

Medizinische Fakultät Charité – Universitätsmedizin Berlin

Campus Benjamin Franklin

aus dem Institut für molekulare Pharmakologie und Zellbiologie

Direktor: Univ. Prof. Dr. med. Walter Rosenthal

**Long-lasting activation of extracellular signal-regulated kinases 1/2:
importance of G protein-coupled receptor localisation and
transcriptional responses**

Inaugural-Dissertation

zur Erlangung des Grades

Doctor rerum medicarum

Charité – Universitätsmedizin Berlin

Campus Benjamin Franklin

vorgelegt von

Solveig Großmann

aus Berlin

Referent: Prof. Dr. med. Michael Schaefer

Koreferent: Prof. Dr. med. Wolfgang. M. Kübler

Gedruckt mit Genehmigung der Charité - Universitätsmedizin Berlin

Campus Benjamin Franklin

Promoviert am: 30.01.2009

Contents

Contents	III
Abbreviations	VII
1 Introduction	1
1.1 Endothelin system	5
1.2 Thrombin and protease-activated receptors	9
1.3 GPCR-mediated transactivation of the EGFR	14
1.4 Lipid rafts and caveolae	16
2 Aims	19
3 Materials and Methods	21
3.1 Chemicals and Reagents	21
3.2 Buffers and Media	23
3.3 Generation of ET _B receptor constructs	25
3.4 Restriction digest	26
3.5 Agarose gel electrophoresis	26
3.6 DNA sequencing	27
3.7 Cell culture	27
3.8 Passaging of cells	28
3.9 Transient transfection of cells	28
3.10 Generation of MDCK cell clones stably expressing ET _B receptor constructs	29
3.11 RNA extraction	30
3.12 cDNA synthesis	30
3.13 Caveolae preparation	30
3.14 ET-1 binding analysis	31
3.15 Microarray analysis	31
3.16 Semi-quantitative multiplex RT-PCR	31

3.17	<i>SDS-PAGE and immunoblotting</i>	32
3.18	<i>Immunoblot analysis of whole-cell lysates</i>	33
3.19	<i>Immunoblot analysis of caveolae-containing fractions</i>	34
3.20	<i>Ectodomain shedding</i>	34
3.21	<i>Total internal reflection fluorescence microscopy</i>	35
3.22	<i>Immunofluorescence</i>	35
3.23	<i>Confocal microscopy</i>	36
3.24	<i>Calcium measurements</i>	36
4	Results	37
4.1	<i>ET_B receptor localisation and downstream signalling</i>	37
4.1.1	Characterisation of endothelin B receptor constructs	37
4.1.2	Localisation of endothelin B receptor constructs to caveolae	40
4.1.3	ET _B receptor-induced shedding of EGFR ligands	44
4.1.4	The EGFR and its ligands do not localise to caveolae	46
4.1.5	Localisation of ET _B receptors does not affect the activation of ERK1/2	48
4.2	<i>Short-term modification of gene expression in vascular smooth muscle cells</i>	51
4.2.1	Confidence analysis	51
4.2.2	Amphiregulin	59
4.2.3	A disintegrin and metalloproteinase with thrombospondin motif 1	60
4.2.4	Tissue inhibitor of metalloproteinases-1	61
4.2.5	MAP3K8	62
4.2.6	Cyclooxygenase 2	62
4.2.7	Other regulated genes	64
5	Discussion	65
5.1	<i>ET_B receptor localisation and its effects on signalling</i>	65
5.1.1	ET _B receptor localisation is cell type-specific	65
5.1.2	ET _B receptor localisation has little impact on EGFR ligand shedding	67
5.1.3	ET _B receptor localisation only poorly correlates with ERK1/2 phosphorylation	69
5.2	<i>Par-mediated gene expression modification</i>	70
5.2.1	Analysis of novel genes involved in the phenotypic modulation of VSM cells	71
5.2.2	Prothrombotic signalling	71
5.2.3	EGFR transactivation	72
5.2.4	MAPK signalling	74

Contents

Summary	77
Zusammenfassung	79
Erklärung	81
Literature	83
Publications list	97
Acknowledgements	99
Curriculum Vitae	101

Abbreviations

4-NPP	4-nitrophenylphosphate
AC	adenylyl cyclase
ADAM	a disintegrin and metalloproteinase
AP	alkaline phosphatase
APS	ammonium persulfate
BSA	bovine serum albumin
CFP	cyan fluorescent protein
COX-2	cyclooxygenase 2
DAG	diacylglycerol
DMEM	Dulbecco's modified Eagle's medium
DMSO	dimethyl sulfoxide
DRM	detergent-resistant membrane
DTT	dithiothreitol
DUSP	dual specificity phosphatase
EDTA	ethylenediamine tetraacetate
EGTA	ethylene glycol tetraacetic acid
eNOS	endothelial nitric oxide synthase
EGF	epidermal growth factor
EGFR	epidermal growth factor receptor
ER	endoplasmatic reticulum
ERK1/2	extracellular signal-regulated kinases 1/2
ET	endothelin
ET-1	endothelin-1
ET-2	endothelin-2
ET-3	endothelin-3
ET _A receptor	endothelin A receptor
ET _B receptor	endothelin B receptor
f.c.	fold change
FCS	fetal calf serum
GEF	guanine nucleotide exchanging factor
GFP	green fluorescent protein
GPCR	G protein-coupled receptor
GPI	glycophosphoinositol
GSL	glycosphingolipids

Abbreviations

HB-EGF	heparin-binding EGF-like growth factor
HDL	high-density lipoprotein
IFN	interferon
IL	interleukin
IP ₃	inositol-1,4,5-trisphosphate
JAK	janus-activated kinase
JNK	c-Jun N-terminal kinase
LBD	light buoyant density
LDL	low-density lipoproteins
l _o	liquid-ordered
MAPK	mitogen-activated protein kinase
MEM Earl's	minimum Eagle's medium with Earl's salts
MHC	major histocompatibility complex
MMP	matrix metalloproteinase
MT-SP	membrane-tethered serine proteinase
NFAT	nuclear factor of activated T cell
NO	nitric oxide
oxLDL	oxidised low-density lipoprotein
PAI	plasminogen activator inhibitor
PAR	protease-activated receptor
PBS	phosphate buffered saline
PFA	paraform aldehyde
PGE ₂	prostaglandin E ₂
PGI ₂	prostacyclin
PI3K	phosphatidylinositol 3-kinase
PIP ₂	phosphatidylinositol 4,5-bisphosphate
PKA	protein kinase A
PKB	protein kinase B
PKC	protein kinase C
PLAU	urinary-type plasminogen activator
PLAUR	urinary-type plasminogen activator receptor
PLC	phospholipase C
PMA	phorbol-12-myristate-13-acetate
PTX	pertussis toxin
ROCK	Rho/Rho-kinase
RTK	receptor tyrosine kinase
SDS	sodiumdodecyle sulfate
SRE	serum response element
STAT	signal transducer and activator of transcription

Abbreviations

TBS	Tris buffered saline
TCA	trichloroacetic acid
TEMED	N,N,N',N'-tetramethylethylenediamine
TIMP	tissue inhibitor of metalloproteinases
TIRFM	total internal reflection fluorescence microscopy
TGF- α	transforming growth factor- α
TMS	triple membrane spanning
TNF	tumour necrosis factor
TRAP	thrombin receptor-activating peptide
T X 100	Triton X 100
VSM	vascular smooth muscle
YFP	yellow fluorescent protein

1 Introduction

Diseases such as arteriosclerosis represent the primary cause of heart disease and stroke in industrial countries (Lusis, 2000). It is a disease mainly affecting large vessels and, thus, is influenced by the regulation of blood vessel constriction also known as vascular tone. All different blood vessels such as arteries and veins exhibit some degree of smooth muscle contraction that determines the diameter, and hence tone, of the vessel. Basal vascular tone is different among organs. Those organs having a large vasodilatory capacity (e.g. skeletal muscle, skin) have high vascular tone, whereas organs having relatively low vasodilatory capacity (e.g. renal circulations) exhibit decreased vascular tone.

Vascular tone is determined by many different competing vasoconstrictor and vasodilator influences acting upon the blood vessel. These influences can be separated into extrinsic factors that originate from outside of the organ or tissue where the blood vessel is located, and intrinsic factors that originate from the vessel itself or the surrounding tissue. Extrinsic factors regulate arterial blood pressure while intrinsic mechanisms are concerned with local blood flow regulation within an organ. But it is not only the vascular tone that promotes the development of arteriosclerosis. Other various changes within the vessel can favour this cardiovascular disease. One of the early recognisable changes within the artery during the development of arteriosclerosis is the formation of fatty streaks (Fig. 1): Cell adhesion molecules (such as VCAM-1, P-selectin, ICAM-1) expressed on the surface of endothelial cells regulate the recruitment of monocytes to lesion-prone sites of arteries in response to inflammation (Glass and Witztum, 2001). Meanwhile, low-density lipoproteins (LDL) undergo oxidative modification (oxLDL), which is a major event in the initial formation of fatty streaks (Napoli et al., 1997). The modified LDL attracts monocytes and induces their migration into the subendothelial space where they differentiate into macrophages. The ongoing accumulation of macrophages and the uptake of oxLDL by scavenger receptors results in the formation of arteriosclerotic lesions (Glass and Witztum, 2001). Scavenger receptors accumulate cholesterol deriving from the oxLDL in macrophages leading to the formation of so-called macrophage foam cells, which is a hallmark of arteriosclerotic lesions (Yamada et al., 1998). The macrophage can dispose of excess cholesterol via membrane transporters with high-density lipoproteins (HDL) acting as an extracellular acceptor.

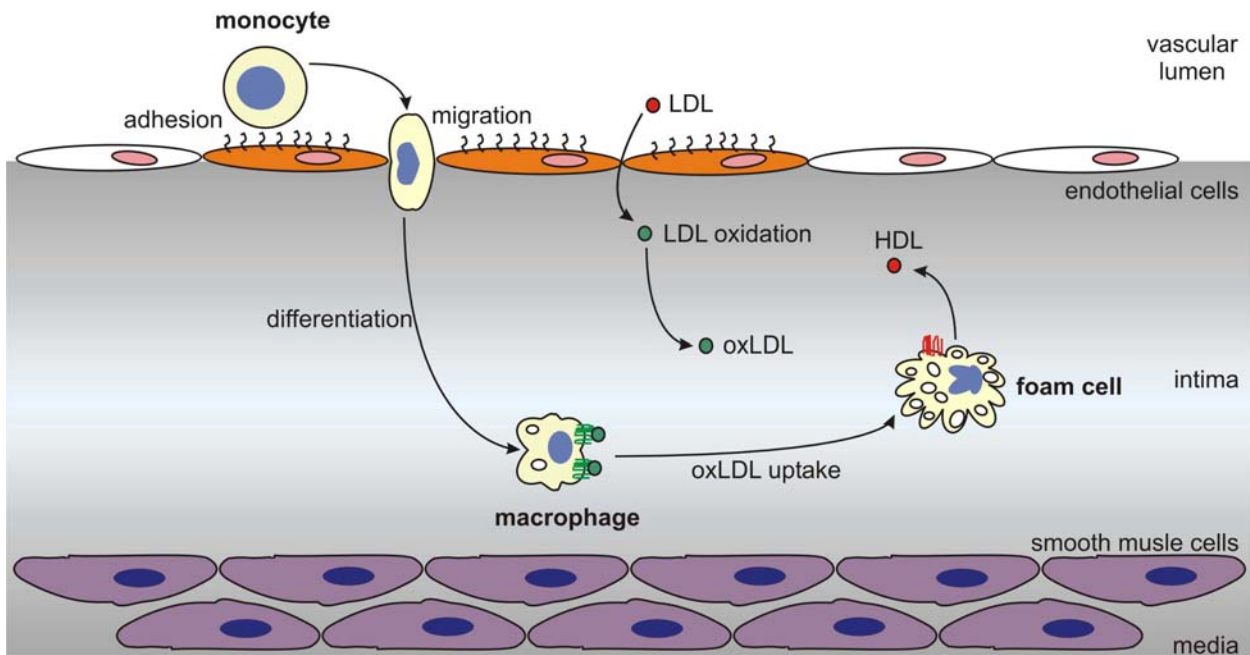


Fig. 1. Development of fatty streaks and arteriosclerotic lesions. Monocytes attach to the endothelial cells expressing adhesion molecules. Adherent monocytes migrate into the subendothelial space and differentiate into macrophages. At the subendothelial space, LDL undergoes oxidative modification and the resulting oxLDL is taken up by scavenger receptors leading to foam cell formation. The oxLDL is then exported to HDL receptors via cholesterol transporters (Figure modified from Glass and Witztum, 2001).

The role for this “reverse cholesterol transport” might explain why arteriosclerosis so often is connected with inversely correlated cholesterol levels (Tall et al., 2000).

The switch from a fatty streak to a more complex lesion is mainly characterised by the immigration of VSM (vascular smooth muscle) cells from the medial layer of an artery into the intimal or subendothelial space (Fig. 2; Glass and Witztum, 2001). In the intima, the innermost layer of an artery or vein, VSM cells can undergo proliferation and take up modified lipoproteins supporting foam cell formation. Furthermore, VSM cells start synthesising extracellular matrix proteins, which ultimately leads to the formation of a fibrous cap (Ross, 1999; Paulsson et al., 2000). Moreover, the cross talk between macrophages and lymphocytes largely influences the development of arteriosclerotic lesions by inducing a broad range of cellular and humoral responses thereby inducing a chronic inflammatory state. Lesional T cells are activated and express Th1 and Th2 cytokines (Hansson, 1997); endothelial cells, macrophages and VSM cells appear to be activated based on the expression of MHC (major histocompatibility complex) class II molecules and inflammatory products such as interleukin (IL)-6 or tumour necrosis factor (TNF) α . The immune response induced can exert atherogenic and antiatherogenic effects.

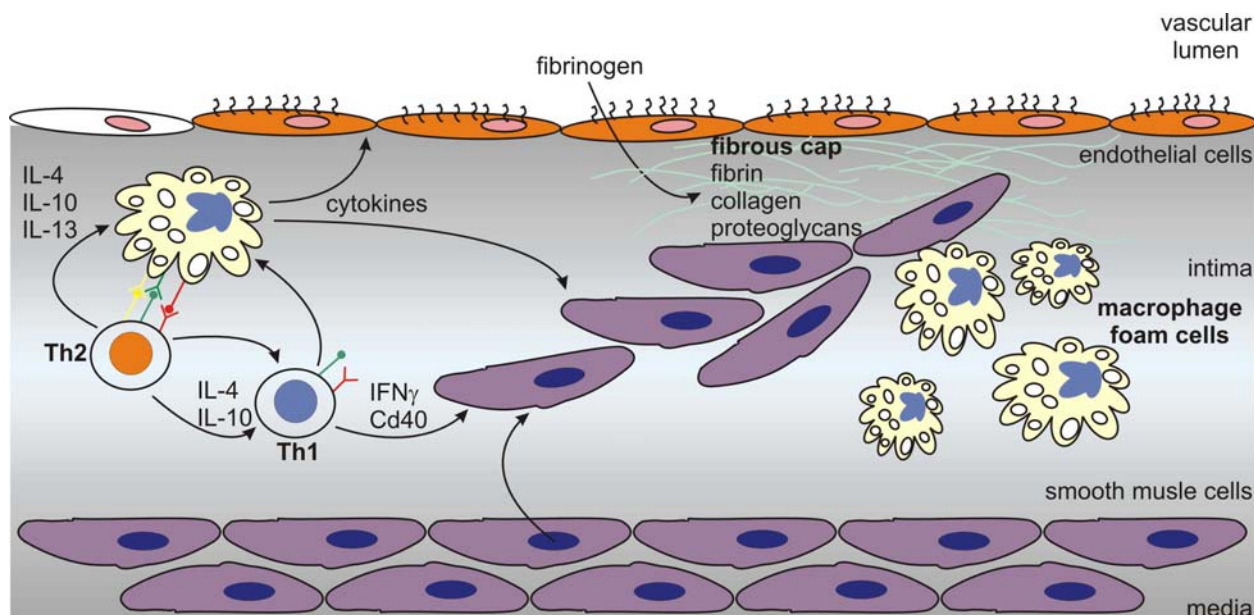


Fig. 2. Lesion progression. Lymphocytes and macrophages secrete cytokines that exert both, pro- and antiatherogenic effects, on cellular elements of the arterial wall. VSM cells migrate from the medial layer into the intimal and subendothelial space where they proliferate and secrete extracellular matrix proteins to form a fibrous cap (Figure modified from Glass and Witztum, 2001).

For example, the Th2-derived IL-4 cytokine is predicted to be antiatherogenic by antagonising the effects of interferon (IFN) γ activity and by inhibiting Th2 cell function. On the other hand, IL-4 also promotes LDL oxidation (Glass and Witztum, 2001).

Even though progressive narrowing of the artery as a result from arteriosclerotic lesions can lead to cardiovascular events such as myocardial infarction and stroke, it is generally thought that a plaque rupture and thrombosis is responsible for these diseases (Davies et al., 1993; Lee and Libby, 1997). Plaque rupture initiates the coagulation cascade, platelet adherence and thrombosis by exposing lipids and the tissue factor to blood components (Fig. 3).

Specific cell-cell interactions as well as the enrichment of cytokines in the arterial wall might account for the apoptosis of macrophages and VSM cells. Moreover, oxidised sterols from oxLDL are known to promote apoptosis and necrosis in arterial lesions (Colles et al., 1996). Oxidised lipids, that are released from necrotic cells, further contribute to the formation of “gruel” advanced lesions, and lipids within the necrotic core are suggested to increase the capability for thrombosis (Glass and Witztum, 2001). Furthermore, most complex lesions exert an extensive fibrin deposition (Fig. 2) resulting from decreased fibrinolytic activity. This deposition accelerates arterial atherogenesis by facilitating thrombosis and fibrin deposition within developing arteriosclerotic lesions (Lee and Libby, 1997).

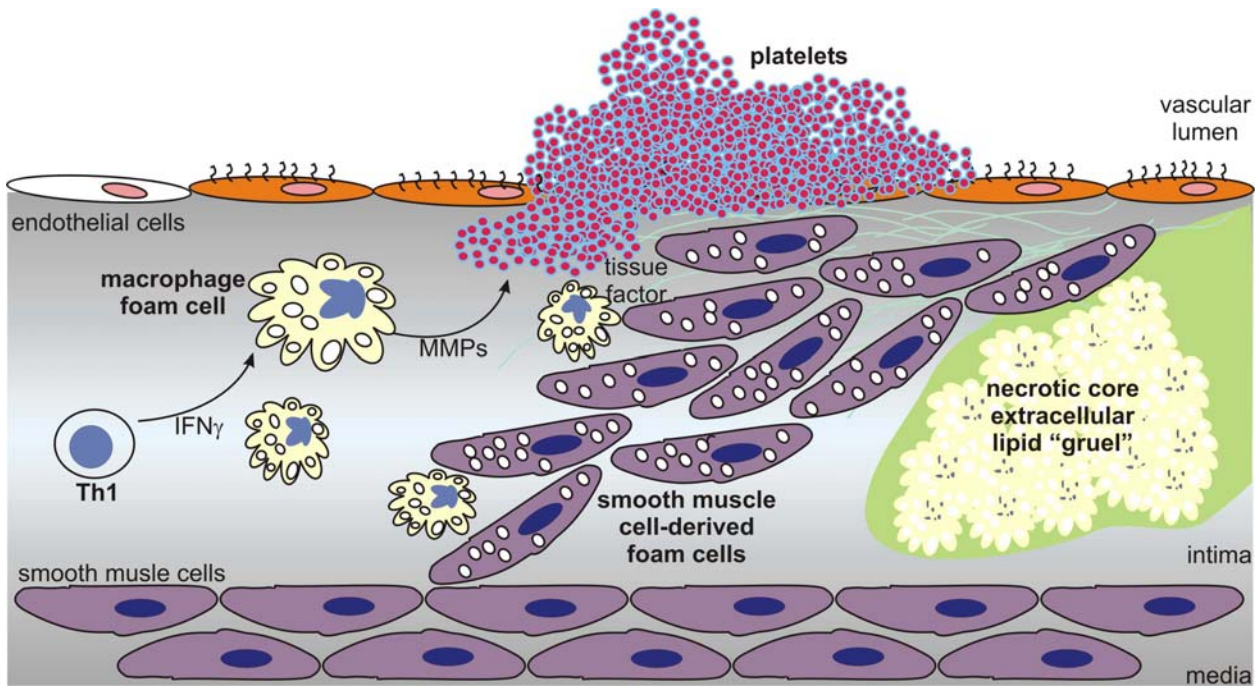


Fig. 3. Plaque rupture and thrombosis. The formation of a necrotic core and the accumulation of extracellular cholesterol as a result from necrosis of macrophages and VSM cells initiate the rupture of a plaque. Plaque rupture exposes blood components to lipids and the tissue factor thereby initiating coagulation, recruitment of platelets and thrombus formation (Figure modified from Glass and Witztum, 2001).

The plaque stability is further influenced by matrix metalloproteinases (MMP) that are released from macrophages and degrade extracellular matrix proteins (Galis et al., 1994; Carmeliet, 2000). In association with protease activation and remodelling, angiogenesis occurs in the vessel wall indicating that neovascularisation also contributes to plaque rupture (Glass and Witztum, 2001).

Besides the molecules and proteins mentioned above many other proteins can be involved in the development of arteriosclerosis. Amongst them is the endothelin system that also plays an important role in the regulation of vascular tone and is implied to be involved in the progression of diseases such as hypertension and arteriosclerosis (Kedzierski and Yanagisawa, 2001). Moreover, protease-activated receptors (PARs) are upregulated in arteriosclerotic plaques (Nelken et al., 1992) and thereby might contribute to the development of arteriosclerosis.

1.1 Endothelin system

The endothelin system consists of two G protein-coupled receptors (GPCRs), three peptide ligands and two activating peptidases. The peptide ligand endothelin-1 (ET-1) leads to both, constriction via smooth muscle cell endothelin A (ET_A) receptor, and dilation via endothelial cell endothelin B (ET_B) receptor (Kedzierski and Yanagisawa, 2001).

Endothelin (ET) is a potent vasoconstrictive peptide consisting of 21 amino acids. Three endogenous isoforms of endothelin, ET-1, ET-2 and ET-3 (Fig. 4), are known (Inoue et al., 1989) of which ET-1 is predominantly produced in endothelial cells.

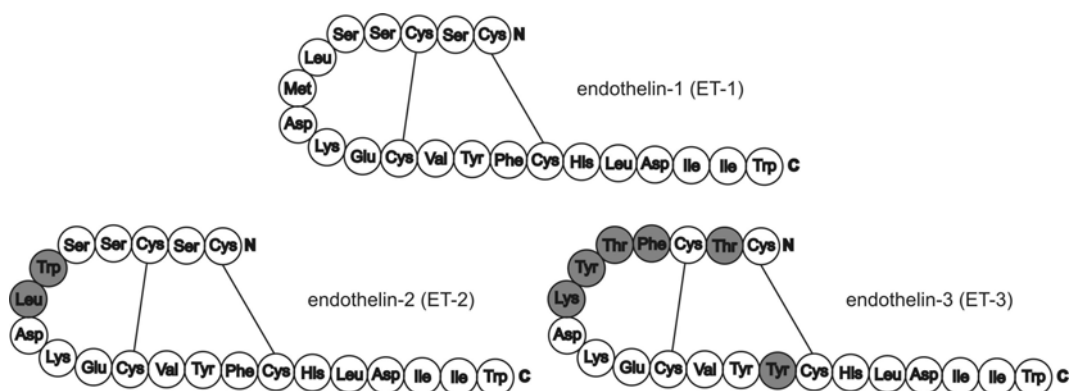


Fig. 4. Endothelin isoforms. The three endothelin isoforms, ET-1, ET-2, ET-3, consist of 21 amino acids. All three ETs possess two intrachain disulfide bridges in a hairpin loop and a conserved, hydrophobic C-terminal tail. Grey residues indicate those that are different from ET-1 (Masaki, 2004).

The human endothelin gene is localised on chromosome 6 and consists of 212 amino acids, which encode the preproendothelin-1 precursor. Preproendothelin-1 undergoes a proteolytic cleavage by the endopeptidase furin to release an intermediary structure, big ET-1. Big ET-1 is then cleaved to mature ET-1 by an endothelin-converting enzyme (ECE) (Russell et al., 1998). Synthesis of ET-2 and ET-3 proceeds in a similar way.

Endothelin-1 is continuously released from vascular endothelial cells by a constitutive pathway, producing intense constriction of the underlying smooth muscle and contributing to the maintenance of endogenous vascular tone (Haynes and Webb, 1994). It elicits smooth muscle contraction mostly via the ET_A receptor, which causes a transient increase in free, intracellular Ca²⁺ ions that leads to sustained contraction (Miwa et al., 1999). In addition to the constitutive pathway it is also released from endothelial cell-specific storage granules in response to external physiological stimuli producing further vasoconstriction (Russell et al., 1998). Only in

inflammatory states ET-1 is also secreted by smooth muscle cells (Tonnessen et al., 1998). Studies on ET-2 are not as extensive as on ET-1. This ET isoform is present in human cardiovascular tissues and is as potent a vasoconstrictor as ET-1 (Maguire and Davenport, 1995). ET-3 is not synthesised by endothelial cells. It is the only ET isoform that distinguishes between the two endothelin receptors (Davenport, 2002).

So far two endothelin receptors, ET_A and ET_B receptor, have been described in mammals. The affinities of the receptors for the different isoforms of endothelin are different. The ET_A receptor binds ET-1 and ET-2 with greater affinity than ET-3, whereas the ET_B receptor binds all isoforms with equal affinity (Masaki, 2004) (Table 1).

Table 1. Functions and distribution of the ET_A and ET_B receptor (Davenport, 2002; Kusserow and Unger, 2004)

receptor	peptide	function	distribution
ET _A	ET-1 ET-2 (ET-3)	long-lasting vasoconstriction, cell proliferation	mainly vascular smooth muscle cells and therefore in all tissues receiving blood supply, including heart, lung and brain
ET _B	ET-1 ET-2 ET-3	clearance of ET-1, inhibition of endothelial apoptosis, release of nitric oxide and prostacyclin, inhibition of endothelin-converting enzyme-1 expression	vascular, endothelial cells; high densities present in the brain, lung, heart and intestine

Both ET receptors belong to the family of heptahelical GPCRs. The human ET_A receptor is encoded on chromosome 4 and consists of 427 amino acids and the human ET_B receptor is encoded on chromosome 13 and has 442 amino acids (Hunley and Kon, 2001). Both proteins contain seven stretches of 20 to 27 hydrophobic amino acid residues. They have an N-terminal signal sequence, which is rare among GPCRs, with a relatively long extracellular N-terminal portion preceding the first transmembrane domain (Fig 5).

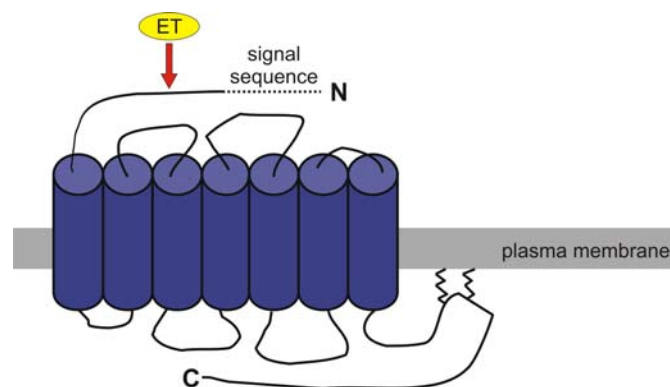


Fig. 5. Structure of endothelin receptors. Both ET receptors belong to the family of G protein-coupled receptors containing seven transmembrane domains. The N-terminal signal sequence is cleaved off upon ligand binding. ET_A and ET_B receptor vary slightly in their number of amino acids within the different domains (Davenport, 2002).

The ET_A receptor is found in most vascular smooth muscle cells but is absent in endothelial cells (Iwasaki et al., 1995). On the other hand, the ET_B receptor is expressed in endothelial cells and in very little amounts in VSM cells (Maguire and Davenport, 1995). Both receptors are also expressed in nonvascular tissues, such as epithelial cells, and occur in the central nervous system in glia and neurones (Table 1; Kusserow and Unger, 2004). Only in diseased states, such as arteriosclerosis, acute renal failure, and focal ischemia, an upregulation of the ET_B receptor in VSM cells has been reported (Roubert et al., 1994; Dagassan et al., 1996; Wackenfors et al., 2004) suggesting an important, however, yet not fully understood role of the ET_B receptor in these cells. A small fraction of ET_B receptor, about 10%, has been described to be located in lipid rafts, which are plasma membrane microdomains that are involved in the regulation of various cell functions (Chapter 1.4; Davenport, 2002).

In general, the ET_A receptor modulates vasoconstriction, cellular proliferation and matrix deposition (Iwasaki et al., 1995) via activation of phospholipase C (PLC) and subsequent conversion of phosphatidylinositol 4,5-bisphosphate (PIP₂) into inositol-1,4,5-trisphosphate (IP₃) and diacylglycerol (DAG) (Fig. 6). The ET_B receptor contributes little to vasoconstriction in tissues due to its low abundance on smooth muscle cells (Maguire and Davenport, 1995). It is prominent in the aorta, brain and lung. In some tissues the ET_B receptor has vasoconstrictive and proliferative activity. In endothelial cells, the ET_B receptor activates the endothelial nitric oxide synthase (eNOS), which mediates the release of prostaglandins and nitric oxide (NO). The subsequent increase in cGMP offsets the vasoconstrictive and mitogenic effects of ET-1 through the ET_A receptor. Finally, the ET_B receptor upregulates the synthesis of ET-1, so that ET-1 is available to interact with the ET_A or ET_B receptor (Fig. 6, Table 1; Iwasaki et al., 1995). Binding of ET-1 to the ET_B receptor occurs in an almost irreversible manner. Therefore, the ET_B receptor acts as a “clearing receptor” and is responsible for the clearing of ET-1 from the extracellular space (Fig. 6, Table 1; Fukuroda et al., 1994).

After ligand binding, the ET_A receptor is internalised rapidly via caveolae or clathrin-coated pits, and follows a recycling pathway, in which it is directed to recycling endosomes and subsequently reappears at the plasma membrane (Chun et al., 1995). The ET_B-ET-1 complex is internalised at a very high constitutive rate and then sorted to lysosomes. Controversial observations exist in regard to what happens to receptor-ligand complexes in lysosomes. While Bremnes et al. (2000) observed a degradation, Foster et al. (2003) found that the complex stays intact for up to 17 hours.

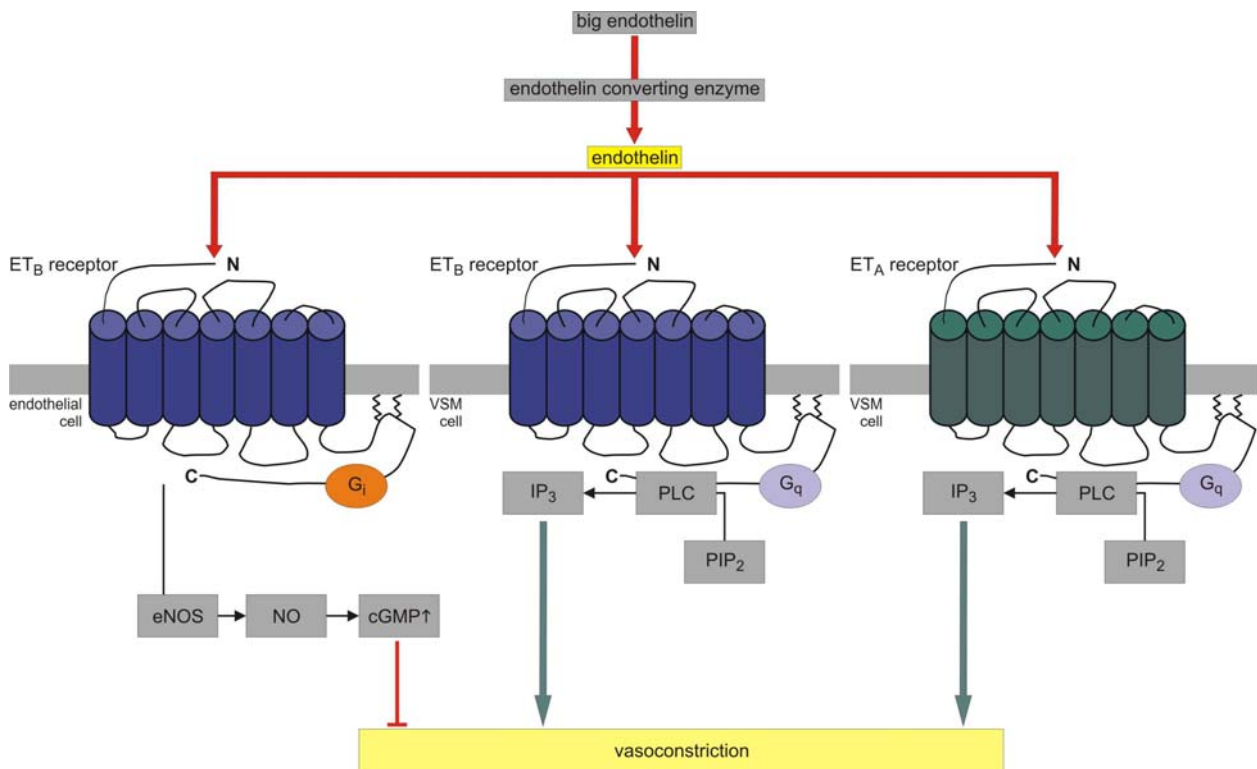


Fig. 6. Signalling cascades induced by ET receptors. Upon synthesis of endothelin, the peptide can bind to the ET_A and ET_B receptor. Stimulation of the smooth muscle cell ET_A receptor triggers vasoconstriction via activation of PLC and subsequent production of IP₃. Activation of the endothelial ET_B receptor prevents vasoconstriction via activation of eNOS and subsequent NO and cGMP production. In diseased states the ET_B receptor can also be localised on VSM cells. There it also triggers vasoconstrictive effects.

A unique feature of the ET_B receptor is the proteolysis of its N terminus. The receptor possesses a 26 amino acid signal peptide, which is cleaved off during receptor synthesis (Akiyama et al., 1992; Kochl et al., 2002). In addition, Akiyama et al. discovered a further proteolytic cleavage site between arginine 64 and serine 65 (R64/S65). Since the proteolytically released N-terminal peptide fragment harbours the only N-linked glycosylation, proteolysis results in a truncated, unglycosylated receptor (Fig. 7). An N-terminal cleavage has been demonstrated for ET_B receptors of various bovine (Hagiwara et al., 1991; Saito et al., 1991), canine (Takasuka et al., 1991), and porcine (Takayanagi et al., 1991) tissues. Moreover, it could be shown that in HEK293 and VSMC this proteolytic cleavage occurs upon ligand binding at the plasma membrane and is most probably triggered by a metalloproteinase (Grantcharova et al., 2002). However, the physiological significance of this proteolytic cleavage remains largely unknown.

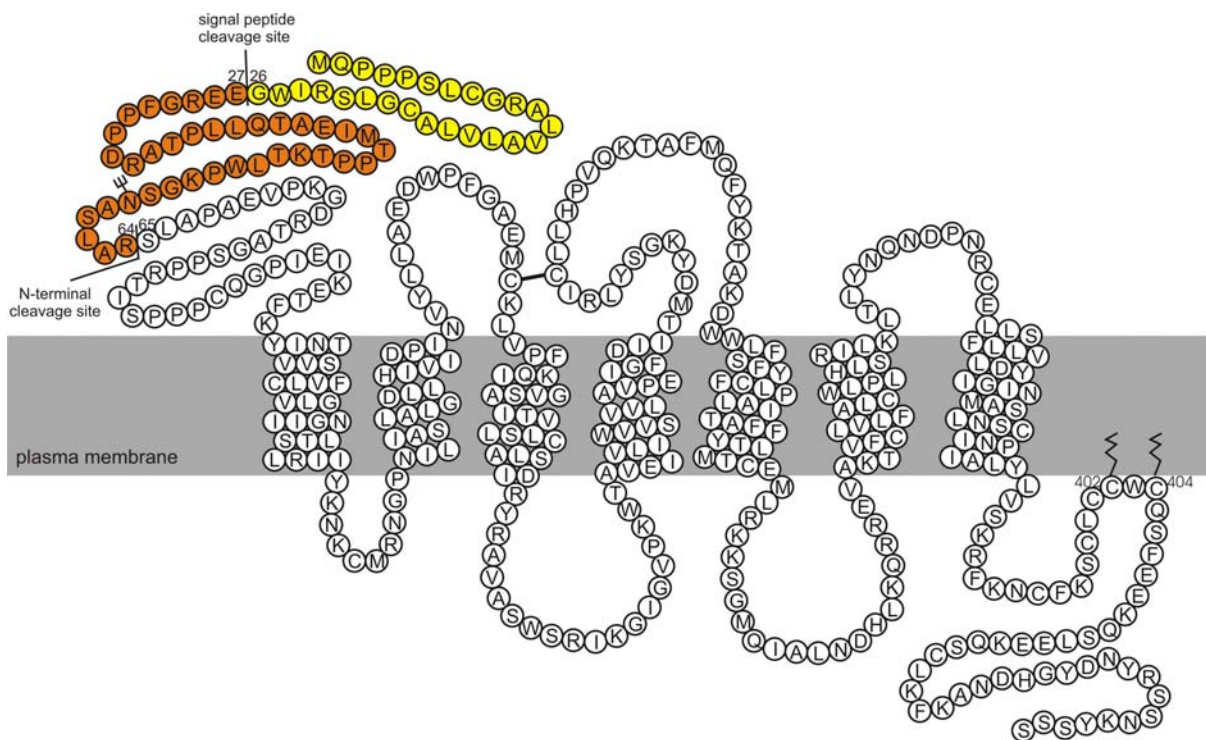


Fig. 7. Cleavage sites of the ET_B receptor. During receptor synthesis, the 26 amino acid signal peptide (yellow) is cleaved off by a signal peptidase in the ER lumen. A metalloproteinase further cleaves the receptor after 64 amino acids (orange). The ET_B receptor harbours an N-glycosylation site at N59. The receptor is posttranslationally modified (palmitoylated) at C402 and C404.

1.2 Thrombin and protease-activated receptors

The serine protease thrombin is activated when thrombosis, inflammation or tissue damage occurs (Martorell et al., 2008). The short-lived thrombin is “persistently” generated by extracellular matrix components in arteriosclerotic lesions (Bar-Shavit et al., 1990). Thrombin converts fibrinogen to fibrin, which forms the fibrous matrix of blood clots and thrombi on arteriosclerotic plaques (Badimon et al., 1994a; Badimon et al., 1994b). Moreover, thrombin induces platelet activation and deposition at the site of injury even in presence of the blood coagulation inhibitor heparin (Badimon et al., 1991). Thrombin generation does not only play an important role in thrombus formation but also produces delayed vascular effects by acting on platelets and VSM cells through protease-activated receptors (“PAR”s in humans; “Par”s in mice and rats; Noorbakhsh et al., 2003) that can be upregulated in arteriosclerotic plaques (Nelken et al., 1992; Coughlin, 2005; Steinberg, 2005; Leger et al., 2006; Hirano, 2007). PARs belong to the family of GPCRs and mediate cellular effects induced by various proteases including thrombin. So far, four different PARs that are differentially expressed in VSM cells, endothelial

cells, platelets and other circulating cells where they exert different physiological effects, have been identified (Table 2; Martorell et al., 2008).

Table 2. Functions and distribution of the different PARs (Noorbakhsh et al., 2003; Hirano, 2007; Martorell et al., 2008)

receptor	activating proteinases	inactivating proteinases	function	distribution
PAR-1	thrombin, trypsin, cathepsin G, granzyme A, factor VIIa/factor X, plasmin, activated protein C, tryptase, MMP 1	plasmin, trypsin, cathepsin G, proteinase 3, elastase, chymotrypsin	platelet activation and thrombosis; embryogenic development; vasoregulation; tissue remodelling	platelets; endothelium; VSM cells; leukocytes
PAR-2	trypsin, tryptase, factor VIIa/tissue factor/factor X, membrane-type serine protease A, activated protein C, MT-SP 1, proteinase 3, acrosin	plasmin, cathepsin G, proteinase 3, elastase	inflammation and vasoregulation	endothelium; VSM cells; leukocytes
PAR-3	thrombin, trypsin	cathepsin G, elastase	platelet activation and thrombosis	platelets; endothelium
PAR-4	thrombin, trypsin, cathepsin G, factor VIIa/factor X, plasmin		platelet activation and thrombosis; inflammation	platelets; endothelium; VSM cells; leukocytes

PARs have a unique mechanism of activation: they carry their own activating peptide and receptor activation is achieved through a proteolytic cleavage within the N terminus of the receptor, which reveals a tethered ligand that binds to and activates the PAR (Fig. 8; Hollenberg and Compton, 2002; Coughlin, 2005; Steinhoff et al., 2005). Furthermore, PAR-1, PAR-2, and PAR-4 but not PAR-3 can also be activated by short synthetic peptide sequences derived from the sequences of the proteolytically revealed tethered ligands (Ramachandran and Hollenberg, 2007). Proteinases do not only activate PARs but can also negatively regulate them by cleaving the receptor at a non-receptor activating site thereby removing the tethered ligand. These receptors do not signal in a physiological setting even though they are still able to bind their activating peptides (Ramachandran and Hollenberg, 2007). The overall effects of proteinases on the receptor may be influenced by the primary sequences of the extracellular region, the state of glycosylation of the receptor, and the difference in the kinetics of the enzymatic reaction at the different cleavage sites (Fig. 9; Hirano, 2007).

Thrombin is one of the most potent agonists for PAR-1 and to a lesser extent for PAR-4 (Hirano, 2007). In the vascular system, low concentrations are sufficient to activate PAR-1 whereas PAR-4-mediated responses are limited to PAR-1-deficient systems or where high thrombin concentrations are employed (Ramachandran and Hollenberg, 2007).

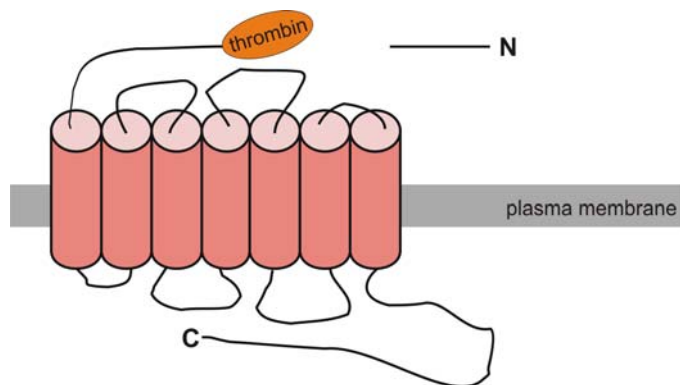


Fig. 8. Structure of protease-activated receptors. All PARs belong to the family of G protein-coupled receptors containing seven transmembrane domains. An N-terminal domain is cleaved off, exposes a tethered ligand and activates the receptor. (Figure modified from Traynelis and Trejo, 2007)

The thrombin-activated PAR-3 functions as a co-factor for PAR-4 but does not directly initiate intracellular signalling (Ishihara et al., 1997; Nakanishi-Matsui et al., 2000). The last PAR, PAR-2, is not directly activated by thrombin but can be transactivated by the thrombin-cleaved PAR-1 (O'Brien et al., 2000). Activated receptors signal through various signalling pathways as they are coupled to different G proteins (Fig. 10).

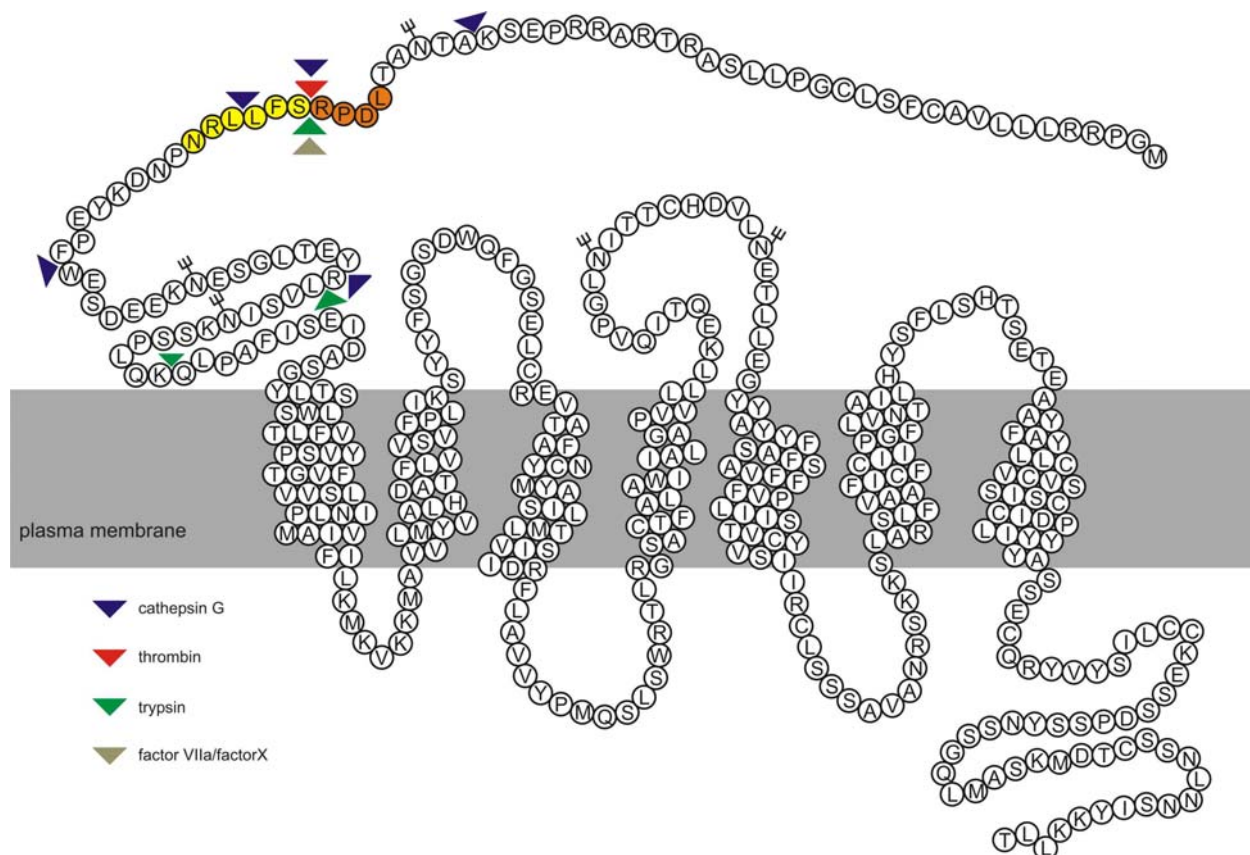


Fig. 9. Topology of PAR-1. Binding of thrombin or other proteinases to its cleavage site (LDPR↓SFLLRN; orange/yellow) within the N-terminal exodomain of PAR-1 exposes a new N terminus beginning with the tethered ligand sequence (yellow). The locations of potential cathepsin G, thrombin, trypsin, and factor VIIa/factorX cleavage sites on PAR-1's N terminus are indicated (Figure modified from Steinberg, 2005).

The PAR-1 couples to G proteins of the $G\alpha_{12/13}$, $G\alpha_{q11}$ and $G\alpha_i$ family (Fig. 10; Macfarlane et al., 2001; Steinhoff et al., 2005). $G\alpha_{12/13}$ couples to guanine nucleotide exchanging factors (GEFs), which results in an activation of Rho/Rho-kinase (ROCK) and serum response element (SRE). Moreover, this G protein can activate c-Jun N-terminal kinase (JNK), which in turn activates the transcription factor c-Jun. Via $G\alpha_{q11}$, PLC β generates IP₃ that mobilises Ca²⁺ and induces the nuclear factor of activated T cell (NFAT) pathway, and DAG, which activates protein kinase C (PKC). This kinase can activate the extracellular signal-regulated kinases 1/2 (ERK1/2) via Raf. Coupling to $G\alpha_i$ inhibits the activity of adenylyl cyclase (AC) and reduces the cAMP production. In addition, G $\beta\gamma$ subunits couple to phosphatidylinositol 3-kinase (PI3K) and protein kinase B (PKB)/Akt. Besides being able to also activate signalling cascades downstream of coupling to G proteins, PAR-1 can also induce the transactivation of the EGFR (see Chapter 1.3). Ras then induces the activation of the mitogen-activated protein kinases (MAPKs) ERK1/2 and p38. Moreover, Rho and Rac lead to the activation of janus-activated kinase (JAK), which induces the signal transducer and activator of transcription 1 and 3 (STAT 1/3) (Fig. 10; Coughlin, 2000; Coughlin, 2005).

Depending on the type of vessel, PAR-1 can lead to an endothelin-dependent relaxation or contraction (Coughlin, 2000; Macfarlane et al., 2001; Hollenberg and Compton, 2002; Steinberg, 2005). In endothelial cells, PAR-1 further contributes to angiogenesis and to the regulation of a number of genes including cytokines, chemokines and cell adhesion molecules (Coughlin, 2000; Steinberg, 2005). When expressed in VSM cells, PAR-1 triggers contraction, migration, proliferation, hypertrophy, and production of extracellular matrix components (Coughlin, 2000; Macfarlane et al., 2001; Hollenberg and Compton, 2002; Steinberg, 2005)

Signalling of PAR-2 has not been studied as extensively as PAR-1 signalling. PAR-2 most probably signals through $G\alpha_{q11}$ and $G\alpha_i$ as its activation leads to the release of IP₃ and DAG followed by an elevation of intracellular Ca²⁺ (Macfarlane et al., 2001). PAR-2 can further signal via an arrestin-mediated process independent of G protein interactions, which might explain the dual actions of PAR-2 in certain settings where it can trigger either inflammatory or anti-inflammatory responses (Ramachandran and Hollenberg, 2007). In different cell types, PAR-2 has also been shown to activate various signalling molecules such as JNK, PLC, Rho, Rac, PKC, ERK1/2, and p38 thereby most probably triggering cytoskeletal effects possibly involving the already mentioned arrestin-mediated signalling (reviewed in Ramachandran and Hollenberg, 2007). Similar to PAR-1, PAR-2 also mediates endothelium-dependent relaxation and

angiogenesis in endothelial cells, whereas it triggers constriction, migration, proliferation, hypertrophy, and production of extracellular matrix components in VSM cells (Coughlin, 2000; Macfarlane et al., 2001; Hollenberg and Compton, 2002; Steinberg, 2005).

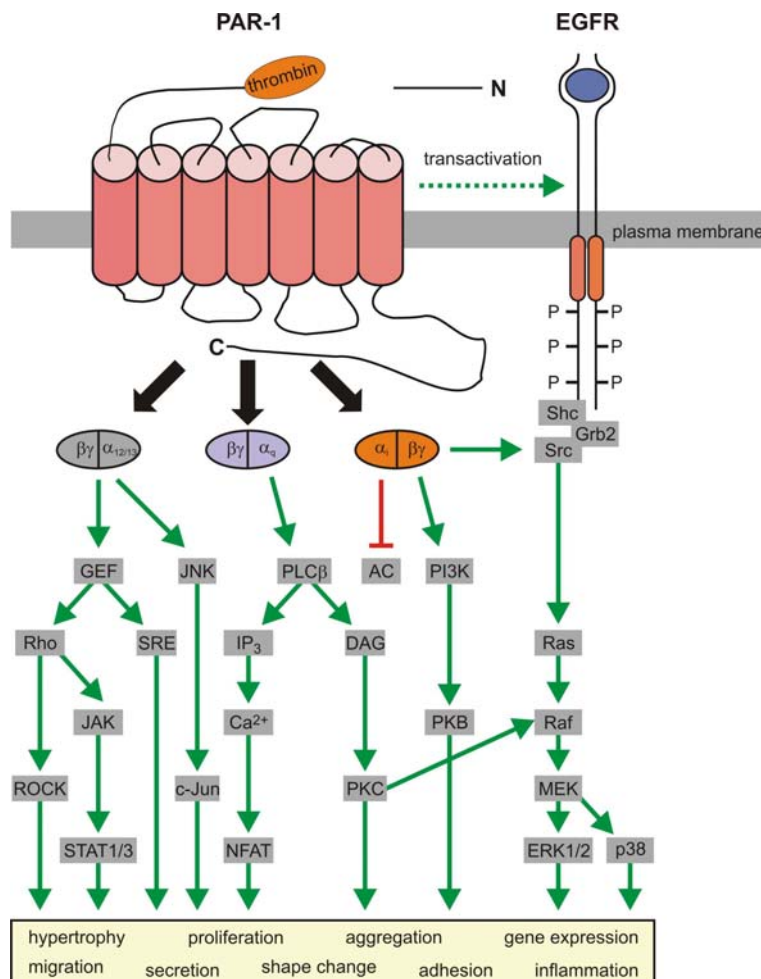


Fig. 10. Signalling cascades induced by PAR-1. The activated PAR-1 couples to $G_{\alpha_{12/13}}$, G_{α_q} and G_{α_i} proteins that signal through multiple signalling pathways that lead to the activation of various transcription factors. PAR-1 activation can also lead to EGFR transactivation thereby inducing further signalling cascades (Figure modified from Martorell et al., 2008)

Except for its ability to act as a co-factor for PAR-1 and PAR-4 signalling, PAR-3 does not seem to signal on its own or to directly elicit intracellular signals (Coughlin, 2000; Nakanishi-Matsui et al., 2000). The PAR-3 tethered ligand sequence can activate other PARs, however, the fact that PAR-3 dimerises with other PARs suggests a mechanism through which PAR-3 can regulate signalling apart from employing its tethered ligand (reviewed in Ramachandran and Hollenberg, 2007).

The last PAR, PAR-4, most probably triggers its signalling via proteins of the $G\alpha_{q/11}$ family. It is known that stimulation of PAR-4 leads to the elevation of intracellular Ca^{2+} via activation of PLC. Moreover, PAR-4 can mediate the phosphorylation of the MAPKs ERK1/2 and p38 (reviewed in Ramachandran and Hollenberg, 2007). It is known that PAR-4 contributes to endothelium-dependent relaxation by inducing NO production in endothelial cells, however, its role in VSM cells remains unknown (Hirano, 2007).

Upon activation, PARs are rapidly internalised in a clathrin-dependent way and transported to lysosomes where they are degraded (Trejo et al., 2000).

1.3 GPCR-mediated transactivation of the EGFR

In diseased states, such as arteriosclerosis, VSM cells undergo a phenotypic modulation switching between proliferation and dedifferentiation (Owens et al., 2004). This phenotypic modulation is characterised by the loss of contractile function, but the exact mechanisms and signalling events underlying this switch remain largely elusive (Ross, 1995). It has been suggested that the strength and duration of MAPK phosphorylation - especially of ERK1/2 - defines the phenotypic outcome of cells (Marshall, 1995).

At least three mitogenic pathways from GPCRs to ERK1/2 are known: the transactivation pathway, the PKC pathway and the cAMP/PKA pathway (Liebmann, 2001). The so-called “triple membrane-spanning” (TMS) pathway, which includes a GPCR-mediated transactivation of the EGFR, is an interesting but not fully understood way of ERK1/2 activation (Fig. 11). The EGFR (also known as ErbB1 or HER1), as well as HER2 (ErbB2), HER3 (ErbB3), and HER4 (ErbB4), belong to the family of receptor tyrosine kinases (RTKs), which may form active homo- or heterodimers upon interaction with their agonistic ligands (Rozenfurt, 2007).

The GPCR-induced EGFR transactivation is often mediated by the release of proforms of the EGFR ligands EGF, heparin-binding EGF-like growth factor (HB-EGF), amphiregulin, betacellulin, epiregulin or transforming growth factor- α (TGF- α) (Prenzel et al., 1999; Gschwind et al., 2003; Shah and Catt, 2004; Schafer et al., 2004a). Conversion of the proforms into active ligand requires MMP activity. It is suggested that MMPs of the zinc dependent ADAM (a disintegrin and metalloproteinase) family trigger this conversion (Asakura et al., 2002; Yan et al., 2002; Gschwind et al., 2003; Schafer et al., 2004b). The exact mechanism by which ADAMs such as ADAM10, ADAM12 and ADAM17, that have already been implicated in the GPCR-induced transactivation, are activated remains largely elusive (for review see Ohtsu et al., 2006).

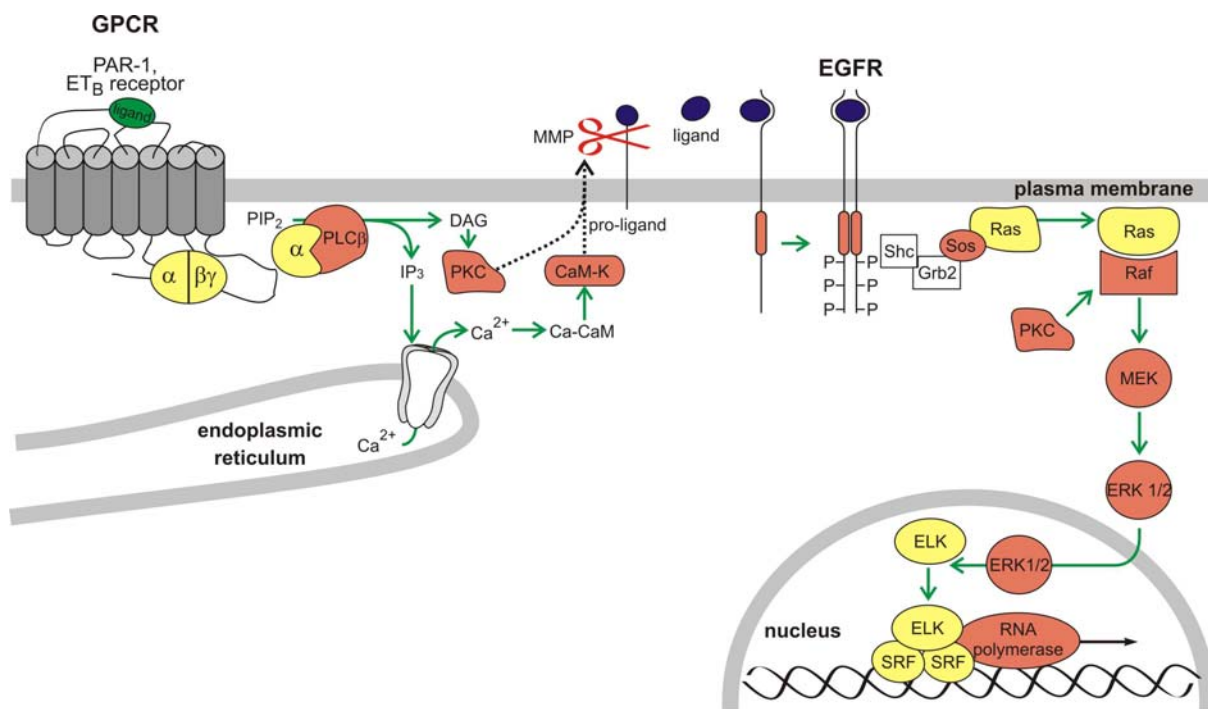


Fig. 11. Triple membrane-spanning pathway. Following GPCR activation, MMPs initiate the shedding of the EGFR ligands, which leads to autophosphorylation of the EGFR, and subsequently activates the canonical Ras/Raf/MEK/ERK signalling cascade.

The EGFR autophosphorylates at Tyr¹⁰⁶⁸ upon interaction with its ligand. Moreover, GPCR agonists induce a rapid and transient activation of Src-family members, which directly induce the phosphorylation of the EGFR at Tyr⁸⁴⁵. Since Src can also trigger the release of EGFR ligands, it is likely that Src contributes to a number of signalling mechanisms during the GPCR-mediated transactivation of the EGFR (Rozengurt, 2007). Another signalling molecule that is very likely to be involved in this process is the PKC. In a number of different cells it could be shown that PKC negatively regulates the EGFR signalling indicating a regulated feedback inhibition. In this manner, PKC modulates the intensity and duration of EGFR transactivation and signalling (Crotty et al., 2006; Oster and Leitges, 2006). Once activated, the EGFR triggers the canonical Ras/Raf/MEK/ERK signalling cascade (Prenzel et al., 2000). Phosphorylated ERK1/2 then translocate to the nucleus and in turn phosphorylate nuclear transcription factors or transcriptional coactivators (Torii et al., 2004). Depending on the kinetic of ERK1/2 activation (Marshall, 1995), the Ras/Raf/MEK/ERK cascade promotes cell proliferation or differentiation (Gerits et al., 2007).

Various GPCRs have been implicated to induce the transactivation of the EGFR: in thrombin-stimulated VSM cells, Par-1 induces a biphasic and long-lasting activation of ERK1/2 with the subsequent expression of contractile proteins and differentiation markers such as smooth muscle-

specific α -actin and smooth muscle-specific myosin heavy chain (Reusch et al., 2001b). Similar results were obtained for the stimulated ET_B receptor in VSM cells (Grantcharova et al., 2006b). Both receptors induced an EGFR transactivation and subsequent signal propagation through the Ras/Raf signalling module that resulted in a long-lasting phosphorylation of ERK1/2, however, the molecular basis of this differentiation-promoting signalling cascades is still not fully understood.

It is possible that small signalling platforms within the plasma membrane, such as lipid rafts and caveolae, could also be of importance in the phenotypic modulation of VSM cells. It has been described that the angiotensin-mediated transactivation of the EGFR is influenced by the enrichment of the angiotensin receptor in those plasma membrane microdomains (Ushio-Fukai et al., 2001; Shah, 2002). Moreover, it has been shown that the oxytocin receptor changes between a proliferative and growth-inhibiting phenotype depending on whether it is enriched in caveolin-1-containing plasma membrane microdomains or not (Rimoldi et al., 2003).

1.4 Lipid rafts and caveolae

Lipid rafts are plasma membrane microdomains that are involved in the regulation of a number of cell functions such as the sorting of proteins and endocytosis (Johannes and Lamaze, 2002). They are planar domains of the outer leaflet of the cell membrane enriched in glycosphingolipids and cholesterol (Fig. 12A; Brown and London, 1998). The sphingolipids aggregate into a distinct domain in the Golgi apparatus and form a unit-membrane patch, which is then trafficked to the plasma membrane. Lipid rafts appear as rather small (in the nanometre range) dynamic structures, which are stabilised through interactions with the cytoskeleton that can aggregate into larger platforms in response to various stimuli (Harder et al., 1998).

Lipid rafts belong to the group of detergent-resistant membranes (DRMs) as they resist low-temperature solubilisation by non-ionic detergents like Triton X 100 at 4°C. This allows their separation by differential flotation after density-gradient centrifugation (London and Brown, 2000). Lipid rafts are described as having a light buoyant density (LBD) and they literally “float” like rafts to the top of a density-gradient.

Caveolae are a subfamily of lipid rafts first described more than 50 years ago (Palade, 1953). They are non-planar membrane domains highly enriched in cholesterol and glycosphingolipids (GSL), just like rafts. Caveolae form flask-shaped invaginations, with a diameter of 50-100 nm

and are located at or near the plasma membrane of some, but not all cells. A specific set of proteins, caveolin-1, -2, and -3, self-assembles in high-mass oligomers to form a cytoplasmic coat on the membrane invaginations, which leads to the shape and structural organisation of caveolae (Fig. 12B). Each caveolin protein has a size of 22 kDa and contains a 33 amino acid hydrophobic domain that anchors the protein in the membrane, leaving the amino and carboxyl portions free in the cytoplasm (Kurzchalia et al., 1994).

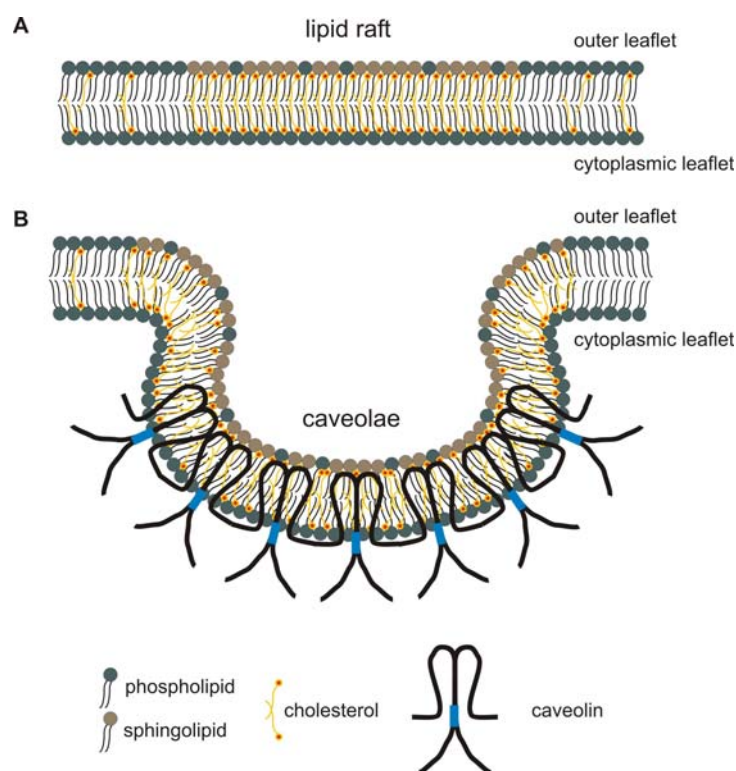


Fig. 12. Structure of lipid rafts and caveolae. (A) Lipid rafts are planar membrane microdomains highly enriched in sphingolipids and cholesterol. Due to their composition and low density they are resistant to solubilisation by detergents and can be isolated by density gradient centrifugation; (B) Caveolae are a subfamily of lipid rafts. The flask-like shape of caveolae derives from the caveolin protein. The model was modified from Galbiati et al., (2001).

Caveolin-1 is associated not only with the plasma membrane but also with the trans-Golgi network, where it is synthesised, and with endosomes and caveosomes (caveolar vesicles), which suggest a role in endocytosis (Pelkmans and Helenius, 2002). Caveolin-1 acts as a marker for the identification of caveolae and the presence of caveolin-1 alone distinguishes caveolae from other lipid rafts, although some evidence is given for the existence of some caveolae without caveolin-1 (Anderson and Jacobson, 2002). Caveolin-1 interacts with glycosphosphoinositol (GPI)-proteins as well as other proteins including endothelin and the ET_A receptor (Chun et al., 1994). However, caveolin-1 does not appear to induce raft invagination but rather stabilises the plasma membrane association of invaginated rafts retarding their dynamin-dependent budding (Le et al.,

2002). The fact that the motor protein dynamin, which is important for vesicle separation, localises to caveolae and the morphological similarity to clathrin-coated pits again suggests an endocytic role for caveolae (Oh et al., 1998; Henley et al., 1998).

The formation of caveolae is a multistep process. The glycosphingolipids/ sphingomyelin/ cholesterol lipid core of caveolae forms in the Golgi apparatus. GPI proteins and caveolin-1 arrive from the endoplasmic reticulum (ER) and are then incorporated into the membrane (Lisanti et al., 1993). Caveolae are shipped to the cell surface embedded in the membrane of exocytic vesicles (Dupree et al., 1993) where the 'lipid shuttle' begins transporting cholesterol and other lipids from the ER. The lipid shuttle maintains the liquid-ordered (l_o) phase of caveolae, which is essential for concentrating GPI and acylated proteins migrating in and out of the domain. Once the assembly step is completed, caveolae internalise molecules and deliver them to specific locations in the cell (Anderson, 1998).

Like lipid rafts, caveolae can also be isolated as DRMs (Johannes and Lamaze, 2002) as they float on both velocity (Smart et al., 1995) and equilibrium (Sargiacomo et al., 1993) gradients. Caveolae contribute to a number of signalling events (Lisanti et al., 1995; Kurzchalia and Parton, 1999), therefore, the localisation of a receptor to caveolae might influence its signalling cascades. Some GPCRs, such as the ET_B receptor, are reported to be located in both lipid rafts and caveolae and it seems as if lipid rafts/caveolae are actively regulating their signalling and trafficking (Chini and Parenti, 2004). The importance of localisation of proteins to caveolae for their signalling events is still not fully understood.

2 Aims

The ET_B receptor can undergo a proteolytic cleavage resulting in an N-terminally truncated and unglycosylated receptor. Activation of the full-length ET_B receptor leads to the transactivation of the EGFR but the EGFR ligands involved remain unknown. The stimulation of the full-length ET_B receptor further leads to a long-lasting, biphasic phosphorylation of ERK1/2 in VSM and HEK293 cells (Grantcharova et al., 2006b). In contrast, activation of the truncated ET_B receptor leads to monophasic activation of ERK1/2. The reasons for these differences are not understood. One hypothesis explaining this phenomenon could be different localisations of the receptor isoforms within these cells. Moreover, stimulation of either of the two receptor variants could determine the phenotypic outcome of a cell since the pattern of MAPK activation - especially of ERK1/2 - has been shown to define the proliferation or differentiation of cells (Reusch et al., 2001a). In this study, it was investigated whether the localisation of distinct ET_B receptor isoforms to caveolae leads to different ERK1/2 activation patterns in COS7, HEK293 and MDCK cells. It was further studied, which EGFR ligands might account for the transactivation of the EGFR upon stimulation of the ET_B receptor.

Stimulation of PARs with thrombin or with a thrombin receptor-activating peptide (TRAP) also leads to a strong and biphasic activation of ERK1/2 and subsequent expression of contractile proteins in VSM cells (Reusch et al., 2001b). Both, thrombin and TRAP activate PARs but differ in their selectivity. Whilst the peptidase thrombin acts upon PAR-1, PAR-3 and PAR-4, TRAP is a selective PAR-1-activating peptide. Neither thrombin nor TRAP activate PAR-2 (Noorbakhsh et al., 2003). It has been shown that the second phase of ERK1/2 activation results from an MMP-mediated shedding of pro-HB-EGF and pro-amphiregulin followed by the transactivation of the EGFR (Higashiyama et al., 1991; Reusch et al., 2001a;) and the Ras/Raf/MEK/ERK signalling cascade (Reusch et al., 2001b). Moreover, treatment of VSM cells with pertussis toxin (PTX) showed that the late phase of ERK1/2 activation requires signalling by G_i proteins (Reusch et al., 2001a). All these studies imply that it is the late phase of ERK1/2 phosphorylation that defines the PAR-1- and G_i-mediated differentiation of VSM cells, however, the exact signalling cascade underlying these events remains largely elusive. This study aimed to reveal new candidate genes that function as novel intermediates in the PAR-1 and PAR-4-induced signalling cascade leading to the expression of contractile proteins.

3 Materials and Methods

3.1 Chemicals and Reagents

¹²⁵ I-Endothelin-1	Amersham Biosciences, USA
4-Nitrophenylphosphate (4-NPP)	Sigma-Aldrich, Steinheim, Germany
Acetone	J.T.Baker, Netherlands
Acrylamide/Bis (30%)	Carl Roth, Karlsruhe, Germany
Agar-agar	Carl Roth, Karlsruhe, Germany
Agarose	Carl Roth, Karlsruhe, Germany
Ammonium persulfate (APS)	Sigma-Aldrich, Steinheim, Germany
Aprotinine	MERCK, Darmstadt, Germany
Bacitracine	MERCK, Darmstadt, Germany
Benzamidine	Sigma-Aldrich, Steinheim, Germany
BigDye Terminator Cycle Sequencing mix	Applied Biosystems, USA
Boric acid	MERCK, Darmstadt, Germany
Bovine serum albumin (BSA)	Sigma-Aldrich, Steinheim, Germany
Bromphenol blue	Carl Roth, Karlsruhe, Germany
Cacodylat solution	Carl Roth, Karlsruhe, Germany
Calcium chloride (CaCl ₂)	MERCK, Darmstadt, Germany
Dimethylsulfoxide (DMSO)	Sigma-Aldrich, Steinheim, Germany
Disodium-hydrogen phosphate (Na ₂ HPO ₄)	MERCK, Darmstadt, Germany
Dithiothreitol (DTT)	Sigma-Aldrich, Steinheim, Germany
Endothelin-1 (ET-1)	Sigma-Aldrich, Steinheim, Germany
Ethanol	J.T.Baker, Netherlands
Ethidium bromide solution (1%)	Carl Roth, Karlsruhe, Germany
Ethylendiamine-tetraacetate (EDTA)	Carl Roth, Karlsruhe, Germany
Ethylene glycol tetraacetic acid (EGTA)	Carl Roth, Karlsruhe, Germany
Fetal calf serum (FCS)	Biochrom, Berlin, Germany
G-418	PAA Laboratories, Austria
Glucose	Carl Roth, Karlsruhe, Germany
Glutamine	Biochrom, Berlin, Germany

Glycerine	MERCK, Darmstadt, Germany
Glycine	Carl Roth, Karlsruhe, Germany
HEPES	Carl Roth, Karlsruhe, Germany
IRL1620	Sigma-Aldrich, Steinheim, Germany
Magnesium acetate (C ₄ H ₆ MgO ₄)	New England Biolabs, United Kingdom
Magnesium chloride-6-hydrate (MgCl ₂ ·6H ₂ O)	J.T.Baker, Netherlands
N,N,N',N'-tetramethylethylenediamine (TEMED)	Sigma-Aldrich, Steinheim, Germany
Optiprep	Axis-Shield, Norway
Paraformaldehyde (PFA)	Applichem, Darmstadt, Germany
Penicillin/Streptomycin	Sigma-Aldrich, Steinheim, Germany
Peptone	Carl Roth, Karlsruhe, Germany
Percoll	Amersham Biosciences, USA
Pertussis toxin (PTX)	Calbiochem, Darmstadt, Germany
Phorbol-12-myristate-13-acetate (PMA)	Calbiochem, Darmstadt, Germany
Potassium acetate (CH ₃ COOK)	New England Biolabs, United Kingdom
Potassium chloride (KCl)	Sigma-Aldrich, Steinheim, Germany
Potassium dihydrogen phosphate (KH ₂ PO ₄)	J.T.Baker, Netherlands
Sodium acetate (C ₂ H ₃ NaO ₂)	Applichem, Darmstadt, Germany
Sodium chloride (NaCl)	J.T.Baker, Netherlands
Sodiumdodecylsulfate (SDS)	Carl Roth, Karlsruhe, Germany
Sucrose	Carl Roth, Karlsruhe, Germany
Thrombin	Calbiochem, Darmstadt, Germany
Thrombin receptor-activating peptide FLLRN (TRAP)	Tocris, USA
Trichloroacetic acid (TCA)	Sigma-Aldrich, Steinheim, Germany
Triton X 100 (T X 100)	Sigma-Aldrich, Steinheim, Germany
Tris	Applichem, Darmstadt, Germany
Tris acetate	New England Biolabs, United Kingdom
Trypsin/EDTA	Biochrom, Berlin, Germany
Trypsin inhibitor	Sigma-Aldrich, Steinheim, Germany
Tryptose phosphate broth	Sigma-Aldrich, Steinheim, Germany
Tween 20	Sigma-Aldrich, Steinheim, Germany
Xylenol orange	Serva, Heidelberg, Germany
Yeast extract	Carl Roth, Karlsruhe, Germany

3.2 Buffers and Media

Agarose gel sample buffer, 10 x	50% glycerol 0.4% xylenol orange 1 mM EDTA, pH 8
Blocking buffer	2% BSA in permeabilisation buffer
Blocking solution	5% nonfat dried milk powder in TBS/Tween buffer
Buffer A, pH 7.8	0.25 M sucrose 1 mM EDTA 20 mM Tris
Buffer C, pH 7.8	50% Optiprep 0.25 M sucrose 6 mM EDTA 120 mM Tris
Fixans, pH 7.5	100 mM cacodylat 100 mM sucrose 1% PFA
Laemmli buffer, 3x	0.3% bromphenol blue 150 mM DTT 30% glycerine 6% SDS 90 mM Tris; pH 6.8
LB medium (Luria-Bertani medium) pH 7.4	10 g peptone 5 g yeast extract 10 g NaCl ad 1 l with dH ₂ O autoclave
LB plates	add 15 g of agar-agar to LB medium autoclave
NEBuffer2, 1x; pH 7.9	10 mM Tris acetate 50 mM NaCl 10 mM MgCl ₂ 1 mM DTT
NEBuffer3, 1x; pH 7.9	50 mM Tris acetate 100 mM NaCl 10 mM MgCl ₂ 1 mM DTT

NEBuffer4, 1x; pH 7.5	20 mM Tris acetate 50 mM potassium acetate 10 mM magnesium acetate 1 mM DTT
PBS (phosphate buffered saline), 1 x pH 7.5	140 mM NaCl 8.1 mM Na ₂ HPO ₄ 2.5 mM KCl 1.5 mM KH ₂ PO ₄ autoclave
Permeabilisation buffer	% T X 100 in PBS
Protease inhibitor mix	100 mM benzamidine 2 µg/ml trypsin inhibitor 1µg/ml aprotinine
SDS running buffer, 10 x	14.4% glycine 10% SDS 3% Tris
SDS reducing sample buffer, 5 x	12.5 ml 0.5 M Tris, pH 6.8 12.5 ml glycerol 1 ml 0.05% Bromphenol blue 1.875 g DTT 1.25 g SDS
SOB medium	20g/l peptone 5g/l yeast extract 0.5 g/l NaCl 2.6 mM KCl
SOC medium	20 mM MgCl ₂ 20 mM glucose in SOB medium
TBE (Tris-borate/EDTA electrophoresis buffer), 1 x	100 mM Tris 100 mM boric acid 2.5 mM EDTA autoclave
TBS (Tris buffered saline), 10x	20mM Tris 137 mM NaCl
TBS/Tween, 1x	99.9% 1 x TBS 0.1% Tween [®] 20

Tris/BAME buffer	50 mM Tris 2 mM EGTA 10 mM MgCl ₂ 0.15 mM bacitracin 0.0015% aprotinin
SDS transfer buffer, 10 x	10.5% glycine 2.85% Tris

3.3 Generation of ET_B receptor constructs

The generation of a plasmid encoding a fusion protein consisting of the human ET_B receptor fused to GFP at its C terminus (ET_B.GFP), and of a plasmid encoding an ET_B receptor with a truncated extracellular N terminus (Δ 2-64.ET_B.GFP) was described before (Oksche et al., 2000; Grantcharova et al., 2002). Briefly, the cDNA encoding the human ET_B receptor (Frank Zollmann, Berlin, Germany) was amplified with the ET_B.GFP primers given in Table 3.

Table 3. Primers for the generation of ET_B receptor constructs

Primer		sequence (5'→3')	restriction site
ET _B .GFP	forward	AGATACTGCAGCAGGTAGCAGCATGCAGCCG	<i>Pst</i> I
ET _B .GFP	reverse	CCAGTAATAAATACAGCTCATCGGATCCATT	<i>Bam</i> HI
Δ 2-64.ET _B .GFP	forward	CTGCAGCAAGCAGCATGTCGTTGGCACCTGCGGAG	<i>Pst</i> I
Δ 2-64.ET _B .GFP	reverse	CTCCGCAGGTGCCAACGACATGCTGCTTGCTGCAG	<i>Pst</i> I
Δ Glc.ET _B .GFP	forward	GCCAGTCTGGCGCACGCGTTGGCACCTG	
Δ Glc.ET _B .GFP	reverse	CAGGTGCCAACGCGTGCGCCAGACTGGC	
ET _B .GFP.Xba	forward	GGTCTAGAGGTGAGCAAGGGCGAG	<i>Xba</i> I
ET _B .GFP.Apa	reverse	GAGGGGGCCCTTAATCCTGGCTCAGTTGC	<i>Apa</i> I

The forward primer introduced a *Pst*I site; the reverse primer replaced the original stop codon with an aspartate codon and introduced a *Bam*HI site. The *Pst*I/*Bam*HI cut PCR fragment was cloned into the pEGFPN1 plasmid (Invitrogen, USA). Site-directed mutagenesis (Quikchange, Stratagene, Heidelberg) using appropriate primers (Table 3) was performed according to the manufacturer's protocol to generate an N-terminally truncated Δ 2-64.ET_B.GFP and a glycosylation-deficient Δ Glc.ET_B.GFP receptor that cannot be cleaved proteolytically and is lacking an asparagine-linked glycosylation site. An OTR.GFP.cav2 plasmid (Guzzi et al., 2002) was used to generate fusion proteins consisting of ET_B.GFP or Δ Glc.ET_B.GFP fused to caveolin-2 (ET_B.GFP.cav2 and Δ Glc.ET_B.GFP.cav2 respectively). Briefly, the GFP.cav2 cDNA was amplified using a forward primer including an *Xba*I site and a reverse primer including an *Apa*I site (Table 3) and subcloned to obtain a pcDNA3.GFP.cav2 vector (pcDNA3 plasmid from Invitrogen, USA). cDNAs of ET_B and Δ Glc.ET_B.GFP receptors were then amplified and in-

frame ligated into pCDNA3.GFP.cav2 after a *HindIII/XbaI* cut. All constructs were verified by cDNA sequencing (Chapter 3.6) of the entire open reading frames.

3.4 Restriction digest

Plasmid DNA was digested using different restriction endonucleases provided by New England Biolabs (United Kingdom). Briefly, 0.5 µg of DNA were digested with 1 U of restriction enzyme in its required incubation buffer (1 x) in a 20 µl reaction. If required, 100 µg/ml BSA were added to the sample. Table 4 summarises all restriction enzymes and their properties. Samples were incubated at the required temperature for 1 hour and then run on an agarose gel as described in Chapter 3.5.

If the DNA was digested with two restriction endonucleases, and the incubation buffers for each enzyme were different, the DNA was incubated for 1 h with the buffer (+ enzyme) containing the lower salt concentration before adding the second enzyme in its incubation buffer. Samples were then incubated at the appropriate temperature for another hour.

Table 4. Restriction endonucleases and their properties

restriction endonuclease	incubation buffer	temperature	BSA
<i>ApaI</i>	NEBuffer 4	25°C	yes
<i>BamHI</i>	NEBuffer 3	37°C	yes
<i>HindIII</i>	NEBuffer 2	37°C	no
<i>PstI</i>	NEBuffer 3	37°C	yes
<i>XbaI</i>	NEBuffer 2	37°C	yes

3.5 Agarose gel electrophoresis

1.5% agarose gels were prepared as follows: 0.9 g of agarose were added to 60 ml of 1 x TBE. The solution was boiled until all the agarose was completely dissolved. Ethidium bromide was added to give a final concentration of 0.5 µg/ml and the cooled to ~ 60°C before pouring it into the gel chamber. Upon polymerisation, gels were placed into a gel electrophoresis apparatus (Peqlab, Erlangen, Germany) and filled with 1 x TBE ensuring that it was completely covered in buffer. The DNA samples were mixed with 10 x agarose gel sample buffer and 15 µl were loaded into each well. In addition to samples, a DNA marker (1 kb DNA ladder, Fermentas, St. Leon-Rot, Germany) was run as an indicator of molecular weight. Gels were electrophoresed at

80 V for approximately 1 h. Gels were examined under ultraviolet light at 302 nm using an UV-transilluminator (LTF Labortechnik, Wasserburg, Germany).

3.6 DNA sequencing

Sequencing of DNA was performed using the Big Dye Terminator sequencing mix and appropriate primers (Table 5). After the PCR (Table 6), sequencing products were purified and precipitated with ethanol. Briefly, the PCR mixture was mixed with 2 μ l 1.5 M sodium acetate / 250 mM EDTA buffer before adding 80 μ l of 95% ethanol. The mixture was incubated on ice for 20 min and then spun at 13,000 rpm for 15 min. Supernatants were removed and DNA pellets were mixed with 400 μ l of 70% ethanol. The samples were centrifuged again (13,000 rpm, 5 min), the supernatants removed and the DNA pellets air-dried.

For capillary electrophoresis in the ABI Prism 310 Genetic Analyzer (Perkin Elmer, USA), DNA pellets were dissolved in loading dye, incubated for 15 min and mixed by vortexing. Sequencing data analysis was performed with the DNASTAR SeqMan Pro software (DNASTAR Inc, USA.).

Table 5. DNA sequencing primers

primer	forward (5'→3')	reverse (5'→3')
BS1	CCGTGCCAAGGACCCATC	GATGGGTCCTTGGCAC
BS2	GGAATCACTGTG	CACAGTGATTCC
BS3	GACCTGTGAAATGTTGAG	CTCAACATTTACAGGTC
BS4	GGTGAGCAAAAGATTCAA	TTGAATCTTTTGCTCACC
T7	TAATACGACTCACTATAGGG	

Table 6. DNA sequencing PCR

Template	300 ng	<u>94°C – 1 min</u>	
Big Dye Terminator	2.5 μ l	94°C – 16 s	
Half Dye	5 μ l	52°C – 16 s	29 cycles
primer (5 μ M)	2 μ l	60°C – 2 min	
dH ₂ O	ad 20 μ l		

3.7 Cell culture

Primary cultures of newborn rat aortic vascular smooth muscle (VSM) cells (H.P. Reusch, University of Bochum, Germany) were grown in MEM Earl's medium (Biochrom, Berlin, Germany) supplemented with 10% FCS, 2% tryptose phosphate broth, 4 mM glutamine, 100 U/ml penicillin and 100 μ g/ml streptomycin.

HEK293 cells (DMSZ, Braunschweig, Germany) were grown in DMEM (Sigma-Aldrich, Steinheim, Germany) supplemented with 10% FCS, 4 mM glutamine, 100 U/ml penicillin and 100 µg/ml streptomycin.

MDCK cells (G. Papsdorf, Leibniz-Institut für Molekulare Pharmakologie, Berlin, Germany) stably expressing the full-length or glycosylation-deficient ET_B receptor were grown in DMEM (Sigma-Aldrich, Steinheim, Germany) supplemented with 10% FCS, 100 U/ml penicillin, 100 µg/ml streptomycin and 0.4 mg/ml G-418.

COS7 cells (ATCC, USA) were grown in DMEM with 4.5 g/l glucose supplemented with 10% FCS, 4 mM glutamine, 100 µg/ml streptomycin, and 100 U/ml penicillin.

All cells, except for COS7 cells, were grown in T75 flasks at 37°C with 5% CO₂. COS7 cells were grown at 7% CO₂.

3.8 Passaging of cells

The cells were passaged every 3-4 days. Briefly, the medium was aspirated off and cells were washed with 10 ml of 1 x PBS. 2 ml of 1 x trypsin/EDTA were added to the cells and incubated at 37°C until cells detached. Adding fresh FCS-containing medium stopped the reaction. Detached cells were transferred to a new cell culture flask already containing medium and incubated as described previously.

3.9 Transient transfection of cells

Confluent HEK293 and COS7 cells were transfected with the different DNA constructs (Table 7) using a Fugene6 transfection reagent (Roche Applied Science, Mannheim, Germany) following the manufacturer's instructions. The amounts of plasmid DNA and Fugene6 reagent used are summarised in Table 8.

Table 7. DNA plasmids used for transient transfection

name	plasmid	source
caveolin-1	caveolin-1.CFP caveolin-1.YFP	AG Oksche, Berlin, Germany
EGFR	EGFR.CFP EGFR.YFP	AG Oksche, Berlin, Germany
ET _B receptor	ET _B .GFP ET _B .CFP ET _B .cDNA ΔGlc.ET _B .GFP Δ2-64.ET _B .GFP Δ2-64.ET _B .cDNA ET _B .GFP.cav2 ΔGlc.ET _B .GFP.cav2	AG Oksche, Berlin, Germany
PIK3-kinase	p101/p110γ	AG Schaefer, Berlin, Germany
EGFR ligands	amphiregulin.AP betacellulin.AP EGF.AP epiregulin.AP HB-EGF.AP TGF-α.AP	S. Higashiyama, Japan

Table 8. Amounts of plasmid DNA and Fugene used for transient transfection

dish	plasmid DNA (μg)	Fugene6 (μl)
35 mm	1	2
60 mm	4	8
100 mm	6	12
6 well	1/well	2/well

3.10 Generation of MDCK cell clones stably expressing ET_B receptor constructs

MDCK cells were grown in 35-mm dishes until 90% confluency. Cells were then transfected with ET_B.GFP or ΔGlc.ET_B.GFP using the transfection reagent Fugene6 (Roche Applied Science, Mannheim, Germany) according to the manufacturer's protocol. After 48 h, cells were transferred to 60-mm dishes and grown in medium supplemented with G-418 (0.4 mg/ml). The medium was changed every day. After one week a dilution series of the remaining cells was grown in 24-well plates. The G-418 medium was changed every second day. After two weeks, single colonies of fluorescent cell clones were picked and grown for further experiments.

3.11 RNA extraction

RNA was extracted from cells using the RNeasy Mini Kit (Qiagen, Hilden, Germany) following the spin protocol for the 'Isolation of Total RNA from Animal Cells' provided by the manufacturer.

3.12 cDNA synthesis

Complementary DNA (cDNA) was synthesised from 1 µg RNA using the AMV (avian myeloblastosis virus) Reverse Transcriptase Kit (Invitrogen, Leek, Netherlands) following the manufacturer's instructions.

3.13 Caveolae preparation

For preparation of caveolae, COS7 cells and MDCK cells stably expressing ET_B.GFP or ΔGlc.ET_B.GFP were grown in 100-mm dishes until confluency. COS7 cells were transfected with the ET_B receptor constructs as indicated. After starving the cells in serum-free culture medium overnight, caveolae were prepared as described (Smart et al., 1995). Upon washing the cells twice with buffer A they were pelleted and homogenised in buffer A by repetitively (20 times) passing through a 23 G syringe followed by 20 strokes in a glass-teflon homogenisator at 850 rpm (Braun Biotech, USA). After centrifugation (1000 x g, 10 min, 4°C) the post-nuclear supernatant was separated on a 30% Percoll gradient by centrifugation (84,000 x g, 30 min, 4°C) in a Beckman Coulter Optima LE-80K ultracentrifuge (Krefeld, Germany). The plasma membrane fraction was sonicated 6 x 15 s at 70% power (Bandelin Sonopuls, Berlin, Germany) before it was separated on a 10-20% Optiprep (Axis-Shield, Norway) gradient by centrifugation (52,000 x g, 90 min, 4°C) in a Beckman Coulter Optima LE-80K ultracentrifuge (Krefeld, Germany). The top 5 ml of the gradient were mixed with buffer C and overlaid with 5% Optiprep. After another centrifugation step (52,000 x g, 90 min, 4°C), 1 ml fractions were collected and used for subsequent immunoblot analysis and binding studies.

3.14 ET-1 binding analysis

The distribution of ET_B receptor constructs within caveolae-containing fractions was analysed by binding analysis essentially as described before (Oksche et al., 2000). Briefly, 250 µl of each gradient fraction were incubated in a final volume of 500 µl Tris/BAME buffer containing 100 pM ¹²⁵I-ET-1 alone (total binding) or in presence of 1 µM unlabelled ET-1 (unspecific binding) in a shaking water bath at 25°C for 2 h. The samples were transferred onto polyethylenimine-treated GF/C filters (Whatman, Dassel, Germany) and washed twice with PBS using a Brandell cell harvester. Filters were transferred into 5-ml vials, and radioactivity was determined by liquid scintillation counting. Specific binding was calculated by subtracting unspecific binding from total binding.

3.15 Microarray analysis

VSM cells were grown in 100-mm dishes until confluency, serum-starved, treated with 200 ng/ml PTX for 24 h and then stimulated with 2 U/ml thrombin or 25 µM TRAP as indicated. Total RNA of VSM cells was extracted as described in Chapter 3.11. Hybridisation to the Affymetrix Rat Genome 230 2.0 GeneChip (Affymetrix, USA) was performed in collaboration with the Huebner group at the Max-Delbrück-Center in Berlin following the manufacturer's protocols. Confidence analysis was applied to datasets of untreated VSM cells representing means of two independent experiments each. Genes were sorted and grouped according to their expression intensity, and expression-stratified confidence intervals were obtained by calculating means and S.D. of the inter-experimental expression variations for groups of 500 genes, each. Confidence intervals of $p < 0.05$ and $p < 0.003$ were assumed to correspond to expression variations that exceed the S.D. by the 2- and 3-fold, respectively. Confidence analysis was used for the interpretation of raw data files.

3.16 Semi-quantitative multiplex RT-PCR

VSM cells were grown in 60-mm dishes until confluency. Cells were serum-starved overnight, stimulated with thrombin (2 U/ml) or TRAP (25 µM) as indicated. Pre-treatment of cells with pertussis toxin (200 ng/ml) for 24 h was performed as indicated. Total RNA of VSM cells was prepared and reverse transcribed as described (Chapter 3.11-3.12). PCR primers were selected based on published gene sequences for *rattus norvegicus*. Primers used and their characteristics

are summarised in Table 9. For each set of primers a specific PCR protocol (Table 10) was used. PCR was run in a Biometra TRIO-Thermoblock PCR machine (Göttingen, Germany). Amplified products were analysed and stained on a 1.5% agarose gel containing 0.002% ethidium bromide. Quantitative analysis of signals was performed with a fluorescence imaging system (Fujifilm LAS-1000, Straubenhardt, Germany). Signal intensities were corrected for background signals and evaluated using TINA 2.09 software (Raytest, Straubenhardt, Germany).

Table 9. Primers for multiplex PCR and their properties

fragment	target mRNA	forward primer (5'→3')	reverse primer (5'→3')	size (bp)
GAPDH	AF106860	TTA GCC CCC CTG GCC AAG G	CTT ACT CCT TGG AGG CCA TG	541
amphiregulin	NM_017123	CCG CGG AAC CAA TGA GAA C	GAA GCA GGA CGG CGG TAA TG	656
ADAMTS-1	NM_024400	CGC CCC ACG GAG GAA GAC	CCG CCG CCT TCG CCT CAG	431
TIMP-1	NM_053819	ACC GCA GCG AGG AGT TTC TC	GTG GCA GGC AGG CAA AGT GA	272
MAP3K8	NM_053847	CAC CGG AAG CGA CGA GAA AG	GGC CCC TGC ACA GAA TCA C	895
COX-2	NM_017232	GCC CAC CCC AAA CAC AGT A	GGA AGG GCC CTG GTG TAG	212

Table 10. PCR protocols

gene	initial denaturation	denaturation	annealing	extension	final extension	amplification cycles
amphiregulin	94°C, 2 min	94°C, 30 s	58°C, 30 s	72°C, 40 s	72°C, 7 min	33
ADAMTS-1	94°C, 2 min	94°C, 30 s	58°C, 30 s	72°C, 25 s	72°C, 7 min	30
TIMP-1	94°C, 2 min	94°C, 30 s	60°C, 30 s	72°C, 20 s	72°C, 7 min	22
MAP3K8	94°C, 2 min	94°C, 30 s	58°C, 30 s	72°C, 55 s	72°C, 7 min	30
COX-2	94°C, 2 min	94°C, 30 s	55°C, 30 s	72°C, 15 s	72°C, 7 min	30

3.17 SDS-PAGE and immunoblotting

The apparatus for pouring and running SDS-Pages was obtained from Bio-Rad (Mini-Protean 3 system, Bio-Rad, München).

7.5% or 10% acrylamide resolving gels were prepared using the values given in Table 11. The acrylamide solution was carefully overlaid with 20% isopropanol to prevent oxygen from diffusing into the gel. After polymerisation of the gel, the overlay was removed and a 4% polyacrylamide stacking gel prepared using the values given in Table 12. After polymerisation, the gel was mounted in the electrophoresis apparatus. 1 x SDS running buffer was added to the top and bottom reservoirs before applying the samples.

Table 11. Solutions for preparing a 10% or 7.5% resolving gel

component	10%	7.5%
dH ₂ O	3.05 ml	3.675 ml
1.5 M Tris, pH 8.8	1.85 ml	1.85 ml
20% SDS	37.5 μ l	37.5 μ l
30% acrylamide/bis	2.5 ml	1.875
10% APS	37.5 μ l	37.5 μ l
TEMED	5 μ l	5 μ l

Table 12. Solutions for preparing a 4% stacking gel

component	4%
dH ₂ O	2.25 ml
0.5 M Tris, pH 6.8	0.95 ml
20% SDS	20 μ l
30% acrylamide/bis	0.5 ml
10% APS	37.5 μ l
TEMED	5 μ l

Samples to be analysed were diluted in 5 x SDS reducing sample buffer and incubated at 95°C in a Thermomixer 5436 (Eppendorf, Hamburg, Germany) for 5 min. Samples were cooled on ice for 5 min, and up to 25 μ l (depending on the experiment) were loaded into the wells. 5 μ l of a Precision Plus Dual Color Protein Standard (Bio-Rad, München, Germany) were run to monitor protein separation. Gels were run at 20 mA/gel. Separated proteins were transferred to Hybond ECL nitrocellulose membranes (Amersham Pharmacia, Freiburg, Germany) by tank blotting for 90 - 150 min at 100 mA/gel in 1 x SDS transfer buffer. Membranes were blocked in blocking solution for 1 h at room temperature and incubated with primary antibodies (diluted in blocking solution) at 4°C overnight. After washing the membranes three times for 10 min in TBS/Tween buffer, they were incubated with a horseradish peroxidase-coupled secondary antibody (diluted in blocking solution) for 1 h at room temperature. After another washing step (3 x 10 min in TBS/Tween buffer), proteins were detected by adding a chemiluminescent substrate (Applichem, Darmstadt, Germany).

3.18 Immunoblot analysis of whole-cell lysates

Cells were grown in 35-mm dishes until confluency. Cells were transfected as described (Chapter 3.9), serum-starved overnight, stimulated as indicated, and lysed in Laemmli buffer. Whole-cell lysates were subjected to SDS-PAGE and immunoblotting (Chapter 3.17), and probed with the antibodies shown in Table 13 following the manufacturer's instructions. Primary antibodies were detected with a horseradish peroxidase-coupled secondary antibody using a

chemiluminescent substrate (Applichem, Darmstadt, Germany). For densitometry, a cooled CCD camera (Fujifilm LAS-1000, Straubenhardt, Germany) was used. Band intensities were corrected for background signals and evaluated using TINA 2.09 software (Raytest, Straubenhardt, Germany).

Table 13. Antibodies

antibody	synonym	company	dilution
Phospho-p44/42 MAP kinase (Thr202/Tyr204)	pERK1/2	Cell Signaling, USA	1:1000
p44/42 MAP kinase	ERK1/2	Cell Signaling, USA	1:1000
amphiregulin (H-155)		Santa Cruz Biotechnology, USA	1:200
ADAMTS-1 (H-60)		Santa Cruz Biotechnology, USA	1:200
TIMP-1		Acris, Herford, Germany	1:200
MAP3K8	Tpl2/Cot	Aviva, USA	1:400
COX-2		Cayman, USA	1:200
Phospho Akt (Ser473)		Cell Signaling, USA	1:1000
Akt		Cell Signaling, USA	1:1000
GFP		BD Biosciences, Heidelberg, Germany	1:1000
Anti-rabbit IgG (HRP)		Sigma-Aldrich, Steinheim, Germany	1:2000
Anti-mouse IgG (HRP)		Sigma-Aldrich, Steinheim, Germany	1:2000

3.19 Immunoblot analysis of caveolae-containing fractions

Aliquots of each fraction from the caveolae preparation were concentrated by TCA precipitation (5% TCA for at 4°C for 1 h). The pellet was washed in 250 µl acetone twice. After drying, pellets were resuspended in Laemmli buffer and subjected to SDS-PAGE and immunoblotting (Chapter 3.17). Caveolae-containing fractions were detected using an anti-caveolin-1 antibody (1:400, Santa Cruz Biotechnology, USA). The primary antibody was detected with an anti-rabbit horseradish peroxidase-coupled secondary antibody (1:2000, Cell Signaling, USA) using a chemiluminescent substrate (Applichem, Darmstadt, Germany). A cooled CCD camera (Fujifilm LAS-1000, Düsseldorf, Germany) was used to image the signal intensities.

3.20 Ectodomain shedding

Alkaline phosphatase (AP)-tagged precursor proteins of amphiregulin, betacellulin, EGF, epiregulin, HB-EGF and TGF- α (Tokumaru et al., 2000; Sahin et al., 2004) were transiently expressed in COS7 or HEK293 cells to investigate the ectodomain shedding of these EGFR ligands. The shedding assay was performed essentially as described before (Sahin et al., 2006): cells were grown in 6-well plates until 70% confluency. Cells were transfected with the ET_B

receptor constructs and AP-tagged EGFR ligands as indicated. After serum-starving cells overnight, 1 ml fresh serum-free culture medium was given to each well. After 1 h incubation at 37°C the supernatants were collected. Cells were then stimulated with 100 nM IRL1620 or 1 µM PMA for 1 hour at 37°C, and supernatants were collected again. 100 µl of the supernatants were transferred to a 96-well plate and mixed with 100 µl of 2 mg/ml 4-NPP. After incubation for 1 h at 37°C the absorbance was measured at 405 nm in a Multiskan MCC 340 plate reader (Titertek, USA).

3.21 Total internal reflection fluorescence microscopy

COS7 and MDCK cells were grown on coverslips in 35-mm dishes until 70% confluency. The following day COS7 cells were transfected with plasmids encoding for caveolin-1 (coupled to YFP or CFP), for the EGFR (coupled YFP or CFP) or ET_B receptor subtypes (coupled to GFP) as indicated. Total internal reflection fluorescence microscopy (TIRFM) was carried out with a prismless TIRF imaging system as described previously (Axelrod, 2003). For single excitation of GFP or YFP the 488 nm line of an Ar⁺-laser (Lasos GmbH, Ebersberg, Germany) was selected. Fluorescent light was detected using a 514 nm Razor Edge long pass filter (Semrock, Rochester, USA). Image acquisition was performed with a back-illuminated EMCCD camera (iXon DV887, Andor, Belfast, United Kingdom) using TillVision software (TILL Photonics, Gräfelfing, Germany).

For detection of co-localisation, CFP or GFP were excited with the 458-nm laser line using a 458-nm dichroic mirror. Fluorescence was detected through a 490/30 band pass filter (Chroma, Münster, Germany). Excitation of YFP or Alexa 555 (see Chapter 3.22) was performed using the 514-nm laser line and a 514-nm dichroic mirror, YFP-fluorescence was detected using a 514-nm Razor Edge long pass filter. Image acquisition was performed with a cooled CCD camera (Imago, TILL Photonics, Gräfelfing, Germany) using TillVision software (TILL Photonics, Gräfelfing, Germany).

3.22 Immunofluorescence

HEK293 and COS7 cells were grown on coverslips in 35-mm dishes until confluency. Cells were transfected with AP-coupled EGFR ligands and caveolin-1 as indicated and incubated overnight. Upon serum-starving the cells overnight, they were washed with warm PBS twice and

with room temperature PBS thrice. Cells were fixed in Fixans at room temperature for 15 min. After washing cells 3 x for 2 min with ice cold PBS, they were permeabilised in permeabilisation buffer for 3 min. Cells were washed again in ice-cold PBS thrice and then blocked in blocking buffer at 37°C for 20 min. The primary antibody detecting alkaline phosphatase (ALPP, Lifespan Biosciences, USA) was diluted 1:100 in PBS and 50 µl carefully poured onto the cells. Cells were incubated at 37°C for 45 min before washing them 3 x for 5 min in ice cold PBS. The secondary Alexa Fluor 555 goat-anti-rabbit IgG antibody (Invitrogen, USA) was diluted 1:100 in PBS and carefully poured onto the cells. After an incubation for 45 min at 37°C, cells were washed 3 x 5 min in ice cold PBS and subjected to TIRFM (Chapter 3.21).

3.23 Confocal microscopy

For confocal microscopy, an inverted confocal laser scanning microscope (LSM 510META; Carl Zeiss, Jena, Germany) and a Plan-Apochromat 63x/1.4 objective were used. GFP was excited with the 488 nm line of an argon laser and detected through a 505 nm long pass filter. Pinholes were adjusted to yield optical sections of 0.8–1.4 µm. All experiments were performed 24 h after transfection at room temperature in 10 mM HEPES, pH 7.4, 128 mM NaCl, 6 mM KCl, 1 mM MgCl₂, 1 mM CaCl₂, 5.5 mM glucose, and 0.2% bovine serum albumin.

3.24 Calcium measurements

For measurements of intracellular calcium, cells were seeded on glass coverslips, loaded with 3 µM fura-2/AM (Molecular Probes) for 30 min at 37 °C and mounted onto the stage of an inverted microscope (Axiovert 100, Carl Zeiss). Cells were sequentially excited at 340 nm, 358 nm, 380 nm, and 470 nm with a monochromatic light source (Polychrome IV, TILL Photonics, Gräfelfing, Germany). A 505 nm dichroic mirror combined with a 510 nm long pass filter, a 40x/1.3 F-Fluar objective, and a cooled CCD camera (Imago SVGA Sensicam, TILL Photonics/PCO) were used for imaging. Fluorescent signals of GFP, calcium-free and calcium-bound Fura-2 were separated by a linear unmixing procedure applying multivariate linear regression analysis, and calcium concentrations were determined as described previously (Lenz et al., 2002).

4 Results

4.1 ET_B receptor localisation and downstream signalling

4.1.1 Characterisation of endothelin B receptor constructs

To analyse the localisation and downstream signalling of the ET_B receptor various plasmids encoding GFP tagged ET_B receptor variants were generated: a full-length ET_B receptor (ET_B.GFP), an N-terminally truncated ET_B receptor (Δ 2-64.ET_B.GFP), a glycosylation-deficient ET_B receptor (Δ Glc.ET_B.GFP) as well as a full-length and glycosylation-deficient ET_B receptor fused to caveolin-2 (ET_B.GFP.cav2 and Δ Glc.ET_B.GFP.cav2, respectively). To confirm the plasma membrane targeting of the ET_B receptor constructs in COS7, HEK293 and MDCK cells, laser-scanning microscopy was performed (Fig. 13).

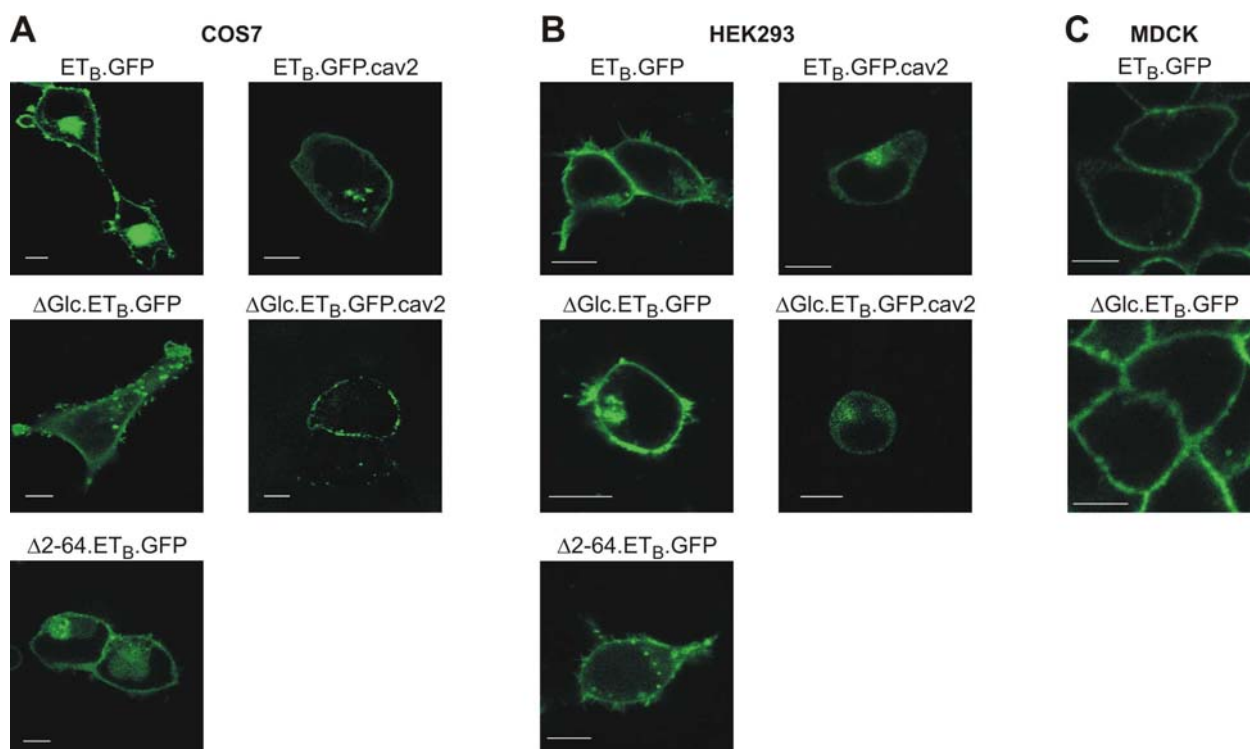


Fig. 13. Plasma membrane integration of ET_B receptor constructs. COS7 (A), HEK293 (B) and MDCK (C) cells expressing ET_B.GFP, Δ Glc.ET_B.GFP, Δ 2-64.ET_B.GFP, ET_B.GFP.cav2 or Δ Glc.ET_B.GFP were analysed by confocal microscopy. Representative images are shown. Bar: 10 μ m.

All receptor constructs, except the ET_B receptors fused to caveolin-2, mainly localised to the plasma membrane of COS7, HEK293 and MDCK cells. The additional C-terminal fusion to caveolin-2 resulted in a less pronounced surface expression of ET_B receptors in COS7 and HEK293 cells.

The receptor expression was further determined by equilibrium binding analysis in plasma membrane-enriched membrane preparations of transfected COS7 cells (Table 14). The results demonstrated an about 2-fold variation between all ET_B receptor constructs, except for the caveolin-2-fused full-length ET_B receptor, which had a lower B_{max} (receptors/cell). It can be concluded that the 4-fold difference in B_{max} is mostly due to the decreased surface targeting of the ET_B.GFP.cav2 construct, whereas all other constructs are expressed at the plasma membrane in similar amounts.

Table 14. ET_B receptor expression in COS7 cells

construct	B _{max} (receptors/cell)
ET _B .GFP	54 600
ΔGlc.ET _B .GFP	30 600
Δ2-64.ET _B .GFP	26 700
ET _B .GFP.cav2	12 100
ΔGlc.ET _B .GFP.cav2	26 700

To find out whether a certain cell type has an effect on the glycosylation pattern or N-terminal processing of the ET_B receptor, whole cell lysates from COS7, HEK293 and MDCK cells expressing ET_B receptor variants were subjected to Western blot analysis (Fig. 14).

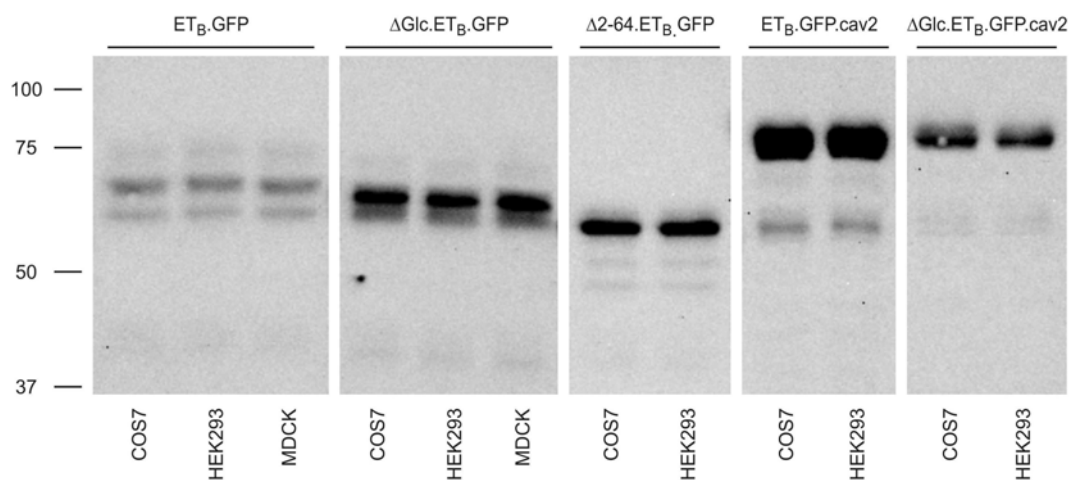


Fig. 14. ET_B receptor expression in different cell types. Whole cell lysates of COS7, HEK293 or MDCK cells expressing ET_B.GFP, ΔGlc.ET_B.GFP, Δ2-64.ET_B.GFP, ET_B.GFP.cav2 or ΔGlc.ET_B.GFP.cav2 were subjected to immunoblot analysis applying an anti-GFP antibody.

All receptor constructs detected an immunoreactive band at ~ 60 kDa. As can be seen for the $\Delta 2$ -64.ET_B.GFP, this band represents the N-terminally truncated ET_B receptor. When the full-length ET_B.GFP is expressed in these cells, a further protein band of about 70 kDa is detected representing the uncleaved ET_B receptor. This band shifts to ~ 65 kDa when the glycosylation site is absent (Δ Glc.ET_B.GFP). Fusion of the 22 kDa protein caveolin-2 to the full-length and glycosylation-deficient ET_B receptor (ET_B.GFP.cav2 and Δ Glc.ET_B.GFP.cav2, respectively) results in a protein size of ~ 90 kDa. The results demonstrate that the ET_B receptor variants show similar sizes and glycosylation patterns between the cell types they were investigated in.

It was further analysed whether the ET_B receptor constructs differ in their early downstream signalling. The ET_B receptor couples to the G_i-family of heterotrimeric G proteins. The G $\beta\gamma$ -induced downstream signalling was assessed by determining PLC β -mediated phosphoinositide hydrolysis causing increases in the intracellular Ca²⁺ concentrations in Fura-2-loaded HEK293 cells expressing the respective receptor variant. A similar transient increase in cytosolic Ca²⁺ was observed for all ET_B receptor constructs (Fig. 15).

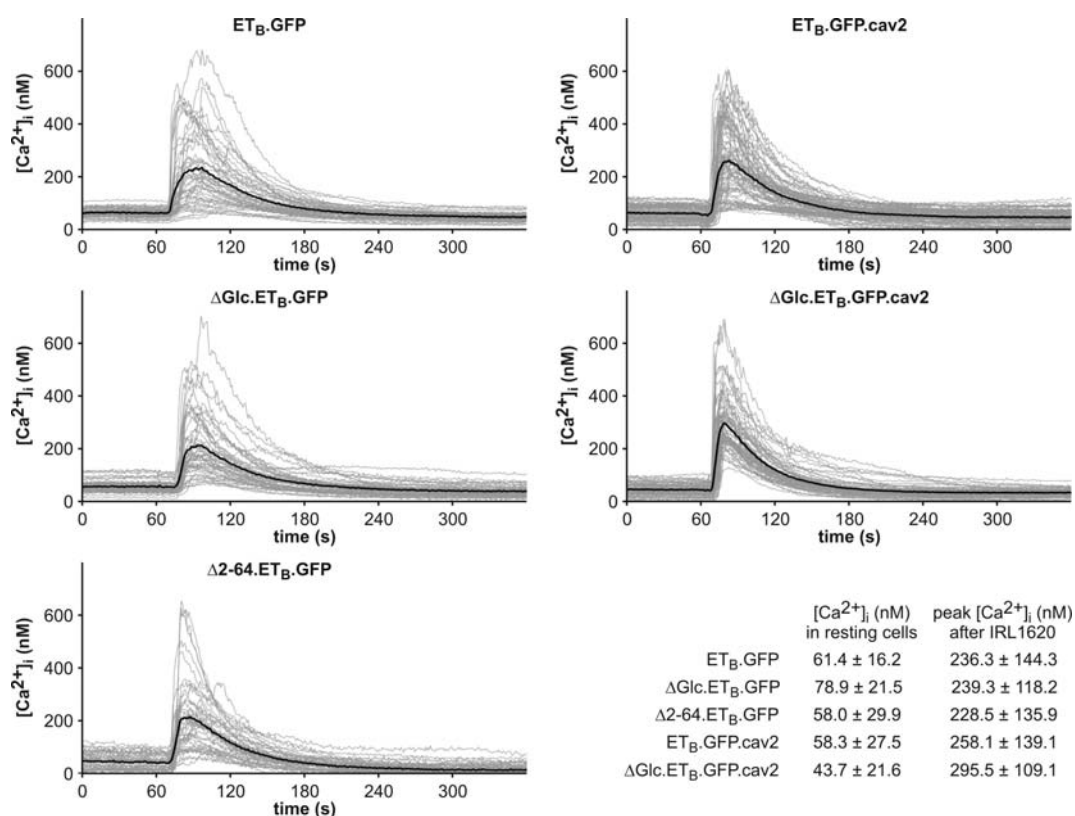


Fig. 15. ET_B receptor-induced Ca²⁺ elevation. Intracellular Ca²⁺ concentrations ([Ca²⁺]_i) were determined before and after stimulation with the ET_B receptor agonist IRL1620 (100 nM) in fura-2-loaded HEK293 cells. [Ca²⁺]_i data represent means \pm S.D. of 45-95 single cells that were identified to express the respective GFP-fused receptor construct. Correction of spectral interferences arising from GFP expression and calibration of [Ca²⁺]_i signals was achieved spectroscopically by a linear unmixing procedure.

The signalling towards the PI3K-Akt/PKB pathway was also tested in COS7 cells that were co-transfected with the respective ET_B receptor variants and expression plasmids encoding the Gβγ-sensitive PIK3-kinase γ (p101/p110γ) (Fig. 16). Stimulation of the transiently transfected COS7 cells resulted in a phosphorylation of Akt on Ser⁴⁷³ for all ET_B receptor constructs. The effect was, however, less pronounced when the ET_B receptor lacked its glycosylation site or was N-terminally truncated.

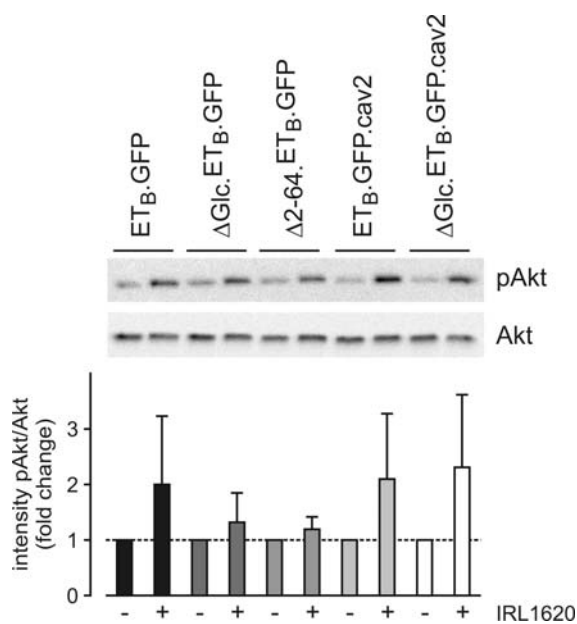


Fig. 16: ET_B receptor-mediated Akt phosphorylation. Serum-starved COS7 cells expressing the distinct ET_B receptor constructs as indicated were stimulated with 100 nM IRL1620 for 5 min. Activated Akt was detected with an anti-phospho-Akt antibody. Total Akt was detected with an anti-Akt antibody. Graphs depict means and S.E. of at least 3 independent experiments.

4.1.2 Localisation of endothelin B receptor constructs to caveolae

Activation of the full-length ET_B receptor leads to a long-lasting activation of ERK1/2 whereas the stimulated N-terminally truncated ET_B receptor triggers a short-term phosphorylation of ERK1/2 (Grantcharova et al., 2002; Grantcharova et al., 2006a; Grantcharova et al., 2006b). The localisation of the two ET_B receptor variants may account for these differences. A full-length (ET_B.GFP), N-terminally truncated (Δ2-64.ET_B.GFP) and a full-length but glycosylation-deficient (ΔGlc.ET_B.GFP) ET_B receptor construct were used to address this question. Furthermore, the caveolae marker protein caveolin-2 was fused to the full-length and to the glycosylation-deficient ET_B receptor (ET_B.GFP.cav2 and ΔGlc.ET_B.GFP.cav2 respectively), which results in the direct targeting of a GPCR to caveolae (Guzzi et al., 2002).

Caveolae-containing fractions of plasma membranes from COS7 and MDCK cells expressing the various ET_B receptor constructs were identified performing Western blot analysis detecting caveolin-1, a major marker protein of caveolae (Fig. 17). Due to their high amount in lipids, caveolae float on top of a density gradient. Caveolin-1 was highly enriched in those low density fractions 1-3. HEK 293 cells were not included in this study as they do not form naturally occurring caveolae due to a lack of caveolin-1 (Fig. 18).

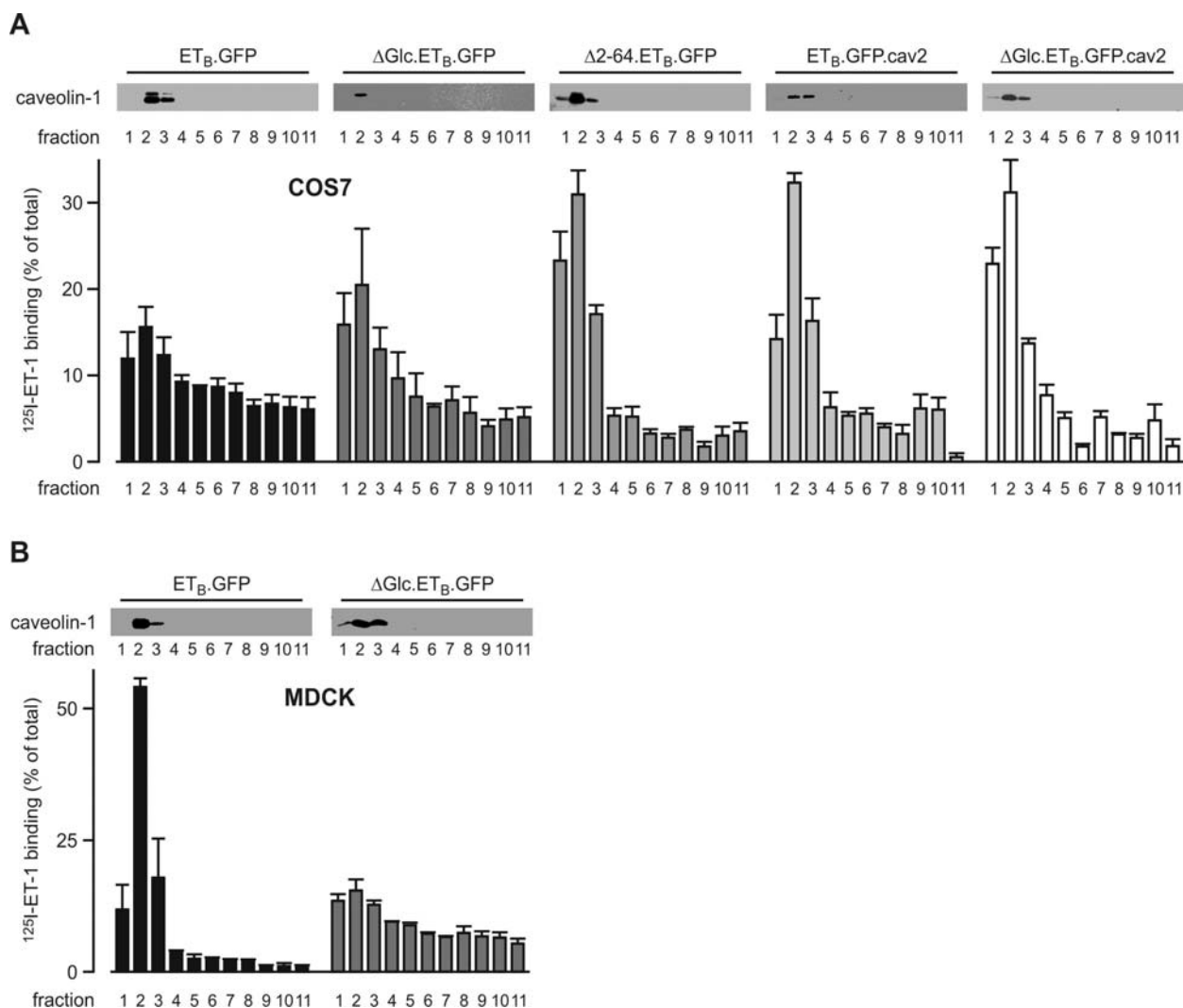


Fig. 17. Localisation of ET_B receptor constructs in COS7 and MDCK cells. Serum-starved COS7 (**A**) and MDCK (**B**) cells expressing the ET_B receptor constructs as indicated were subjected to detergent-free caveolae preparation. Gradient fractions are numbered according to their densities (1 = light fraction, 11 = dense fraction). The distribution of caveolae was determined by Western blot analysis detecting the caveolae marker protein caveolin-1. Binding analysis with ¹²⁵I-ET-1 identified the ET_B receptor constructs present in the different fractions. Graphs depict means and S.E. of at least 3 independent experiments.

To verify equal receptor expression within the caveolae preparations in COS7 and MDCK cells, the receptor expression was calculated and ranged between 12 000 and 54 000 receptors/cell (Table 14) in all experiments. ET-1 binding analysis in single fractions of the density gradient revealed different distribution patterns for the distinct ET_B receptor constructs.

In COS7 cells, the ET_B.GFP receptor and the glycosylation-deficient ET_B receptor were evenly distributed over the plasma membrane, whilst 71.3% of the N-terminally truncated Δ 2-64.ET_B.GFP were enriched in the low density fractions 1-3. When fused to caveolin-2, the full-length and glycosylation-deficient ET_B receptors were enriched in caveolin-1-containing fractions (Fig 17A). Therefore, fusion of caveolin-2 to the ET_B receptor is a good means to artificially target the receptor into caveolae. In MDCK cell lines stably expressing ET_B.GFP or Δ Glc.ET_B.GFP (Fig. 17B), 83.6 % of the plasma membrane expressed ET_B.GFP were enriched in caveolae-containing fractions, whereas the glycosylation-deficient Δ Glc.ET_B.GFP was spread all over the plasma membrane. Since the gel migration properties of ET_B receptor constructs expressed either in COS7, HEK293 or MDCK cells were almost indistinguishable (Fig. 14), it can be assumed that the different localisation patterns of ET_B.GFP or Δ Glc.ET_B.GFP in COS7 and MDCK cells were not caused by gross changes of the attached glycosyl moieties. Due to the low transfection efficiency in MDCK cells, the distribution of the N-terminally truncated and caveolae-targeted ET_B receptors could not be analysed in MDCK cells.

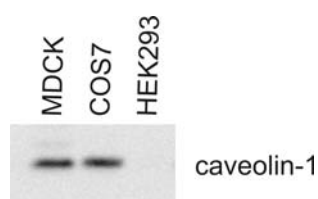


Fig. 18: Expression of caveolin-1 in MDCK, COS7 and HEK293 cells Caveolin-1 expression was detected in whole cell lysates of MDCK, COS7 and HEK293 cells with an anti-caveolin-1 antibody.

Total internal reflection fluorescence microscopy (TIRFM), a highly efficient technique to analyse the distribution of fluorescently tagged proteins within the plasma membrane, was performed to reassess the localisation of the distinct ET_B receptor constructs. Caveolin-1.YFP expression in COS7 and HEK293 shows a punctate pattern, which was used as a reference to recognise caveolae-localised ET_B receptors (Fig. 19A,B). Since, ET_B.GFP and Δ Glc.ET_B.GFP expressed in COS7 cells did not show a punctate pattern as seen for caveolin-1.YFP, these receptor constructs might be expressed throughout the plasma membrane. This pattern remained unchanged even when caveolin-1.YFP was overexpressed (Fig. 20A). By contrast, the N-

terminally truncated ($\Delta 2-64$.ET_B.GFP) and the artificially caveolae-targeted ET_B receptors (ET_B.GFP.cav2 and Δ Glc.ET_B.GFP.cav2) showed a punctate pattern similar to caveolin-1.YFP, suggesting an accumulation in caveolae (Fig. 19A), which is in good agreement with their accumulation as revealed by caveolae preparations (Fig. 17A).

It has been described that the expression of caveolin-1 in HEK293 cells can result in the formation of caveolae-like plasma membrane invaginations (Keren and Sarne, 2003). Accordingly, caveolin-1.YFP expressed in HEK293 cells gave rise to a punctate pattern (Fig. 19B). Only fusion of the ET_B receptors to caveolin-2 resulted in a receptor targeting into punctate structures (Fig. 19B). The full-length and the N-terminally truncated ET_B receptors displayed a more even distribution at the plasma membrane. This distribution was not affected by co-expression of caveolin-1.YFP (Fig. 20B), indicating that the ET_B receptor is not targeted to raft- or caveolin-like structures in HEK293 cells.

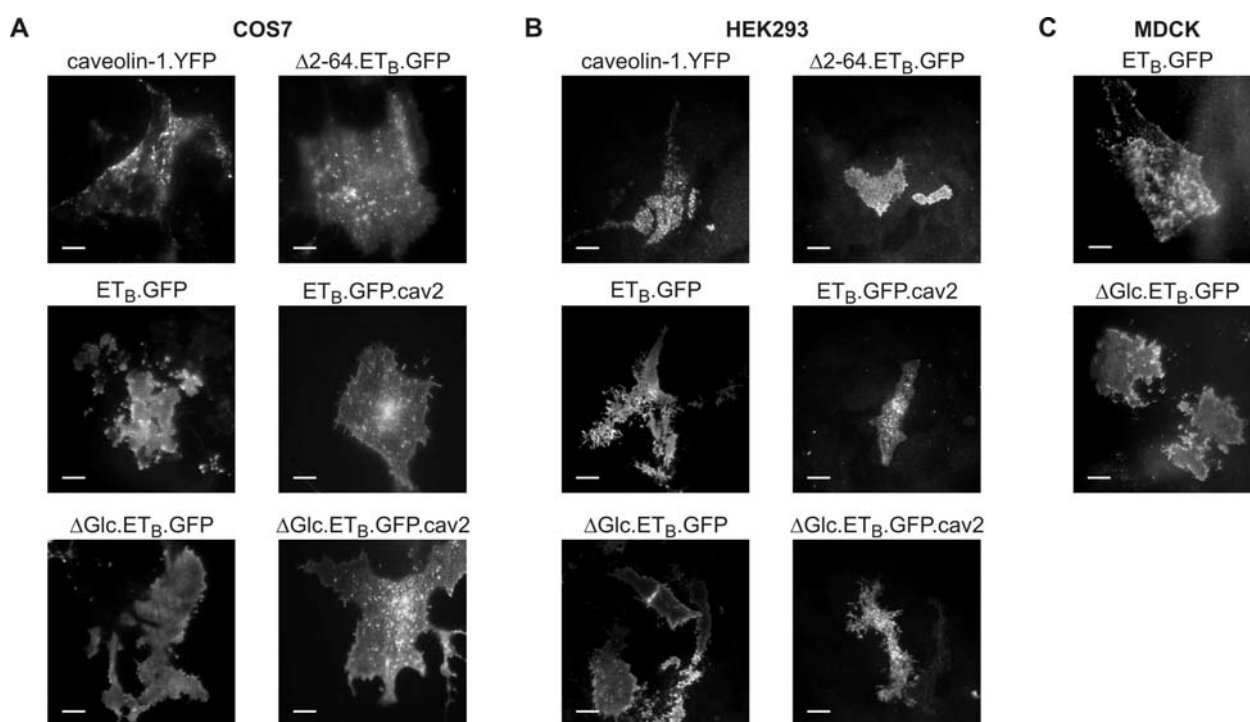


Fig. 19. TIRFM of ET_B receptor constructs reveals cell type-specific differences in their localisation. COS7 (A), HEK293 (B) and MDCK (C) cells expressing caveolin-1.YFP or the ET_B receptor constructs as indicated were grown on coverslips and excited with the 488-nm line of an Ar⁺ laser that was focused into the periphery of the back focal plane of a 100x/1.45 α -Plan Fluor objective to achieve a prismless TIR illumination. Receptor presence in caveolae was determined by comparing the distribution to that of caveolin-1 within the cell. Bar: 10 μ m.

MDCK cells stably expressing ET_B.GFP showed a punctate distribution indicating caveolar localisation (Fig. 19C). In contrast, the Δ Glc.ET_B.GFP receptor did not exhibit this pattern and, thus, is not enriched in or even excluded from caveolae. These results are again consistent with

the data obtained by fractionation analysis (Fig. 17B) and demonstrate that the organisation of full-length or proteolytically cleaved ET_B receptors in membrane microdomains occurs in a cell type-specific manner.

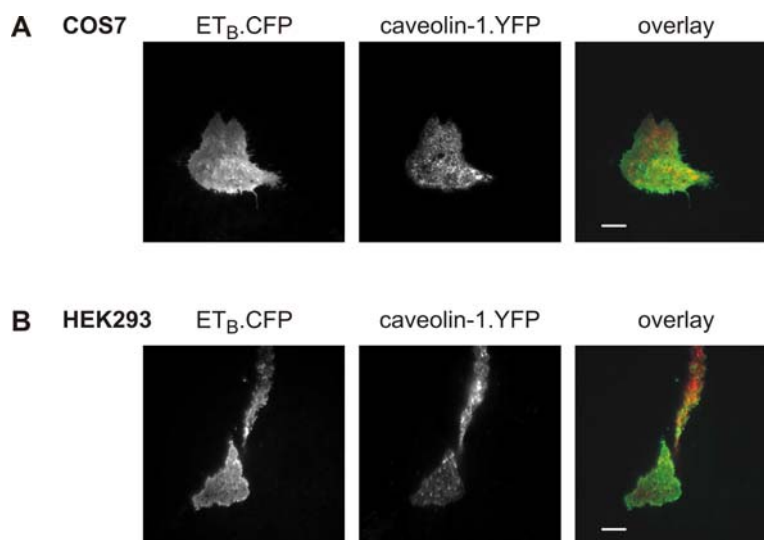


Fig. 20: The full-length ET_B receptor does not co-localise with caveolin-1 in COS7 and HEK293 cells. COS7 (A) and HEK293 (B) cells expressing caveolin-1.YFP and ET_B.CFP were grown on coverslips and imaged by two-colour TIRFM. YFP and CFP were sequentially excited with the 514 nm and 458 nm lines of an Ar⁺ laser, respectively. In the overlay pictures, YFP signals are displayed in the red channel, and CFP is depicted in green. Bar: 10 μm.

4.1.3 ET_B receptor-induced shedding of EGFR ligands

The triple membrane-spanning pathway, which results in the activation of ERK1/2 upon transactivation of the EGFR, is controlled by the shedding of EGFR ligands (Prenzel et al., 1999). The localisation of ET_B receptors could have an influence on this pathway. COS7 and HEK293 cells were co-transfected with the different ET_B receptor constructs and alkaline phosphatase (AP)-fused proforms of the EGFR ligands betacellulin, EGF, TGF- α , epiregulin, HB-EGF or amphiregulin (Tokumaru et al., 2000). Subsequently, the ET_B receptors were stimulated with 100 nM IRL1620, a specific ET_B receptor agonist, and the induced shedding of EGFR ligands analysed. Unfortunately, this experiment could not be performed in MDCK cells due to low transfection efficiencies.

Compared to the constitutive ectodomain shedding in unstimulated COS7 and HEK293 cells, the stimulation of the ET_B receptor constructs resulted in an increased shedding of some, but not all EGFR ligands (Fig. 21).

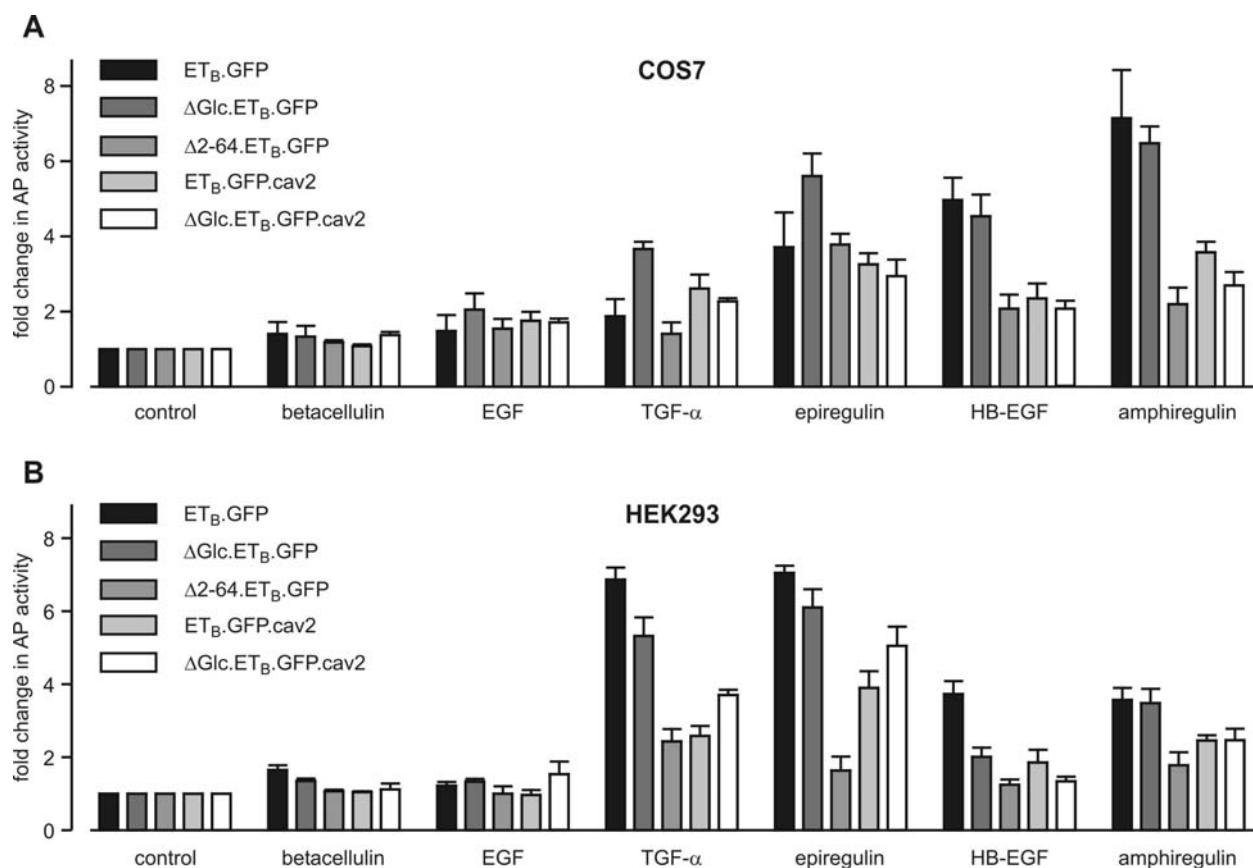


Fig. 21. ET_B receptor-induced ectodomain shedding of EGFR ligands in COS7 and HEK293 cells. COS7 (A) and HEK293 (B) cells were co-transfected with the ET_B receptor constructs and AP-fused proforms of EGFR ligands as indicated. After serum-starving the cells, ectodomain shedding of betacellulin, EGF, TGF- α , epiregulin, HB-EGF and amphiregulin was analysed before and after stimulation with 100 nM IRL1620 for 1 h. AP activity was measured in supernatants after adding the chromogenic AP substrate 4-nitrophenylphosphate. Unstimulated cells (serum-free medium only) were used to measure the constitutive shedding activity. Changes in absorbance between unstimulated and stimulated supernatants reflect fold change in AP activity compared to control. Graphs depict means and S.E. of at least 3 independent experiments.

In COS7 cells, a strong increase in EGFR ligand ectodomain shedding was observed for TGF- α , epiregulin, HB-EGF, and amphiregulin constructs. In contrast, the constitutive shedding of betacellulin and EGF was not changed upon stimulation of any of the ET_B receptor constructs (Fig. 21A). Stimulation of the non-caveolar full-length (ET_B.GFP) and glycosylation-deficient ET_B receptor (Δ Glc.ET_B.GFP; Fig. 17, Fig. 19), resulted in a 5- and 7- fold increase in shedding for HB-EGF and amphiregulin, respectively (Fig. 21A). In contrast, the caveolae-enriched N-terminally truncated (Δ 2-64.ET_B.GFP) and caveolae-targeted ET_B receptor constructs (ET_B.GFP.cav2 and Δ Glc.ET_B.GFP.cav2), exhibited a decreased shedding activity. Interestingly, only the Δ Glc.ET_B.GFP, but not the ET_B.GFP receptor or caveolae-localised ET_B receptors induced the shedding of TGF- α or epiregulin (Fig. 21A). Taken together, these data indicate that the ectodomain shedding of EGFR ligands is influenced by a caveolar localisation of the ET_B receptor in COS7 cells.

In HEK293 cells, stimulation of the distinct ET_B receptor constructs did not result in a shedding of betacellulin and EGF (Fig. 21B). In comparison to COS7 cells, the artificial targeting of ET_B receptors to caveolae did not have a pronounced effect on the shedding activity, which might result from the fact that HEK293 cells do not form caveolae without additional caveolin being transfected. Furthermore, stimulation of the N-terminally truncated ET_B receptor (Δ 2-64.ET_B.GFP) resulted in the weakest shedding signal for TGF- α , epiregulin, HB-EGF and amphiregulin (Fig. 21B), indicating that the N-terminal truncation of the ET_B receptor might result in reduced shedding activities in HEK293 cells. The shedding of TGF- α was only induced when the full-length ET_B receptor (ET_B.GFP) was stimulated. No such influences could be observed for the shedding of epiregulin, HB-EGF and amphiregulin (Fig. 21B). Taken together these results suggest an N-terminal truncation-dependent but localisation-independent shedding activity of ET_B receptors in HEK293 cells.

4.1.4 The EGFR and its ligands do not localise to caveolae

To investigate whether not only the localisation of the ET_B receptor but also the localisation of the EGFR and its ligands might account for different signalling events, co-localisation studies were performed in COS7 and HEK293 cells. Due to very low transfection levels, this experiment could not be performed in MDCK cells. The EGFR and all of its ligands were expressed in the plasma membrane of COS7 and HEK293 cells as revealed by TIRFM. Moreover, neither the EGFR (Fig. 22) nor its ligands (Fig. 23) co-localised with caveolin-1, the marker protein for caveolae. Even though, the EGFR, amphiregulin and HB-EGF seem to partially co-localise with caveolin-1, the major portion of these ligands, does not (Fig. 22, 23A), suggesting that this protein is not enriched in caveolae.

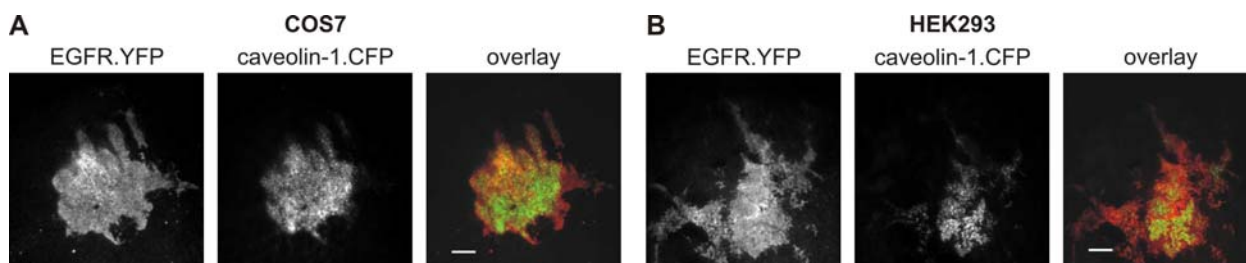


Fig. 22. TIRFM of the EGFR shows partial enrichment in caveolin-1 containing plasma membrane domains of COS7 and HEK293 cells. COS7 (A) and HEK293 (B) cells expressing caveolin-1.CFP and EGFR.YFP were grown on coverslips and excited with the 488-nm (YFP) or 458-nm (CFP) line of an Ar⁺ laser. In the overlay pictures, the YFP line is detected as red and the CFP line as green. Bar, 10 μ m.

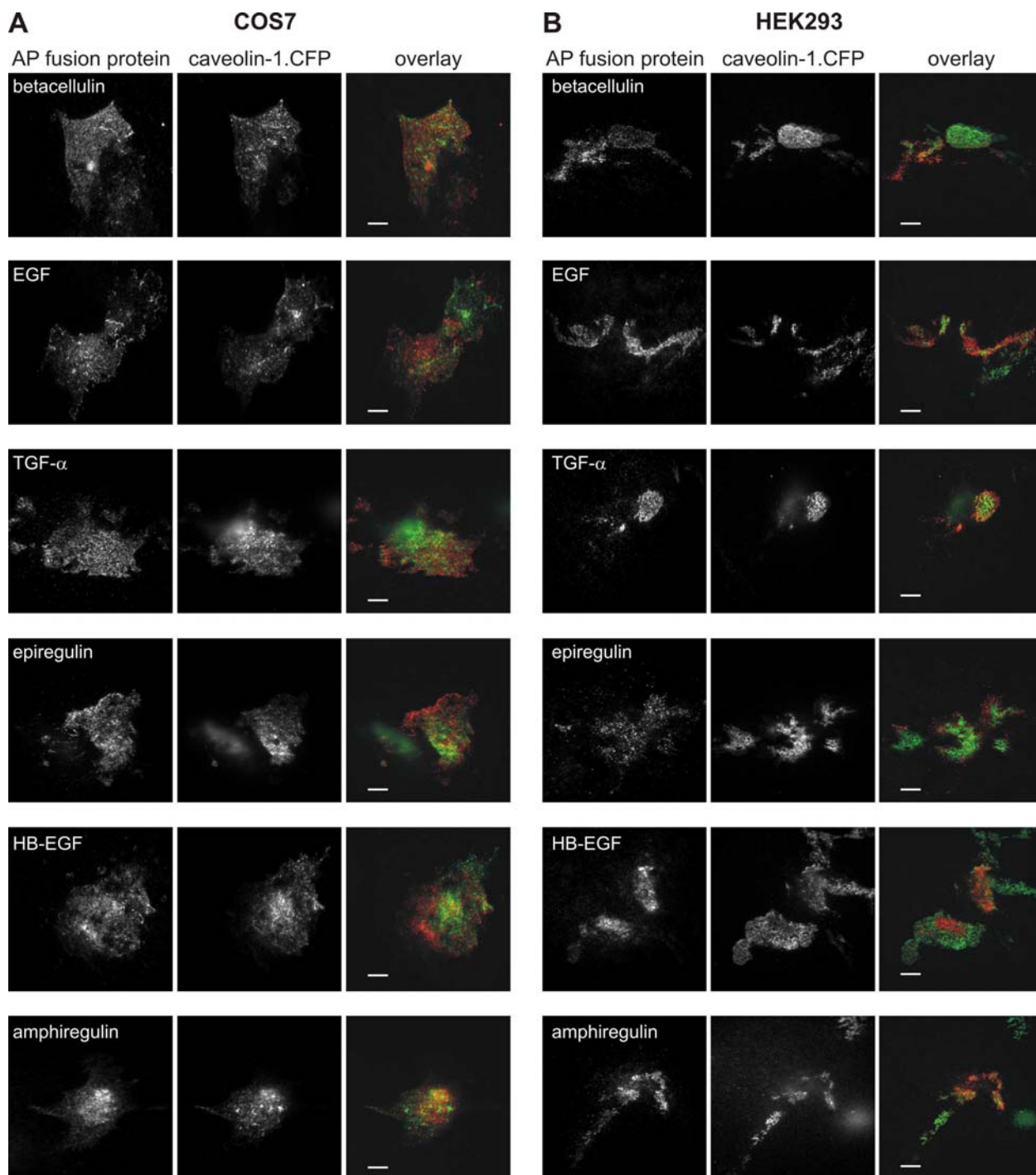


Fig. 23. Localisation of EGFR ligands in COS7 and HEK293 cells. COS7 (A) and HEK293 (B) cells expressing AP-tagged proforms of the EGFR ligands betacellulin, EGF, TGF- α , epiregulin, HB-GFF or amphiregulin and caveolin-1.CFP were subjected to immunofluorescence. A specific AP antibody was detected with an Alexa Fluor 555 antibody. Excitation of Alexa 555 was performed using the 514-nm laser line and a 514-nm dichroic mirror, CFP-fluorescence was detected using a 458-nm laser line. In the overlay pictures, the Alexa 555 line is detected as red and the CFP line as green. Bar, 10 μ m.

Moreover, the localisation of the EGFR seems to be independent of ET_B receptor expression since the detection of the EGFR by Western blot analysis failed within caveolae-containing fractions from gradient centrifugation studies (see Chapter 4.1.2.), suggesting an absence from

caveolae (data not shown). Moreover, neither co-transfection of amphiregulin, caveolin-1 and cDNAs of the full-length and N-terminally truncated ET_B receptor nor the stimulation of the ET_B receptor with IRL1620 for 1 hour changed the localisation of amphiregulin in COS7 and HEK293 cells (Fig. 24). This suggests, that the localisation of EGFR receptor ligands is independent of the ET_B receptor localisation.

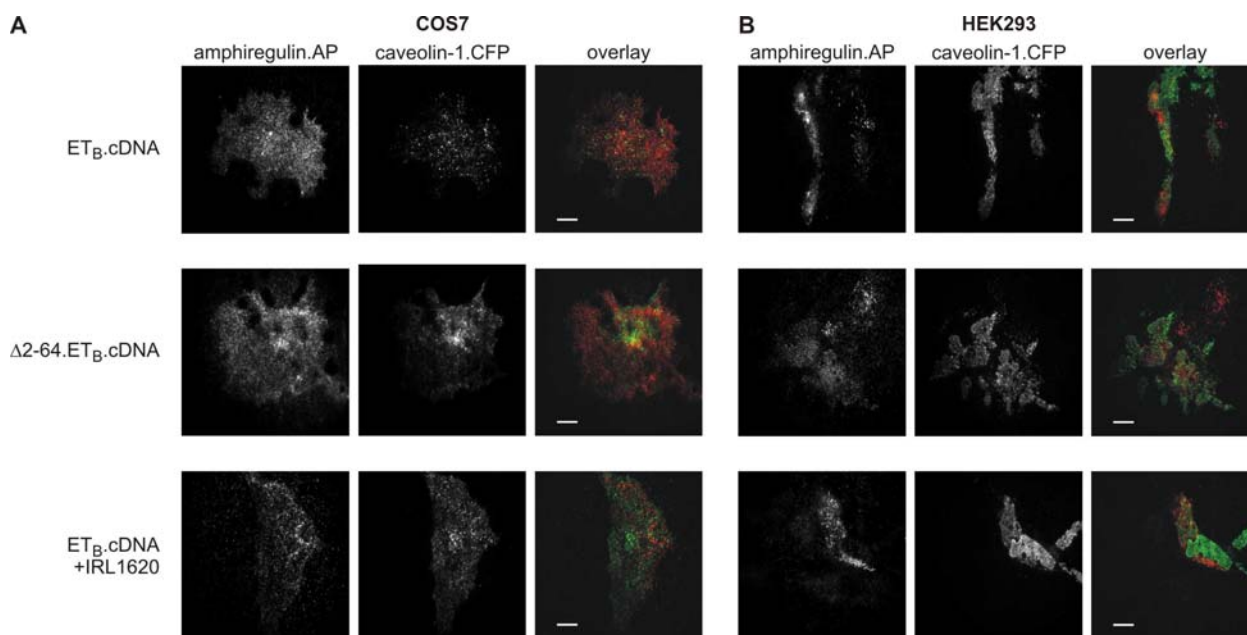


Fig. 24. Localisation of amphiregulin in COS7 and HEK293 cells when co-transfected with ET_B receptor constructs. COS7 (A) and HEK293 (B) cells were transfected with amphiregulin.AP, caveolin-1.CFP and ET_B receptor constructs as indicated. Cells were stimulated with 100 nM IRL1620 for an hour when indicated. A specific AP antibody was detected with an Alexa Fluor 555 antibody. Excitation of Alexa 555 was performed using the 514 nm laser line and a 514-nm dichroic mirror, CFP-fluorescence was detected using a 458-nm laser line. In the overlay pictures, the Alexa 555 line is detected as red and the CFP line as green. Bar, 10µm.

4.1.5 Localisation of ET_B receptors does not affect the activation of ERK1/2

The pattern of ERK1/2 phosphorylation upon stimulation of ET_B receptor variants differs in VSM and HEK293 cells (Grantcharova et al., 2006b). To investigate whether distinct ERK1/2 activation patterns are related to ET_B receptor localisation, COS7, HEK293 and MDCK cells were transfected with the different ET_B receptor constructs and the induced ERK1/2 phosphorylation pattern after ET_B receptor stimulation with IRL1620 analysed (Fig. 25). In COS7 cells, stimulation of the ET_B.GFP resulted in a long-lasting, biphasic phosphorylation of ERK1/2 (Fig. 25A). However, the second phase started after 180 min, which is much later than has been reported in HEK293 or VSM cells (Grantcharova et al., 2006a; Grantcharova et al., 2006b). Stimulation of the glycosylation-deficient ΔGlc.ET_B.GFP and the N-terminally truncated

$\Delta 2-64.ET_B.GFP$ led to a sustained but diminished activation of ERK1/2. In contrast, the stimulation of the caveolar $ET_B.GFP.cav2$ and $\Delta Glc.ET_B.GFP.cav2$ receptors led to a monophasic phosphorylation of ERK1/2. Thus, the activation pattern of ERK1/2 activation cannot be correlated to caveolar localisation but may be linked to ET_B receptor glycosylation.

In HEK293 cells, results from previous studies (Grantcharova et al., 2006a; Grantcharova et al., 2006b) were confirmed: stimulation of the full-length $ET_B.GFP$ resulted in a biphasic activation of ERK1/2 whereas stimulation of the N-terminally truncated $\Delta 2-64.ET_B.GFP$ triggered a monophasic activation (Fig. 25B). From this study it can be added that stimulation of all other constructs with IRL1620 resulted in a monophasic phosphorylation of ERK1/2, indicating that the pattern of ERK1/2 phosphorylation does not only depend on receptor length but also on receptor glycosylation in HEK293 cells. Furthermore, direct targeting of the receptors to artificial caveolae might increase the ERK1/2 signal but not influence the actual ERK1/2 activation kinetics.

Performing the same experiment in MDCK cells stably expressing the full-length $ET_B.GFP$, the activation pattern of ERK1/2 was only transient, as the increased phosphorylation after 10 min diminished after 30 min (Fig. 25C). Activation of the stably expressed glycosylation-deficient $\Delta Glc.ET_B.GFP$ resulted in a weak biphasic phosphorylation of ERK1/2. Moreover, the maximum signal of ERK1/2 activation induced by the glycosylation-deficient receptor was much weaker than that induced by the full-length ET_B receptor. Thus, the caveolar localisation of the ET_B receptor partially influences ERK1/2 activation pattern in MDCK cells. Similar to COS7 cells, the signal intensity of ERK1/2 phosphorylation may be linked to ET_B receptor glycosylation.

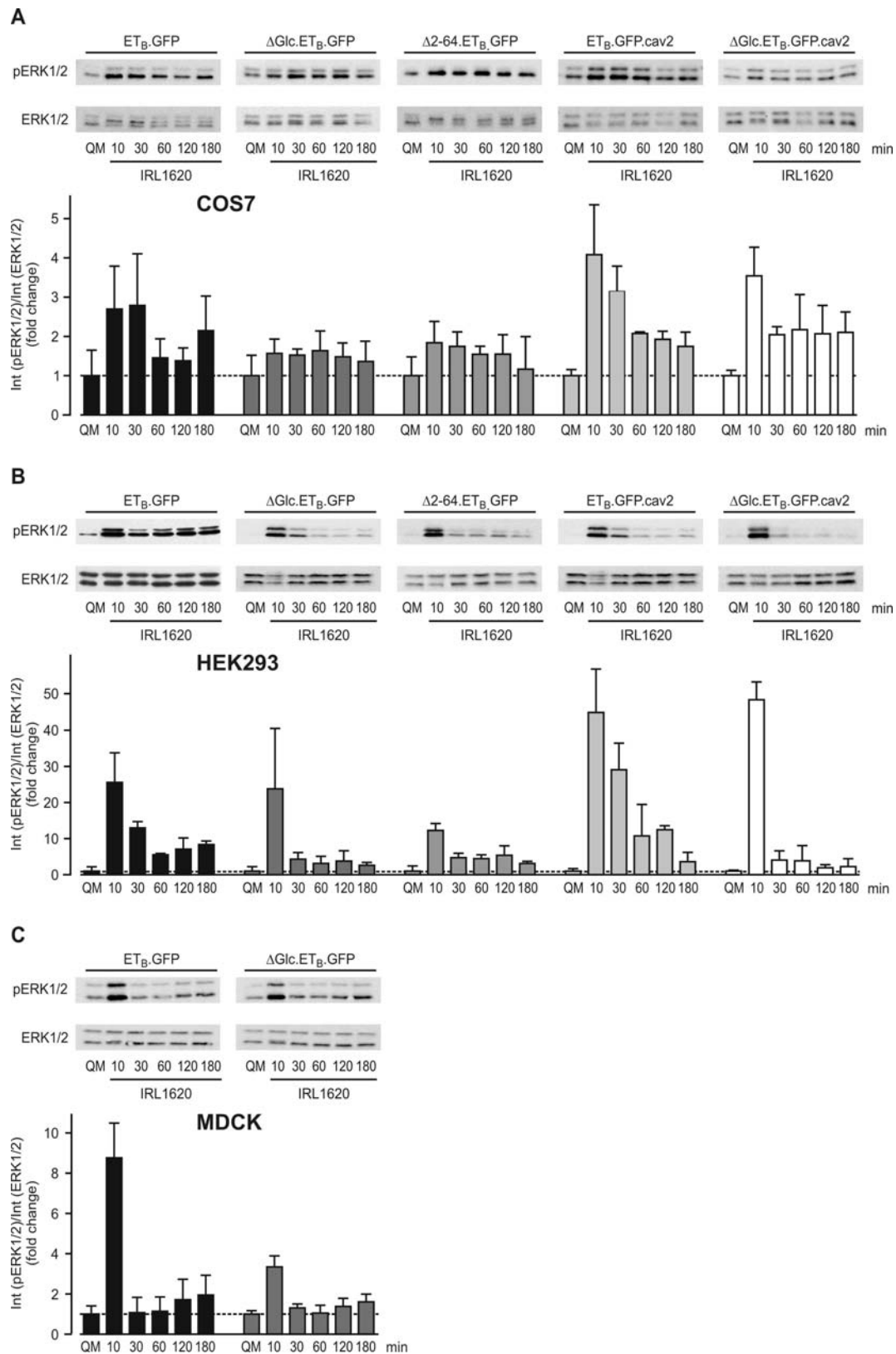


Fig. 25. ET_B receptor-mediated ERK1/2 phosphorylation. Serum-starved COS7 (A), HEK293 (B) and MDCK (C) cells expressing the ET_B receptor constructs as indicated were stimulated with 100 nM IRL1620 for up to 180 min. Activated ERK1/2 was detected with an anti-phospho-ERK1/2 antibody. Total ERK1/2 was detected with an anti-ERK1/2 antibody. Quantitative analysis of signals was performed with a CCD camera-based bioluminescence imaging system. Graphs depict means and S.E. of at least 3 independent experiments. QM: quiescent medium.

4.2 Short-term modification of gene expression in vascular smooth muscle cells

4.2.1 Confidence analysis

It has been suggested that the strength and duration of MAPK phosphorylation - especially of ERK1/2 - defines the phenotypic outcome of cells (Marshall, 1995). Stimulation of PARs with thrombin or with a thrombin receptor-activating peptide (TRAP) also leads to a strong and biphasic activation of ERK1/2 and subsequent expression of contractile proteins in VSM cells (Reusch et al., 2001a). To identify candidate genes that are involved in the long-lasting activation of ERK1/2 that might result in the differentiation of VSM cells, microarray analysis was performed.

To assess the kinetics of ERK1/2 phosphorylation, cell lysates were taken at various time points after stimulation with thrombin or TRAP, and probed for ERK1/2 expression and phosphorylation state (Fig. 26). Confirming previous studies (Reusch et al., 2001a), stimulation of VSM cells with thrombin or TRAP resulted in a biphasic activation pattern of ERK1/2. Pre-treatment of the cells with the G_i -uncoupling PTX abolished the late phase of ERK1/2 phosphorylation. Corresponding to the late phase of ERK1/2 activation, gene expression analysis was performed 120 min after stimulation of VSM cells. As a reference, gene expression analysis of untreated VSM cells was performed simultaneously. Each condition was assayed in duplicates.

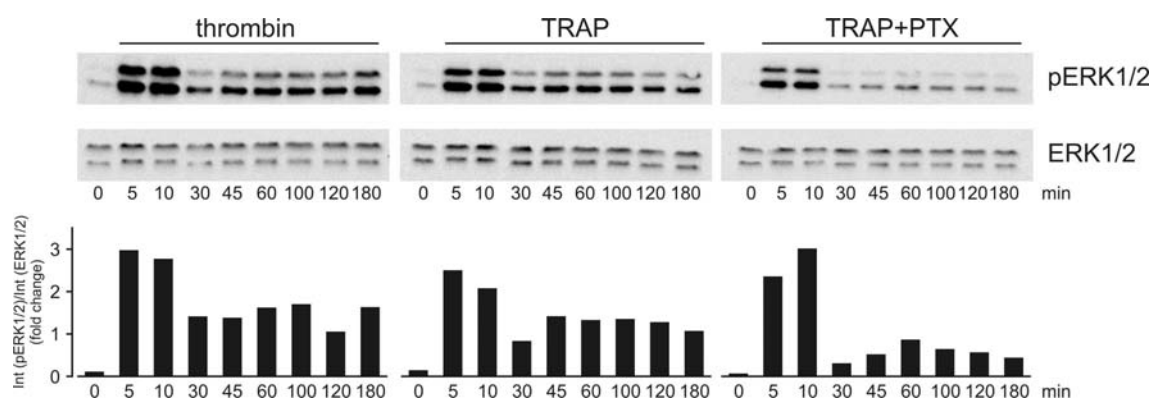


Fig. 26. Long-lived activation of ERK1/2 is inhibited by PTX. VSM cells were stimulated for the indicated times with 2 U/ml thrombin, 25 μ M TRAP or 25 μ M TRAP upon pre-treatment with 200 ng/ml PTX for 24 h. Whole cell lysates were subjected to immunoblot analysis detecting either the phosphorylated (pERK1/2) or the total ERK1/2.

Differentially regulated genes resulting from stimulation of (rat) Par-1 or Par-4 were determined performing confidence analysis applying confidence intervals of $p < 0.05$ and $p < 0.003$. Based on the stimulation applied, genes could be clustered into 3 categories: i) genes regulated upon Par-1 stimulation via G_q and $G_{12/13}$; ii) genes regulated upon Par-1 stimulation via G_i ; and iii) genes regulated upon Par-4 stimulation (Fig. 27).

The clustered genes were analysed using the DAVID (Dennis et al., 2003) database (<http://niaid.abcc.ncifcrf.gov/tools.jsp>). The 20 most strongly upregulated genes upon stimulation with either thrombin, TRAP or TRAP+PTX are summarised in Tables 15-17. Amongst them are a number of transcription factors, kinases, phosphatases and others. Since this study is interested in resolving the molecular mechanisms leading to the Par-induced activation of ERK1/2, regulated genes were further mapped to known pathways from the KEGG database (http://cgap.nci.nih.gov/Pathways/Pathway_Searcher) especially focusing on MAPK signalling and prothrombotic pathways. 33 regulated genes, of which 22 were upregulated, could be mapped to these signalling cascades (Table 18).

A simplified MAPK pathway including most of the regulated genes is shown in Fig. 28. Five genes, namely amphiregulin, a disintegrin and metalloproteinase with thrombospondin motif 1 (ADAMTS-1), tissue inhibitor of matrix metalloproteinases 1 (TIMP-1), MAP3K8 and cyclooxygenase 2 (COX-2) were chosen to confirm the results from the microarray screen by multiplex RT-PCR and immunoblot analysis. A summarising table (Table 19) can be found at the end of Chapter 4.2.6.

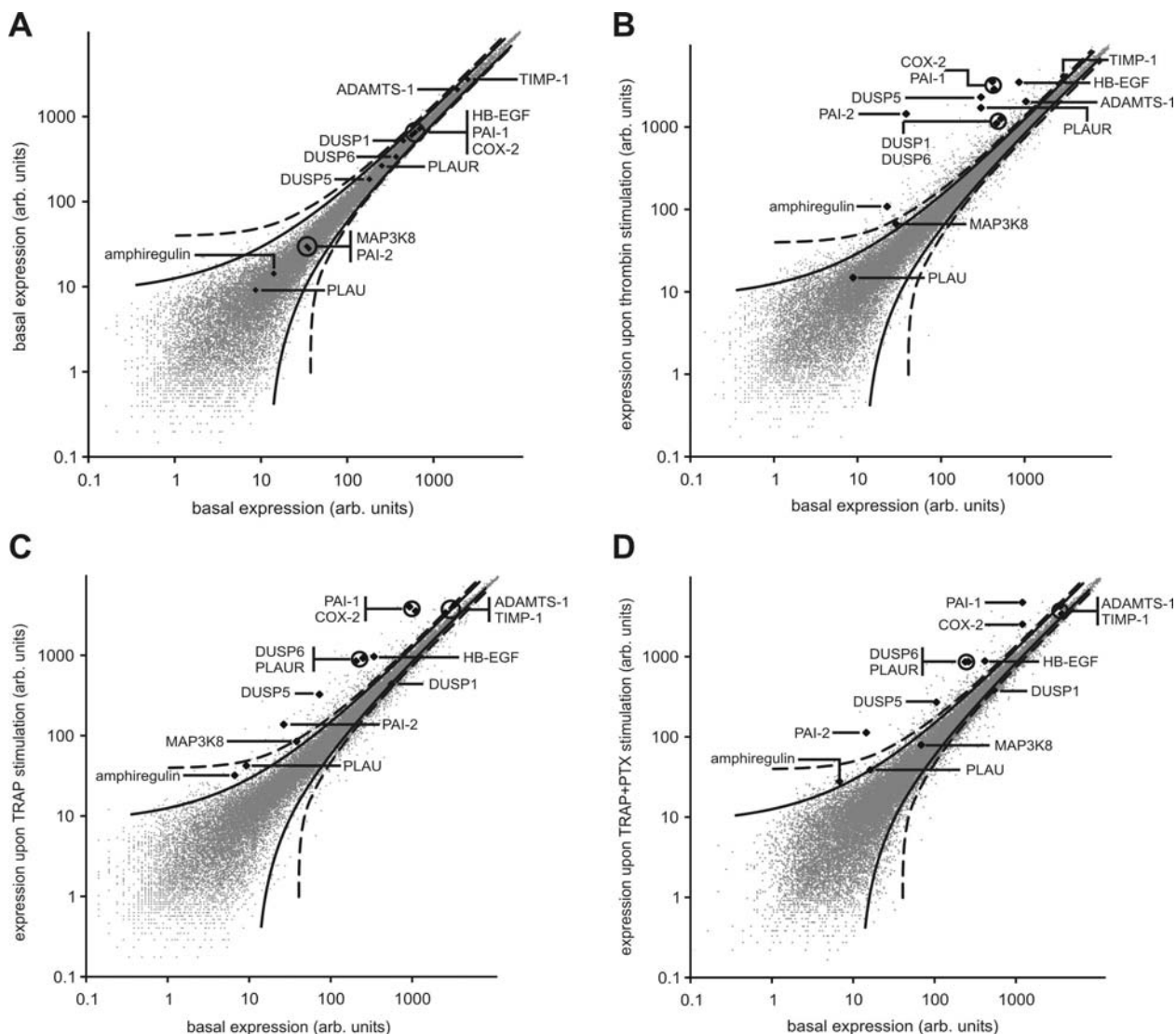


Figure 27. Par-1- and Par-4-dependent gene expression upon stimulation of VSM cells. Total RNA of unstimulated VSM cells (A), VSM cells treated with 2 U/ml thrombin (B), 25 μ M TRAP (C) or 25 μ M TRAP after pre-treatment with 200 ng/ml PTX for 24 h (D) was isolated and probed onto a microarray chip. Confidence analysis using confidence intervals of $p < 0.05$ (solid) and $p < 0.003$ (dashed) was performed to calculate S.D. of the inter-experimental expression variations for groups of 500 genes. Expressed genes were summarised in graphs to reveal differentially regulated genes. Genes of interest were picked and labelled in the graphs.

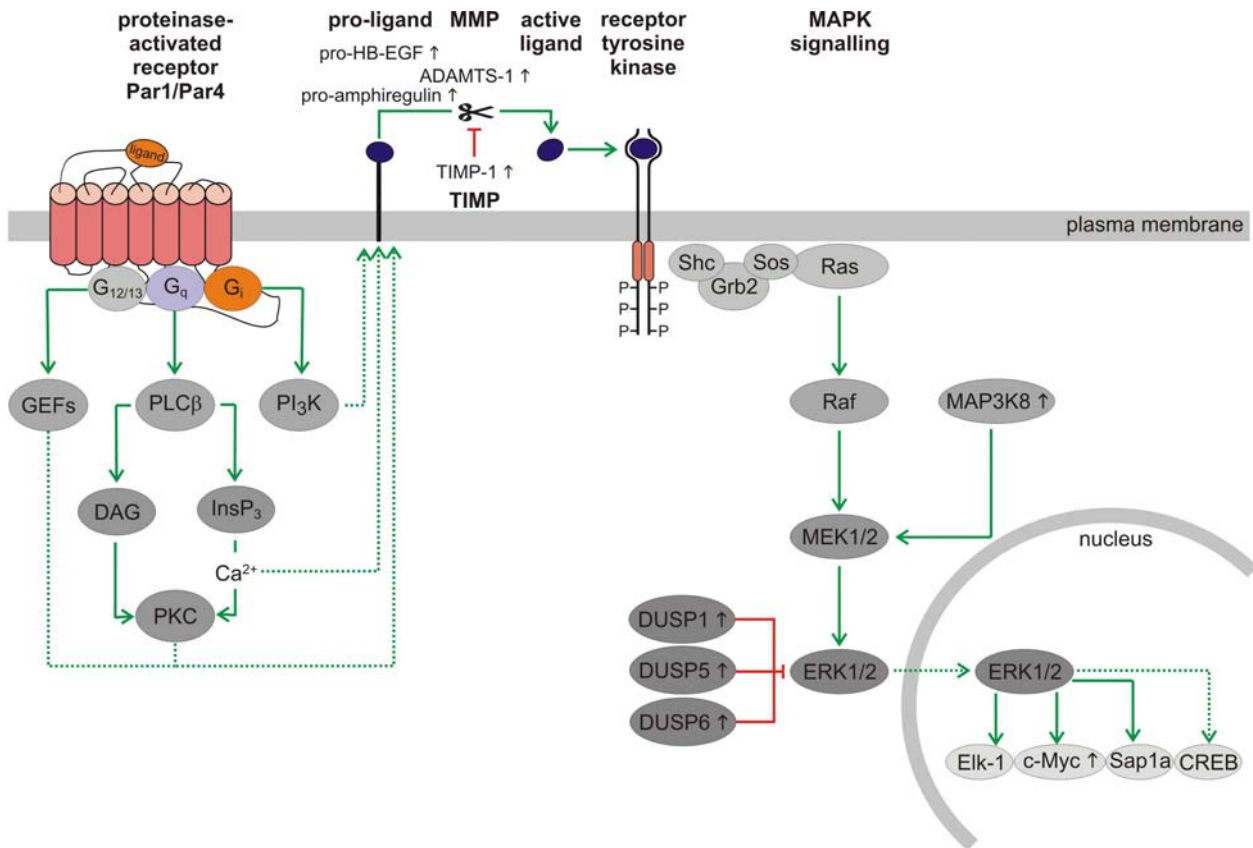


Figure 28. Model of transactivation of receptor tyrosine kinases following stimulation of protease-activated receptors. Activation of Par-1 and Par-4 results in the activation of the G proteins $G_{12/13}$, G_q and G_i . Different signalling pathways then lead to activation of MMPs, followed by shedding of EGFR ligands, subsequent binding to and autophosphorylation of the receptor leading to activation of ERK1/2. Microarray analysis revealed 15 upregulated genes that map to this triple membrane-spanning pathway. Nine of them are included in this schematic and marked with an upright arrow.

Table 15. Upregulated genes 120 min after stimulation of Par-1 and Par-4 receptors with thrombin

gene	Affymetrix ID	accession number	fold change	function
plasminogen activator inhibitor 2 PAI-2	1368487_at	NM_021696.1	38.2	non-conventional serine protease inhibitor
unknown EST	1392791_at	AA964492	21.2	unknown
Fos-like antigen 1 (Fosl1)	1368489_at	NM_012953.1	15.4	related to c-fos; involved in serum-inducible immediate-early transcription
early growth response 2 (Egr2)	1387306_a_at	NM_053633.1	10.6	DNA-binding transcription factor
unknown EST	1392264_s_at	AI500951	9.2	unknown
activity regulated cytoskeletal-associated protein (Arc)	1387068_at	NM_019361.1	9.2	regulates endocytosis of AMPA receptors in response to synaptic activity
sphingosine kinase 1c	1368254_a_at	AB049572.1	8.7	catalyses the conversion of sphingosine to sphingosine 1 phosphate
unknown EST	1375475_at	BE111304	8.7	unknown
cyclooxygenase 2; COX-2	1368527_at	U03389.1	8.5	catalyses the conversion of arachidonic acid products to prostaglandin
EST	1384120_at	BF386877	8.4	unknown
glycine receptor, alpha 1 subunit (Gla1)	1387464_at	NM_013133.1	7.8	glycine receptor strychnine binding subunit
dual specificity phosphatase 5; DUSP5	1368124_at	NM_133578.1	7.6	inactivates MAPKs
EST, highly similar to nocturnin	1377869_at	BI284261	7.5	unknown
immediate early gene transcription factor NGFI-B (Nr4a1)	1386935_at	NM_024388.1	7.3	putative ligand-dependent transcriptional activator
unknown EST	1373759_at	BF522317	6.7	unknown
plasminogen activator inhibitor 1; PAI-1	1368519_at	NM_012620.1	6.5	mediates inhibition of fibrinolysis by inhibiting the plasminogen activator
unknown EST	1381341_at	BE111796	6.1	unknown
beta-nerve growth factor gene, last exon	1371259_at	BM388972	5.9	is involved in the regulation of growth and differentiation of sympathetic and certain sensory neurons
EST, predicted epithelial V-like antigen 1	1375908_at	BI282616	5.9	unknown
regulator of g-protein signalling 16	1373777_at	NM_001077589	5.6	inhibits signal transduction by increasing the GTPase activity of G protein alpha subunits

Table 16. Upregulated genes 120 min after stimulation of Par-1 receptors with TRAP

gene	Affymetrix ID	accession number	fold change	function
chemokine (C-X-C motif) ligand 1	1387316_at	NM_030845.1	40.3	neutrophil chemoattractant
unknown EST	1392791_at	AA964492	18.5	unknown
Fos-like antigen 1 (Fosl1)	1368489_at	NM_012953.1	14.1	related to c-fos; involved in serum-inducible immediate-early transcription
potassium large conductance calcium-activated channel	1372929_at	NM_031828	12.7	large-conductance Ca ²⁺ -activated K ⁺ channel
CC chemokine ST38 precursor	1369814_at	NM_019233.1	10.6	chemotactic factor that attracts lymphocytes and, slightly, neutrophils, but not monocytes
EST, similar to molecule possessing ankyrin-repeats induced by lipopolysaccharide	1378032_at	AI176265	7.7	unknown
tryptophan hydroxylase 1	1392647_at	NM_001100634	7.2	catalyses the conversion of l-tryptophan to 5-hydroxy-l-tryptophan
chemokine (C-C motif) ligand 2	1367973_at	NM_031530.1	6.9	chemotactic factor that attracts monocytes, but not neutrophils
chemokine (C-C motif) ligand 7	1379935_at	NM_001007612	6.8	chemotactic factor that attracts monocytes and eosinophils, but not neutrophils
EST, highly similar to nocturnin	1377869_at	BI284261	6.6	unknown
unknown EST	1373759_at	BF522317	5.7	unknown
plasminogen activator inhibitor 2; PAI-2	1368487_at	NM_021696.1	5.4	non-conventional serine protease inhibitor
metallothionein 1	1371237_a_at	AF411318.1	5.2	binds various heavy metals
serumglucocorticoid regulated kinase (Sgk)	1367802_at	NM_019232.1	4.9	inactivates NEDD4L, which leads to activation of various channels and transporters
unknown EST	1392264_s_at	AI500951	4.8	unknown
plasminogen activator inhibitor 1; PAI-1	1368519_at	NM_012620.1	4.8	mediates inhibition of fibrinolysis by inhibiting the plasminogen activator
dual specificity phosphatase 5; DUSP5	1368124_at	NM_133578.1	4.8	inactivates MAPKs
urokinase-type plasminogen activator; PLAU	1387675_at	NM_013085.1	4.8	specifically cleaves the zymogen plasminogen to form the active enzyme plasmin
unknown EST	1385641_at	AI070558	4.8	unknown
dual specificity phosphatase 6, DUSP6	1382778_at	AAB06202	4.7	involved in regulation of mitogen-activated protein kinase

Table 17. Upregulated genes 120 min after stimulation of Par-1 receptors with TRAP after pre-treatment with PTX

gene	Affymetrix ID	accession number	fold change	function
chemokine (C-X-C motif) ligand 1	1387316_at	NM_030845.1	40.3	acts as a neutrophil chemoattractant
unknown EST	1392791_at	AA964492	18.9	unknown
Fos-like antigen 1 (Fos11)	1368489_at	NM_012953.1	11.5	related to c-fos; involved in serum-inducible immediate-early transcription
EST, predicted serine/threonine protein kinase 2	1380873_at	BF410197	10.4	unknown
laminin gamma1	1396879_at	AI556752	9.6	an extracellular matrix protein
plasminogen activator inhibitor 2; PAI-2	1368487_at	NM_021696.1	8.2	non-conventional serine protease inhibitor
zinc finger protein 313	1395198_at	NM_001001517	7.6	may play a role in spermatogenesis
EST, highly similar to nocturnin	1377869_at	BI284261	6.1	unknown
a kinase (PRKA) anchor protein (gravin) 12	1368869_at	NM_057103.1	6.0	directs the activity of protein kinase A (PKA) by tethering the enzyme near its physiologic substrates
serumglucocorticoid regulated kinase (Sgk)	1367802_at	NM_019232.1	5.8	inactivates NEDD4L, which leads to activation of various channels and transporters
dual specificity phosphatase 6; DUSP6	1377064_at	AAB06202	5.5	involved in regulation of mitogen-activated protein kinase
early growth response 2 (Egr2)	1387306_a_at	NM_053633.1	5.5	DNA-binding transcription factor
early growth response 1 (Egr1)	1368321_at	NM_012551.1	5.3	activates transcription of the LH receptor gene
unknown EST	1381341_at	BE111796	5.0	unknown
peroxisomal acyl-coa thioesterase 1	1394902_at	NM_130756	4.5	involved in conversion of dimethylnonanoyl-CoA and dimethylheptanoyl-CoA into 4,8-dimethylnonanoic acid plus CoASH
EST, predicted WD repeat domain 36	1381070_at	AI233106	4.5	unknown
plasminogen activator inhibitor 1; PAI-1	1368519_at	NM_012620.1	4.4	mediates inhibition of fibrinolysis by inhibiting the plasminogen activator
EST, predicted TCDD-inducible poly(ADP-ribose) polymerase	1385407_at	AI511405	4.4	unknown
CC chemokine ST38 precursor	1369814_at	NM_019233.1	4.2	chemotactic factor that attracts lymphocytes and, slightly, neutrophils, but not monocytes
EST, similar to fli-1rr associated protein-1	1381392_at	BF387435	3.9	unknown

Table 18. Par-1- and Par-4-induced upregulation of genes belonging to the MAPK signalling pathway and the prothrombotic coagulation cascade

gene	synonym	Affymetrix ID	pathway	fold change			description	
				thrombin	TRAP	TRAP+PTX		
TIMP-1	EPA	1367712_at	MAPK signalling	1.4	1.5	1.1	tissue inhibitor of metalloproteinase 1	
MAP3K8	Tpl2/Cot	1369393_at	MAPK signalling	2.3	2.3	1.2	mitogen-activated protein kinase kinase 8	
ADAMTS-1	METH1	1368223_at	MAPK signalling	1.9	1.4	1.4	a disintegrin and metalloproteinase with thrombospondin type 1 motif	
AR	AREG	1369871_at	MAPK signalling	4.8	4.9	4.3	amphiregulin	
c-Jun		1369788_s_at	MAPK signalling	1.3	1.4	2.3	jun oncogene	
EGFR	ERBB	1370830_at	MAPK signalling	1.2	0.9	1.4	epidermal growth factor receptor	
ERK	MAPK3	1387771_a_at	MAPK signalling	1.0	1.1	1.4	mitogen activated protein kinase 3, extracellular signal-regulated kinase	
HB-EGF	DTR	1368983_at	MAPK signalling	4.0	3.1	2.4	diphtheria toxin receptor, heparin-binding EGF-like growth factor	
Hsp72	HSPA1A	1368247_at	MAPK signalling	2.3	1.7	2.0	heat shock 70kd protein 1a	
NGF	NGFB	1371259_at	MAPK signalling	5.9	1.7	2.2	nerve growth factor β	
Nur77	NR4A1	1386935_at	MAPK signalling	7.3	2.7	3.2	nuclear receptor subfamily 4, group a, member 1	
DUSP	MKP	1368124_at	MAPK signalling	7.6	2.4	4.5	3.0	dual specificity phosphatase 5
		1387024_at				4.4	4.2	dual specificity phosphatase 6
		1368147_at				0.9	0.8	dual specificity phosphatase 1
c-Myc		1368308_at	MAPK signalling	2.2	0.8	0.8	myelocytomatosis viral oncogene homologue (avian)	
COX-2	PTGS2	1368527_at	Coagulation cascade	8.5	3.6	2.3	cyclooxygenase 2, prostaglandin-endoperoxide synthase 2	
BDKR	BKR1	1369807_at	Coagulation cascade	4.0	2.3	1.8	bradykinin receptor b1	
Par-1	F2R	1367899_at	Coagulation cascade	1.1	1.1	1.5	coagulation factor ii (thrombin) receptor, protease activated receptor 1	
TF	F3	1369182_at	Coagulation cascade	2.4	2.3	1.4	coagulation factor iii, tissue factor	
PLAU	uPA	1387675_at	Coagulation cascade	1.7	4.9	3.0	plasminogen activator, urokinase	
PLAUR	uPAR	1387269_s_at	Coagulation cascade	5.2	4.1	3.5	plasminogen activator, urokinase receptor	
PAI-1	SERPINE1	1368519_at	Coagulation cascade	6.5	4.8	4.5	plasminogen activator inhibitor 1	

Genes highlighted in grey were chosen to be analysed further.

4.2.2 Amphiregulin

The ligands of the EGFR are a major component in the GPCR-induced transactivation of the EGFR and the subsequent phosphorylation of ERK1/2. However, the ligands involved in the Par-1- and Par-4-induced EGFR transactivation remain largely unknown. Of the six EGFR ligands expressed in VSM cells - amphiregulin, betacellulin, epidermal growth factor (EGF), epiregulin, heparin-binding EGF-like growth factor (HB-EGF) and transforming growth factor- α (TGF- α) - only amphiregulin and HB-EGF were found to be upregulated upon stimulation with thrombin or TRAP (Fig. 27, Table 18). An upregulation of HB-EGF, which has been identified earlier, was confirmed on both transcriptional and protein levels (data not shown) (Pérez Sastre et al., 2008). Amphiregulin was upregulated independent of PTX pre-treatment. Therefore, gene expression of amphiregulin is most probably triggered by the activation of Par-1 and G_{12/13} or G_q proteins. Gene chip analysis revealed an about 4.6-fold increase in expression, 120 min after stimulation with thrombin, TRAP or TRAP+PTX. Multiplex RT-PCR confirmed an upregulation of amphiregulin, however, only by ~2-fold and therefore not as prominent as evident from the microarray (Fig. 29A).

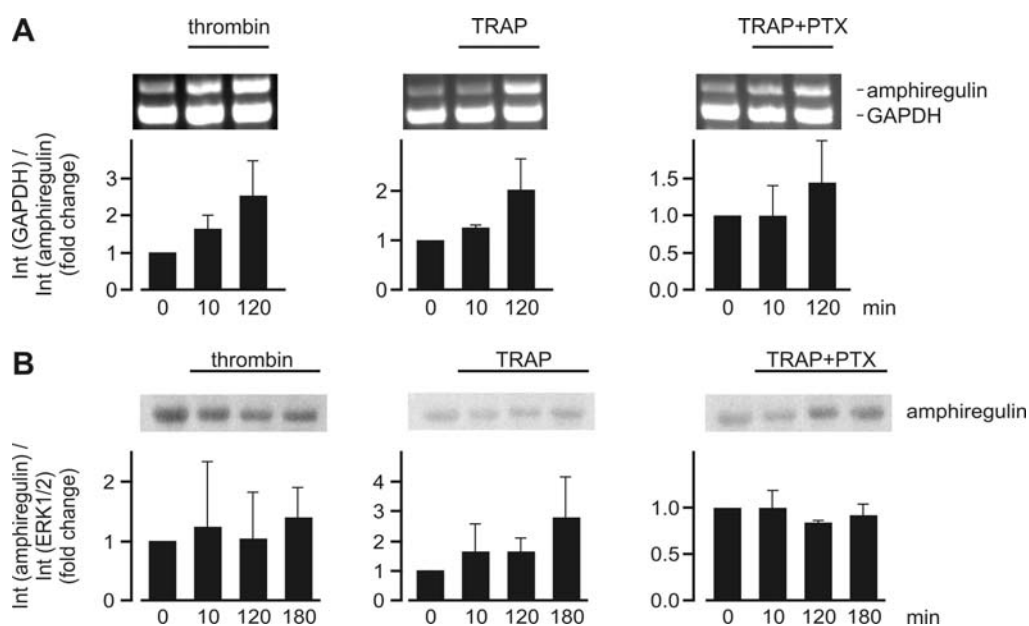


Fig. 29. Multiplex RT-PCR and immunoblot of amphiregulin. VSM cells were stimulated for the indicated times with 2 U/ml thrombin, 25 μ M TRAP or 25 μ M TRAP after pre-treatment with 200 ng/ml PTX for 24 h. (A) Total RNA was isolated and reverse transcribed into cDNA. Appropriate primers detected the expression of amphiregulin. GAPDH was simultaneously co-amplified as an internal reference. Graphs summarise results from at least 3 independent experiments. (B) Whole cell lysates were subjected to immunoblot analysis applying an antibody detecting amphiregulin. ERK1/2 expression was probed as a control (data not shown). Graphs summarise results from at least 3 independent experiments.

At the protein level, only stimulation with TRAP resulted in an upregulation (fold change; f.c.: 1.6 ± 0.5) of amphiregulin, whereas thrombin or TRAP+PTX did not (Fig. 29B). The increase was much weaker than that obtained from the gene chip and RT-PCR.

4.2.3 A disintegrin and metalloproteinase with thrombospondin motif 1

Activation of membrane-bound EGFR ligands requires the activity of MMPs. These shed the ligand proforms to release the active EGFR ligand. In this study, the only MMP found to be upregulated was a disintegrin and metalloproteinase with thrombospondin motif 1 (ADAMTS-1). The regulation of ADAMTS-1 was Par-1-dependent and PTX-insensitive therefore most likely triggered via G proteins of the $G_{12/13}$ - and G_q - families (Fig. 27, Table 18). The TRAP-induced increase in mRNA levels (f.c.: 1.4) was confirmed by multiplex RT-PCR (f.c.: 1.2 ± 0.1) (Fig. 30A).

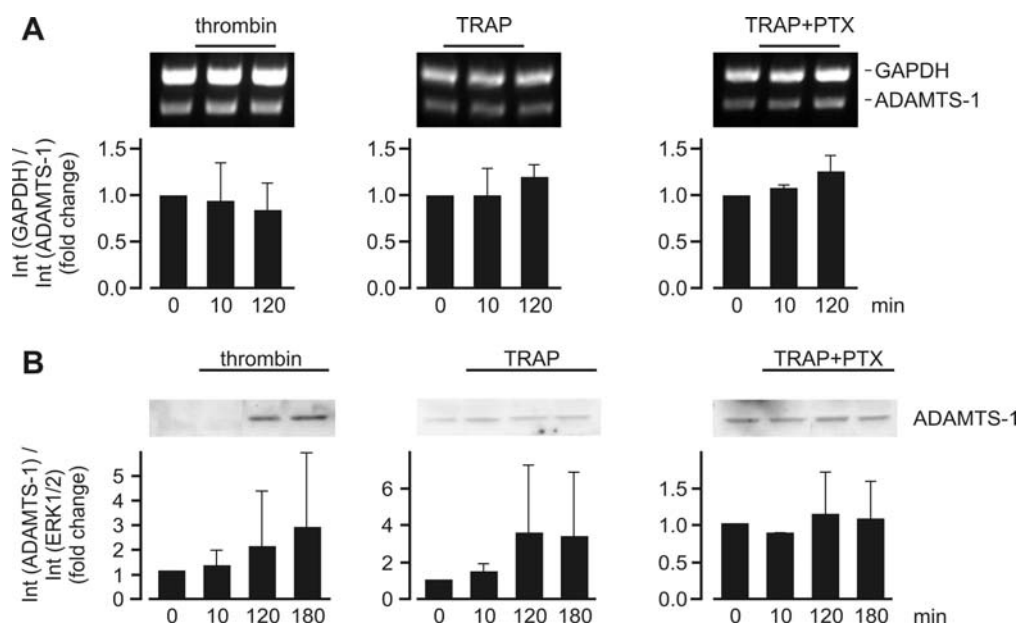


Fig. 30. Multiplex RT-PCR and immunoblot of ADAMTS-1. VSM cells were stimulated for the indicated times with 2 U/ml thrombin, 25 μ M TRAP or 25 μ M TRAP after pre-treatment with 200 ng/ml PTX for 24 h. (A) Total RNA was isolated and reverse transcribed into cDNA. Appropriate primers detected the expression of ADAMTS-1. GAPDH was simultaneously co-amplified as an internal reference. Graphs summarise results from at least 3 independent experiments. (B) Whole cell lysates were subjected to immunoblot analysis applying an antibody detecting ADAMTS-1. ERK1/2 expression was probed as a control (data not shown). Graphs summarise results from at least 3 independent experiments.

In contrast, stimulation of VSM cells with thrombin resulted in a decreased expression on transcript levels as assessed by RT-PCR (f.c.: 0.8 ± 0.3), although immunoblot analysis yielded results similar to the ones obtained from the microarray (f.c.: 1.9 ± 2.0 and 1.9, respectively; Fig.

30B). Stimulation with TRAP resulted in a stronger upregulation on the protein level (f.c.: 3.6 ± 3.7) than on transcript level, where both microarray and RT-PCR analysis, yielded similar results (f.c.: 1.4 and 1.2 ± 0.1 , respectively). PTX pre-treatment did not abolish the upregulation on both mRNA and protein levels.

4.2.4 Tissue inhibitor of metalloproteinases-1

The activity of MMPs is regulated by their inhibitors called tissue inhibitors of MMPs (TIMPs). A number of TIMPs is known but only TIMP-1 was found to be upregulated in this study. Its activation was most probably mediated by Par-1 in a G_i -dependent manner (Fig. 27, Table 18). Multiplex RT-PCR as well as immuno blot analysis (f.c.: 1.4 ± 0.3 and 1.3 ± 0.2 , respectively) confirmed the increased expression of Par-1 upon stimulation with TRAP (f.c.: 1.5; Fig. 31). In contrast to the microarray data, that indicated only a 1.1 fold change in expression upon stimulation with TRAP in presence of PTX, RT-PCR and immunoblot assays resulted in a similar upregulation (f.c.: 1.2 ± 0.0 and 1.3 ± 0.3 , respectively) as obtained after stimulation with thrombin or TRAP.

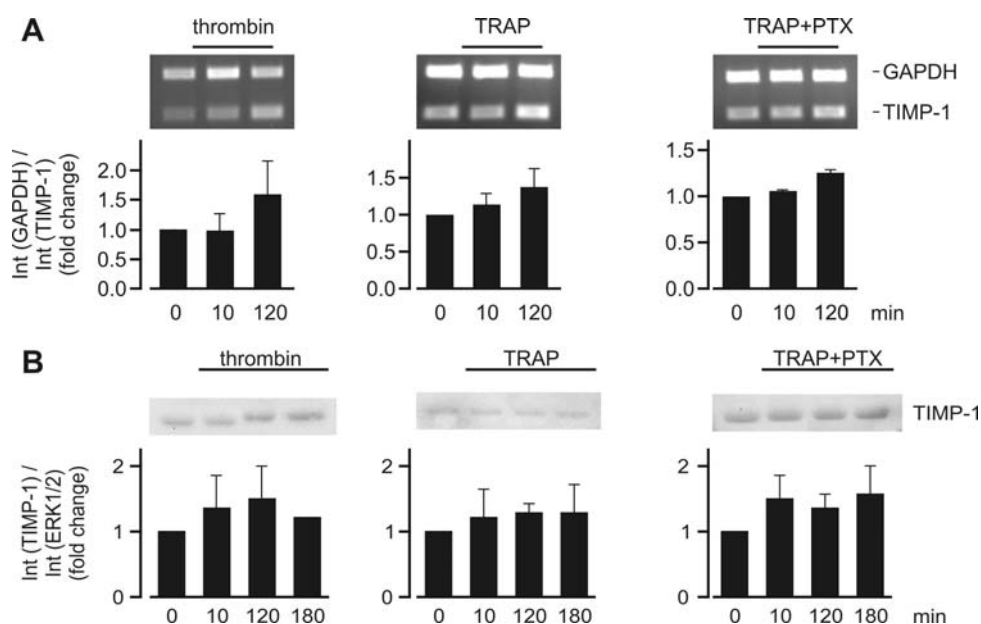


Fig. 31. Multiplex RT-PCR and immunoblot of TIMP-1. VSM cells were stimulated for the indicated times with 2 U/ml thrombin, 25 μ M TRAP or 25 μ M TRAP after pre-treatment with 200 ng/ml PTX for 24 h. **(A)** Total RNA was isolated and reverse transcribed into cDNA. Appropriate primers detected the expression of TIMP-1. GAPDH was simultaneously co-amplified as an internal reference. Graphs summarise results from at least 3 independent experiments. **(B)** Whole cell lysates were subjected to immunoblot analysis applying an antibody detecting TIMP-1. ERK1/2 expression was probed as a control (data not shown). Graphs summarise results from at least 3 independent experiments.

4.2.5 MAP3K8

Upon EGFR transactivation, the canonical Ras/Raf/MEK/ERK pathway is activated. A stimulation of MEK is also possible through MAP3K8, likewise resulting in activation of ERK1/2. In these studies, this kinase was upregulated in a Par-1- and G_i -dependent manner (Fig. 27, Table 18). RT-PCR confirmed the upregulation upon stimulation of VSM cells with TRAP in presence (f.c.: 1.2 ± 0.0 as compared to 1.2) or absence of PTX (f.c.: 1.5 ± 0.2 as compared to 2.3; Fig. 32A). Moreover, the thrombin- and TRAP-dependent upregulation (f.c.: 2.3 for both) was also confirmed by immunoblotting (f.c.: 1.7 ± 0.1 for thrombin and 1.4 ± 0.2 for TRAP; Fig. 32B). It can be concluded that MAP3K8 might be an interesting candidate in the Par-1-triggered phenotypic modulation of VSM cells.

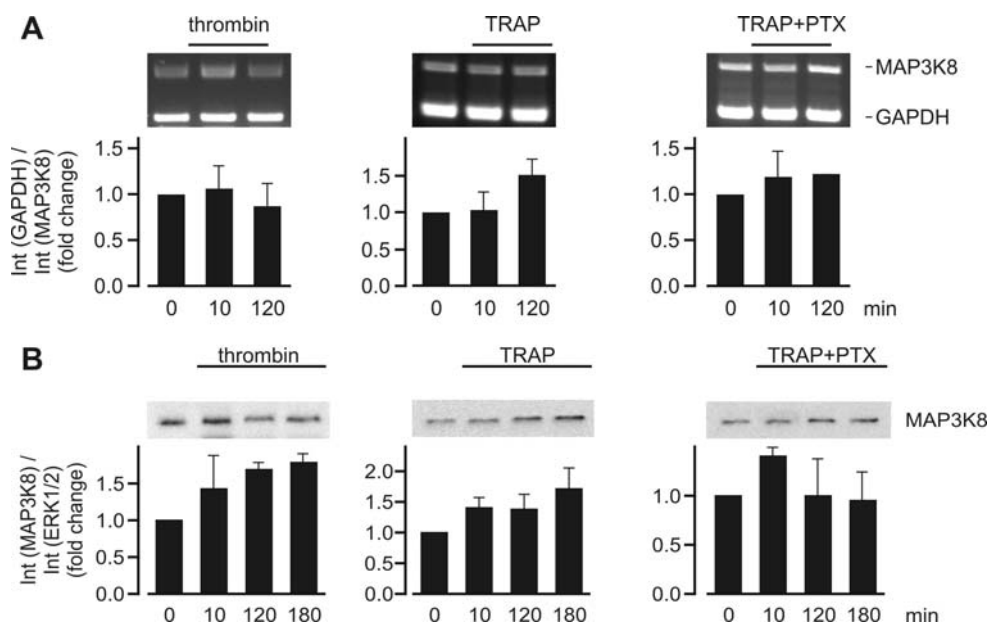


Fig. 32. Multiplex RT-PCR and immunoblot of MAP3K8. VSM cells were stimulated for the indicated times with 2 U/ml thrombin, 25 μ M TRAP or 25 μ M TRAP after pre-treatment with 200 ng/ml PTX for 24 h. (A) Total RNA was isolated and reverse transcribed into cDNA. Appropriate primers detected the expression of MAP3K8. GAPDH was simultaneously co-amplified as an internal reference. Graphs summarise results from at least 3 independent experiments. (B) Whole cell lysates were subjected to immunoblot analysis applying an antibody detecting MAP3K8. ERK1/2 expression was probed as a control (data not shown). Graphs summarise results from at least 3 independent experiments.

4.2.6 Cyclooxygenase 2

Cyclooxygenase 2 (COX-2) has a great influence on the regulation of vascular tone as it is involved in the synthesis of prostaglandins and thereby in the dilation of arteries. COX-2 showed a strong upregulation 120 min after stimulation of VSM cells with thrombin (f.c.: 8.5), TRAP

(f.c.: 3.6) or TRAP+PTX (f.c.: 2.3). This upregulation was, thus, triggered by Par-1 and relayed via G_q and $G_{12/13}$ protein-dependent signalling cascades (Fig. 27, Table 18). Surprisingly, RT-PCR failed to confirm the upregulation upon any stimulation (Fig. 33A). In contrast, performing immunoblot analysis, the microarray results were confirmed upon stimulation with thrombin (f.c.: 13.3 ± 7.7), TRAP (f.c.: 4.1 ± 0.7) or TRAP after pre-treatment with PTX (f.c.: 3.2 ± 1.9 ; Fig. 33B).

In Table 19, the results of all five novel potential candidate genes are summarised according to the stimulation and analysis applied.

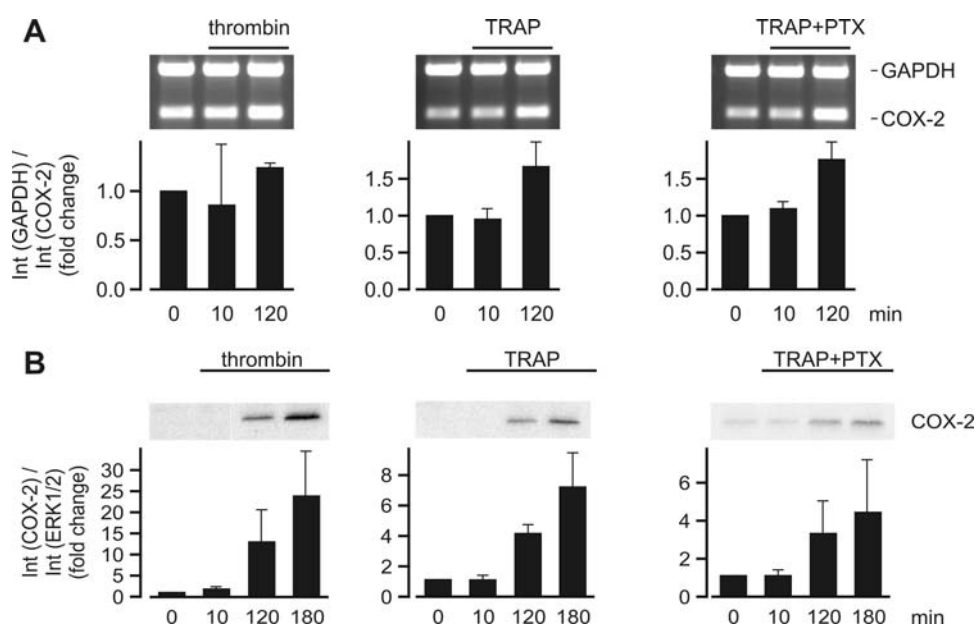


Fig. 33. Multiplex RT-PCR and immunoblot of COX-2. VSM cells were stimulated for the indicated times with 2 U/ml thrombin, 25 μ M TRAP or 25 μ M TRAP after pre-treatment with 200 ng/ml PTX for 24 h. (A) Total RNA was isolated and reverse transcribed into cDNA. Appropriate primers detected the expression of COX-2. GAPDH was simultaneously co-amplified as an internal reference. Graphs summarise results from at least 3 independent experiments. (B) Whole cell lysates were subjected to immunoblot analysis applying an antibody detecting COX-2. ERK1/2 expression was probed as a control (data not shown). Graphs summarise results from at least 3 independent experiments.

Table 19. Par-1 and Par-4-regulated genes 120 min after stimulation with thrombin, TRAP or TRAP+PTX

Gene	Thrombin			TRAP			TRAP+PTX		
	A	PCR	WB	A	PCR	WB	A	PCR	WB
MAP3K8	2.3	0.9 \pm 0.2	1.7 \pm 0.1	2.3	1.5 \pm 0.2	1.4 \pm 0.2	1.2	1.2 \pm 0.0	1.0 \pm 0.4
amphiregulin	4.8	2.5 \pm 1.0	1.0 \pm 0.8	4.9	2.0 \pm 0.7	1.6 \pm 0.5	4.3	1.4 \pm 0.6	0.8 \pm 0.0
ADAMTS-1	1.9	0.8 \pm 0.3	1.9 \pm 2.0	1.4	1.2 \pm 0.1	3.6 \pm 3.7	1.4	1.2 \pm 0.2	1.1 \pm 0.5
TIMP-1	1.5	1.6 \pm 0.6	1.5 \pm 0.5	1.5	1.4 \pm 0.3	1.3 \pm 0.2	0.8	1.2 \pm 0.0	1.3 \pm 0.3
Cox-2	8.5	1.2 \pm 0.1	13.3 \pm 7.7	3.6	1.7 \pm 0.3	4.1 \pm 0.7	2.3	1.8 \pm 0.2	3.2 \pm 1.9

Results are shown as fold change from Affymetrix analysis (A). Gene expression patterns could be partially confirmed by PCR or Western blot (WB). Results shown derive from at least 4 independent experiments.

4.2.7 Other regulated genes

Other genes that showed a strong upregulation and may be worthwhile to investigate further include the MAPK phosphatases (MKPs), also known as dual specificity phosphatases (DUSPs). These phosphatases regulate the activity of MAPKs and could therefore play a major role in the phenotypic modulation of VSM cells. In this study, DUSP1, DUSP5 and DUSP6 were found to be upregulated via either Par-1 or Par-4 (Fig. 27, Tables 15-18). Furthermore, Par-1-regulated prothrombotic gene products (coagulation factors, plasminogen activators and their inhibitors; Fig. 27, Tables 15-18) from the coagulation cascade could play an important role in the phenotypic modulation of VSM cells and require further analysis.

5 Discussion

5.1 ET_B receptor localisation and its effects on signalling

It is known that the localisation of a given GPCR within plasma membrane domains can define the cellular signalling events in both, qualitative and quantitative terms. This study used detergent-free caveolae preparations and total internal reflection fluorescence microscopy (TIRFM) to show that different ET_B receptor constructs are either enriched in caveolae or evenly distributed at the plasma membrane of COS7, HEK293 and MDCK cells. In analogy to the oxytocin receptor (Guzzi et al., 2002), fusing the ET_B receptor to caveolin-2 artificially targeted the receptor to caveolae, thereby serving as a positive control for a caveolae-localised ET_B receptor. It could be shown that N-terminal proteolysis or glycosylation of the ET_B receptor as well as the cellular background determines the caveolar enrichment of this receptor and its subsequent signalling events leading to the transactivation of the EGFR. Surprisingly, these differences had no discernible impact on the EGFR-mediated downstream activation of ERK1/2.

5.1.1 ET_B receptor localisation is cell type-specific

Various methods are in use to investigate the localisation of GPCRs in plasma membrane subdomains, however, they are controversially discussed. A number of approaches have been used to analyse the localisation of the ET_B receptor in caveolae/lipid rafts; yet, they all came up with a less than satisfactory answer. In HEK293 fibroblasts, which natively do not form caveolae, only the co-transfection of caveolin-1 led to an enrichment of the ET_B receptor in detergent-resistant (Triton X 100) membranes (Yamaguchi et al., 2003). However, only 10% of the ET_B receptors expressed were found in these plasma membrane microdomains; a less than satisfactory result. Moreover, it has to be questioned whether these detergent-resistant membranes resemble caveolae or lipid rafts as treatment of cells with detergents may generate clusters of lipid rafts that do not exist in intact cells (Mayor and Maxfield, 1995). In primary astrocytes, it has been shown that the ET-1-induced phosphorylation of ERK1/2 requires a caveolar localisation of the ET_B receptor (Teixeira et al., 1999). These findings are mostly based on cholesterol depletion by filipin III, which is a poorly specific pharmacological modulation. Not only filipin III but also β -methylcyclodextrin is commonly used to disrupt lipid rafts to investigate their role in certain cellular events. However, the specificity of these compounds for

lipid rafts is controversial. Treatment of cells with filipin III leads to leakage of cellular components by inducing a structural disorder in sterol-containing membranes (Gimpl and Gehrig-Burger, 2007). It is very unlikely that only lipid rafts and no other membranes are affected. Moreover, filipin III has cytotoxic properties and the use of it will probably lead to many other, more profound effects than cholesterol depletion. Treatment of cells with β -methylcyclodextrin forms water-soluble inclusion complexes and thereby enhances the solubility of cholesterol (Gimpl and Gehrig-Burger, 2007). It selectively prefers cholesterol to other membrane lipids, but again specificity for lipid rafts is questioned. In this work, caveolar localisation of the ET_B receptor could be studied without gross cellular perturbation by using various ET_B receptor constructs. The localisation of the full-length ET_B receptor in caveolae differs in COS7 and MDCK cells depending on its N-terminal proteolysis. In MDCK cells, only the full-length ET_B receptor was enriched in caveolae, whereas in COS7 cells the N-terminally truncated ET_B receptor was enriched in these plasma membrane microdomains. The receptor construct- and cell type-specific differences of the ET_B receptor localisation were not only determined by detergent-free caveolae preparations but also confirmed by binding analyses and TIRFM, a method that allows the analysis of receptor accumulation in plasma membrane subdomains in living cells (Tagawa et al., 2005). It is noteworthy, that the caveolar localisation of the ET_B receptor is not indicative of its internalisation, as it is well known that the full-length ET_B receptor internalises via a clathrin-dependent mechanism (Oksche et al., 2000). Therefore, caveolar localisation of the receptor might be important for its coupling to downstream signalling molecules.

A cell type-specific difference in the localisation of GPCRs is not a unique feature for the ET_B receptor as it has already been observed for other receptors. In cardiomyocytes, β_1 - and β_2 -adrenoceptors exhibit an enrichment in caveolae (Rybin et al., 2000; Ostrom et al., 2001). In contrast, no such enrichment can be seen for the same receptors expressed in rat aortic smooth muscle cells (Ostrom et al., 2002). So far, the reasons for this distinct localisation patterns in various cell types remain to be resolved. As COS7 cells are unpolarised fibroblast-like kidney cells of a monkey, whereas MDCK cells are polarised epithelial kidney cells of a dog. It is possible that the polarisation of a cell might play a role in caveolae composition. Moreover, the expression pattern of caveolin-1, -2 and -3 and the subsequent lipid and protein recruitment into caveolae might be of interest. Likewise, the importance of caveolar receptor localisation for its downstream signalling may depend on the cell type the receptor is investigated in. Previous experiments (Grantcharova et al., 2006a; Grantcharova et al., 2006b) showed, that activated ET_B

receptor variants differ in their ability to induce the phosphorylation of ERK1/2. Thus, the finding that the phosphorylation of ERK1/2 upon ET_B receptor stimulation is largely independent of the ET_B receptor localisation in COS7, HEK293 and MDCK cells, does not exclude receptor-dependent differences of downstream events in other cell types. Vice versa, the finding that receptor localisation in caveolae triggers specific signalling cascades in a certain cell type should not be generalised regarding other cell types.

5.1.2 ET_B receptor localisation has little impact on EGFR ligand shedding

To find out, which EGFR ligands are shed upon ET_B receptor stimulation and whether the localisation of the ET_B receptors is important for the EGFR ligand shedding and subsequent transactivation of the EGFR, transfection of COS7 and HEK293 cells with the different ET_B receptor constructs and AP-tagged EGFR ligand proforms were performed according to Sahin and colleagues (2006). It could be shown that none of the ET_B receptor constructs used, induced the shedding of betacellulin and EGF upon stimulation with IRL1620 in either cell type. An increased shedding of betacellulin in VSM cells was described by Sanderson et al. (2006) upon stimulation with ET-1. This was, however, most likely triggered by the ET_A receptor, as this is the endothelin receptor predominantly expressed in VSM cells.

It is well known that the ectodomain shedding of EGFR ligands can be induced via GPCR stimulation or via phorbol ester-induced activation of classical or novel protein kinase C isoenzymes. The pattern of ET_B receptor-induced ectodomain shedding of betacellulin and EGF as revealed in this study, resembles that of phorbol ester-stimulated mouse embryonic fibroblasts (Sahin et al., 2004). One has to note, however, that despite mimicking a protein kinase C pattern, the GPCR-induced EGFR transactivation might involve independent or redundant pathways, as the GPCR-induced transactivation is not sensitive to protein kinase C inhibition in COS7 cells (Prenzel et al., 1999).

The shedding of amphiregulin and HB-EGF seemed to be disfavoured if receptors were localised to caveolae in COS7 but not HEK293 cells. Both ligands were shed more efficiently when the respective stimulated ET_B receptor construct was evenly distributed over the plasma membrane of COS7 cells. Even though the shedding of HB-EGF and amphiregulin has been reported in various cell types after stimulation of different GPCRs (see Tokumaru et al., 2000; Gschwind et al., 2003; Higashiyama and Nanba, 2005; Mifune et al., 2005 for examples), the importance of caveolar localisation has not been investigated.

The shedding of TGF- α and epiregulin seemed to occur independent of caveolar localisation of the ET_B receptor constructs in COS7 cells. In caveolae-free HEK293 cells, the shedding could not depend on a caveolar localisation of the ET_B receptor. In this cell type the shedding of TGF- α was highest, when the stimulated receptor was not truncated or coupled to caveolin-2. Furthermore, in HEK293 cells, N-terminal truncation of the ET_B receptor might have a large impact on EGFR shedding as none of the ligands was processed upon stimulation of the Δ 2-64.ET_B.GFP. Thus, the GPCR-induced shedding and EGFR transactivation may not only depend on the localisation of the GPCR, but also on its processing and on the cellular expression of different EGFR ligands in different cell types.

It can be concluded that the signalling of stimulated ET_B receptor constructs differed depending on the cell type. In COS7 cells, ET_B receptor-induced shedding of EGFR ligands was stronger when the receptor was evenly distributed over the plasma membrane, whereas in HEK293 cells the shedding was reduced when the ET_B receptor was N-terminally truncated. In addition, the co-localisation of GPCRs with EGFR ligands or the EGFR may further modulate the shedding activity and the resulting EGFR transactivation. It is noteworthy, that the EGFR, which has recently been shown to accumulate in flat cholesterol-rich lipid rafts, but not in caveolae (reviewed in Pike, 2005), was also not found to co-localise with caveolin-1 in this study. However, it should be noted that the localisation of the EGFR seems to vary a lot. It was found to localise to caveolae as well as to non-caveolin fractions in different cell types, among others, in A431 and PAC-I (a VSM cell line) cells (Waugh et al., 1999; Waugh et al., 2001; Liu et al., 2007). Even less is known about the localisation of EGFR ligands in plasma membrane microdomains. In the present work, the EGFR ligands poorly co-localised with caveolin-1, indicating no caveolar enrichment of these proteins. Thus, non-caveolar ET_B receptor variants may induce shedding of EGFR ligands more efficiently due to their proximity. The differential localisation of caveolin-1 and EGFR ligands provides no clear information about their possible localisation in non-caveolar, but cholesterol-enriched rafts. It is therefore necessary to characterise the targeting of EGFR ligands into plasma membrane microdomains in more detail and thereby get a better understanding of the GPCR-induced transactivation of the EGFR.

5.1.3 ET_B receptor localisation only poorly correlates with ERK1/2 phosphorylation

The EGFR transactivation is one possibility to control the phosphorylation state of MAPKs via the canonical Ras/Raf/MEK/ERK signalling cascade. The intensity and kinetics of ERK1/2 phosphorylation can define the proliferation or differentiation of a cell (Reusch et al., 2001a; Rimoldi et al., 2003; Grantcharova et al., 2006b). An activation of the ET_B receptor leads to the phosphorylation of ERK1/2 in various cell types (see Vichi et al., 1999; Schinelli et al., 2001; Cheng et al., 2003; Dschietzig et al., 2003 for examples). Furthermore it has been shown that, upon stimulation of Rat-1 cells with ET-1, an EGF receptor transactivation occurs (Daub et al., 1996; Gschwind et al., 2001). However, ET-1 does not distinguish between ET_A and ET_B receptors. Therefore it is difficult to conclude which of the two receptors was activated and led to the transactivation. In another study it has been shown that the angiotensin-1 receptor localises to caveolae and that caveolin is essential for the angiotensin II induced EGF receptor transactivation in VSM cells (Shah, 2002). Relying on these previous studies, this work focused on the ET_B receptor-induced activation of ERK1/2 with regard to the caveolar localisation of the ET_B receptor in COS7, HEK293 and MDCK cells. In contrast to HEK293 and VSM cells (Grantcharova et al., 2006b), stimulation of various ET_B receptor constructs induced no significant differences in ERK1/2 activation in COS7 or MDCK cells. In COS7 cells, caveolae-localised ET_B receptors induced a less sustained activation of ERK1/2 as compared to non-caveolar ET_B receptor variants. Interestingly, in MDCK cells no such differences were observed and the ERK1/2 phosphorylation was only transient. This in contrast to a study on the oxytocin receptor, where the localisation outside of caveolae triggered a long-lasting activation of ERK1/2 in MDCK cells (Rimoldi et al., 2003).

In HEK293 cells, stimulation of ERK1/2 was only long-lasting, when the full-length unmodified ET_B receptor was stimulated. The localisation-independent activation patterns of ERK1/2 are in contrast to a study focusing on the localisation of the oxytocin receptor and its effects on signalling: stimulation of the oxytocin receptor results in either a proliferative or growth-inhibitory response of MDCK cells (Rimoldi et al., 2003). In that case, localisation in caveolae favoured a transient activation of ERK1/2 and a mitogenic response, whereas the activation was persistent (leading to cell growth inhibition) when the receptor was not enriched in plasma membrane subdomains.

These results indicate that the cell type in which the receptor is expressed appears to play a major role for receptor localisation and subsequent signalling. It is possible that the predominance of the cellular background for the determination of the kinetic and intensity of downstream signalling towards ERK1/2 include further signal integration downstream of the transactivated EGFR, e.g. via arrestin-mediated mechanisms (DeWire et al., 2007), via signalling through the non-receptor tyrosine kinases Pyk2 and Src (Shah et al., 2006) or via a PKC-mediated phosphorylation of the Ras/Raf complex (Marais et al., 1998). Besides the feed of pre-existing signalling proteins into the mitogenic pathway, a transcriptional regulation level may provide an additional mechanism for cell type-specific responses such as a long-lasting kinetic of ERK1/2 phosphorylation.

5.2 Par-mediated gene expression modification

To obtain a better insight into the molecular basis of phenotypic modulation of VSM cells upon stimulation of Par-1 or Par-4 with thrombin or TRAP (Reusch et al., 2001a), a genome-wide microarray approach was used to identify novel genes that might account for the phenotypic outcome of VSM cells. As it has been suggested that the activation kinetics ERK1/2 can define the proliferation or differentiation of a cell (Marshall, 1995), a specific focus was laid on mechanisms that may contribute to the induction of a long-lasting activity of this kinase. Since the onset of a second phase of sustained ERK1/2 activation is observed about 60 min after thrombin or TRAP stimulation, downregulation of genes, which would not immediately translate into a lower protein expression, were considered to be less important for this process.

Of the 31099 genes screened, 22 upregulated genes could be related to ERK1/2 signalling and prothrombotic pathways. More detailed analyses on four MAPK signalling-related genes, namely amphiregulin, ADAMTS-1, TIMP-1 and MAP3K8, was then performed. Another gene that was highly upregulated, COX-2, was included in this work, as it has been shown to contribute to the regulation of vascular tone by synthesising prostaglandins or prostacyclins (Bagi et al., 2005).

5.2.1 Analysis of novel genes involved in the phenotypic modulation of VSM cells

Expression of all of the selected genes is affected by stimulation of Par-1. However, they differ with respect to the G proteins triggering the alteration in expression. TIMP-1 and MAP3K8 were induced via proteins of the G_i family downstream of Par-1, whereas amphiregulin, ADAMTS-1 and COX-2 were upregulated via $G_{12/13}$ upon Par-1 stimulation. It is well known that different G proteins trigger different signalling events. In one study, the influence of different $G\alpha_q$ family members on VSM cell gene expression was analysed (Peavy et al., 2005), showing similarities to the results obtained in this study. The introduction of constitutive active forms of $G\alpha_q$, $G\alpha_{14}$, and $G\alpha_{15}$ led to induction of overlapping and distinct signalling pathways in VSM cells. Peavy et al. were especially focusing on pro-apoptotic pathways, chiefly investigating the expression of caspase-3. However, they also found a downregulation of amphiregulin mediated by $G\alpha_q$ whereas this study revealed G_i -dependent upregulation. This might represent novel regulation mechanisms of amphiregulin expression. They also observed an upregulation of ADAMTS-1 by $G\alpha_q$ and $G\alpha_{14}$, but not $G\alpha_{15}$. From the microarray analysis obtained in this work it can be added that upon stimulation of the Par-1 receptor this MMP is also regulated by $G_{12/13}$ but not G_i . The same dependency as for ADAMTS-1 (upregulation by $G\alpha_q$ and $G\alpha_{14}$ but not $G\alpha_{15}$) was found for MAP3K8 (also known as Tpl2 or Cot). In contrast, this microarray analysis revealed a regulation of MAP3K8 through G_i proteins. This might be an exclusive signalling event upon Par-1 stimulation. Moreover, Peavy et al. found a remarkable upregulation of COX-2 upon introduction of all different $G\alpha_q$ family members, which they linked to a functional overlap with inositol lipid signalling.

In conclusion, this study confirmed results from previous publications, indicating that the microarray approach is indeed a useful means to analyse gene expression profiles.

5.2.2 Prothrombotic signalling

Confirming earlier expression profiling studies in VSM cells exposed to atherogenic stimuli (Beauchamp et al., 2003), this study found an upregulation of prothrombotic pathways upon Par-1/Par-4 stimulation. With a 38.2 fold change in expression (Fig. 27, Tables 15-17), the plasminogen activator inhibitor (PAI) 2, a serine protease inhibitor with as yet poorly defined function (Medcalf and Stasinopoulos, 2005), was most strongly upregulated in thrombin-stimulated VSM cells. Its closest relative, PAI-1, was also upregulated (6.5 fold; Fig. 27, Tables

15, 17, 18), and appears to be strongly expressed in VSM cells. The upregulation of prothrombotic genes was paralleled by upregulation of the urinary-type plasminogen activator (PLAU) and its receptor PLAUR (Fig. 27, Tables 16, 18). Signalling via PLAU/PLAUR induces a growth arrest of VSM cells (Kunigal et al., 2003) and contributes to the neointima formation in damaged arteries (Carmeliet et al., 1997). These data imply that, upon endothelial damage, the thrombin-induced transcriptional regulation may be part of the signalling mechanism leading to the migration of VSM cells and subsequent neointima formation.

The gene expression pattern found in thrombin-stimulated rat aortic VSM cells in this study partially overlaps with that found in human umbilical artery VSM cells that were exposed to atherogenic stimulation (Beauchamp et al., 2003). In VSM cells, thrombin leads to an upregulation of COX-2 and a subsequent release of prostaglandin E₂ (PGE₂) and prostacyclin (PGI₂) (Hsieh et al., 2008). Alternatively, COX-2 may be induced via sphingosine 1 phosphate (Hsieh et al., 2006), a product of sphingosine kinase 1, which was found to be strongly upregulated upon stimulation with thrombin (Table 15). Despite its well-described upregulation in diseased vessel walls (Pritchard, Jr. et al., 1994), the biological role of COX-2-induced prostaglandin synthesis in VSM cells is less well understood. Microsomal PGE synthase-1 is responsible for both COX-1- and COX-2-dependent PGE₂ synthesis (Camacho et al., 2007). The resulting pro- or antiatherogenic effects of VSM cell-derived prostaglandin synthesis may be controlled by the balance of specific prostaglandin synthases rather than by the global COX activity (Wang et al., 2006). In agreement with biochemical data presented by Wang et al., this present work also found a predominant expression of prostacyclin synthase, which was slightly (statistically not significant) upregulated in TRAP-stimulated VSM cells (data not shown).

5.2.3 EGFR transactivation

Phosphorylation of ERK1/2 via Par-1/Par-4 activation depends on the continuous presence of the activator and is abrogated by inhibition of RNA synthesis or translation (Pérez Sastre et al., 2008). Since thrombin stimulation results in a cleavage of Par-1, either *de novo* synthesis or membrane integration of preformed receptors into the plasma membrane is required. This microarray approach revealed a strong and constant, even slightly increasing expression of Par-1 (fluorescence intensities among the 500 strongest signals). It can be concluded, that the receptor expression may not be a limiting factor for different ERK1/2 signalling kinetics. Of the immediate downstream signalling proteins upon Par-1 and Par-4 stimulation, neither

heterotrimeric G proteins nor PLC β , PKC or Rho-dependent kinase 1 were upregulated upon thrombin or TRAP stimulation. Therefore, the thrombin- and TRAP-induced upregulation of the membrane-attached EGFR ligand proforms amphiregulin and HB-EGF may assist in maintaining the ERK1/2 activation kinetics. In line with this assumption, amphiregulin has been described to promote a long-lived ERK1/2 activation and DNA synthesis in VSM cells (Shin et al., 2003). Moreover, studies on the B cell neoplasia multiple myeloma revealed an upregulation of amphiregulin in primary myeloma cells as compared to normal plasma-blastic cells (Mahtouk et al., 2005). They imply that amphiregulin is responsible for EGFR activation in primary myeloma cells and that it plays a major role in mature plasma cell differentiation. A similar role for amphiregulin in the phenotypic modulation of VSM cells may be conceivable. In the context of neuronal survival and regulation, amphiregulin was observed to be upregulated 12 hours after sciatic nerve injury (Nilsson et al., 2005). Combined with additional findings showing that the EGFR is upregulated upon neuron injury and that amphiregulin also promotes the survival and differentiation of PC12 cells (Kimura and Schubert, 1992), it was suggested that amphiregulin is crucial for nerve regeneration. It is possible that the effect on the phenotypic modulation on nerve cells triggered by amphiregulin, might also account for the phenotypic modulation of VSM cells during the development of arteriosclerosis.

The membrane-bound EGFR ligand proforms are processed by ectodomain shedding through matrix metalloproteinases such as gelatinase- or ADAM-type MMPs. In VSM cells, the gelatinase MMP2, but not MMP9 was found to be constitutively expressed. ADAMTS-1, which is known to be strongly expressed in aortic vascular smooth muscle cells (Jönsson-Rylander et al., 2005), also yielded strong signals in the gene array analysis and was further upregulated after thrombin or TRAP stimulation, indicating that it could be crucial for the ectodomain shedding of amphiregulin and HB-EGF. It should be mentioned that immunoblot analysis of ADAMTS-1 in VSM cells showed a 56-kDa band, which is not compatible with the full-length ADAMTS-1 protein, but may reflect a proteolytic fragment as described earlier (Liu et al., 2005). The expression and regulation of ADAMTS-1 has been studied rather extensively. One work analysed gene expression profiles of ADAMTS-1 upon acute ischemia reperfusion injury, which leads to the lack of effective vascular repair responses. ADAMTS-1 showed an increased expression following an ischemia reperfusion protocol, which was confirmed by RT-PCR and immunoblot analysis (Basile et al., 2008). The authors suggest that ADAMTS-1 acts as an inhibitor of angiogenesis by sequestration of VEGF or by activating the release of anti-angiogenic peptides, thereby inhibiting proliferation of cells. This again underlines the potential

of ADAMTS-1 as a mediator in the differentiation of VSM cells. Likewise, ADAMTS-1 has also been suggested as an important biomarker for the phenotypic state of VSM cells. Genes whose expression was regulated in opposing directions by PDGF and hypertrophic stimuli were identified (Kaplan-Albuquerque et al., 2005). It was hypothesised that expression of these genes would be altered during vascular injury. Upon stimulation with PDGF, inducing proliferation of VSM cells, ADAMTS-1 was downregulated (Kaplan-Albuquerque et al., 2005). These observations support our results implying that the upregulation of ADAMTS-1 is a characteristic for the differentiation of VSM cells.

Isoforms of tissue inhibitors of MMPs (TIMPs) regulate the activity of MMPs. TIMP-1 was upregulated in thrombin- and TRAP-treated VSM cells, an effect that is reminiscent of changes of TIMP-1 expression detected after balloon angioplasty in iliac arteries in hypercholesterolemic rabbits (Feldman et al., 2001). Like ADAMTS-1, TIMP-1 was also found to be upregulated by PDGF, whereas a hypertrophic stimulus induced a downregulation (Kaplan-Albuquerque et al., 2005). The opposing expression patterns for ADAMTS-1 and TIMP-1 correlate well with their opposing actions, as TIMP-1 is an inhibitor of ADAMTS-1. Surprisingly, this work does not reveal such opposing regulation. However, it was found that ADAMTS-1 is regulated via $G_{12/13}$ and TIMP-1 via G_i proteins, suggesting that the different G proteins that are coupled to Par1 can induce different signalling cascades. A similar effect to TIMP-1, but slightly weaker, was found for TIMP-3 (about 1.3-fold induction), whereas TIMP-2 was not affected by the Par-1- or Par-4-mediated signalling even though it was strongly expressed. In conclusion, beyond their substrate expression, the transcriptional regulation of MMPs and their inhibitors does not provide additional clues for the understanding of the sustained kinetic of EGFR transactivation.

5.2.4 MAPK signalling

Like in Rat-1, COS7 and HEK293 cells (Prenzel et al., 1999), the thrombin- and TRAP-induced transactivation of the EGFR feeds into the intracellular Ras/Raf/MEK/ERK signalling cascade in VSM cells (Reusch et al., 2001a). None of the signalling proteins that are part of the canonical MAPK cascade (EGFR, Grb2, Sos1/2, Ras-isoforms, c-Raf, MEK1/2 and ERK1/2) were upregulated by more than 1.4-fold upon thrombin or TRAP stimulation of VSM cells. Interestingly, another kinase leading to the downstream activation of MEK1/2 (Dumitru et al., 2000) and ERK1/2 -MAP3K8 (synonyms: Cot, Tpl2)- was upregulated upon stimulation with thrombin or TRAP. An HGF- or VEGF-induced upregulation of MAP3K8 leading to a robust

proliferative response of human endothelial cells has been shown before (Gerritsen et al., 2003), however, only little is known about the upstream regulators of MAP3K8. It has been suggested that TNF α and IL-1 β could activate MAP3K8 and, in turn, the ERK1/2- and JNK-families of MAPK in MEF cells (Das et al., 2005). From this study it can be added that the Par-1-induced transcriptional regulation of MAP3K8 is relayed via PTX-sensitive G_i proteins. It is tempting to speculate that Par1-activated G_i proteins activate ERK1/2 via MAP3K8 whereas the G_{12/13} proteins might address the classic Ras/Raf/MEK/ERK signalling cascade. More detailed information about biological functions of MAP3K8 and its regulatory networks could come forward in the near future due to the recent development of small molecule inhibitors that selectively target this kinase (Hall et al., 2007).

Dual specificity phosphatases (DUSPs) regulate the activity of MAPKs including ERK1/2 by inducing signal termination. All DUSPs have different substrate specificities (Owens and Keyse, 2007), but the phosphatases upregulated in this study all have the potential to dephosphorylate and inactivate ERK1/2. The data from this work confirms recent results on the thrombin-induced upregulation of DUSP1 expression (Kinney et al., 2008) and upholds the concept that an upregulation of DUSP1 represents a transcriptionally regulated negative feedback loop (Bokemeyer et al., 1998). It is however noteworthy, this upregulation of DUSP1 (Fig. 27, Tables 15-18) is not strictly restricted to ERK1/2 signalling (Zhao et al., 2003; Sarközi et al., 2007; Kinney et al., 2008) and that a vascular injury, induced by e.g. balloon catheter, can result in a downregulation of DUSP1 expression (Lai et al., 1996). This genome wide microarray analysis showed, that besides DUSP1 also DUSP5 and DUSP6 (Fig. 27, Tables 15-18) are strongly upregulated upon stimulation with thrombin or TRAP and therefore may be able to terminate ERK1/2 signalling. DUSP5 and DUSP6 show a more pronounced selectivity towards ERK1/2 (Muda et al., 1996; Mandl et al., 2005) and, thus, these two DUSPs could be required for the ERK1/2 signal termination in VSM cells. In human proximal tubular cells that overexpress a constitutively active MEK1 construct (Sarközi et al., 2007), a similar pattern of DUSP1, DUSP5 and DUSP6 expression has been found. It is likely that the MEK/ERK pathway also accounts for this feedback regulation in VSM cells. In the near future, detailed investigations should be undergone to understand the possible role of DUSPs in the phenotypic modulation of VSM cells.

In conclusion, we provide novel insights in the complex signalling cascade of long-lived ERK1/2 phosphorylation and subsequent phenotypic modulation of VSM cells. Regulated genes such as the DUSPs as well as MAP3K8, but also PAI-2 and PLA2 seem to be of great importance and require further analysis to determine their role in the phenotypic outcome of cells. However, it

should be noted that the exact regulatory mechanisms underlying this complex long-lasting ERK1/2 signalling cascade are still not fully understood. More information needs to be gained to provide novel ideas for a more efficient pharmacological modulation in diseased states. These approaches could help to prevent the progression of arteriosclerosis or exposure of VSM cells to serum components and stimulation of protease-activated receptors after vascular injury.

Summary

Despite compelling evidence that the phenotypic modulation of vascular smooth muscle (VSM) cells plays a key role in the development and progression of arteriosclerosis, we are just beginning to unravel the molecular mechanisms and factors that control this process. It is proposed that the duration of an epidermal growth factor receptor (EGFR)-mediated ERK1/2 (extracellular signal-regulated kinases 1/2) phosphorylation controls the phenotypic outcome of a cell. In that context, long-lasting ERK1/2 kinetics, as opposed to short-lived kinetics, have been linked to cellular differentiation in various cell types. However, the exact mechanisms controlling the activation of ERK1/2 are still not fully understood. This study sought to understand the phosphorylation kinetics of ERK1/2 by focusing on two different aspects.

The endothelin B (ET_B) receptor is a G protein-coupled receptor (GPCR) mainly expressed in endothelial cells. In diseased states, however, it is highly upregulated in VSM cells, suggesting an important role during the development of arteriosclerosis. Upon ligand binding the ET_B receptor can undergo a proteolytic N-terminal cleavage resulting in an unglycosylated, truncated receptor. It was investigated whether the ET_B receptor processing affects its localisation to plasma membrane microdomains and whether the localisation of the receptor has an impact on its mitogenic signalling in COS7, HEK293 and MDCK cells. The subcellular localisation of various ET_B receptor constructs, EGFR ligands and the EGFR itself was analysed by performing detergent-free caveolae preparations and total internal reflection fluorescence microscopy (TIRFM). Furthermore, the ET_B receptor-induced ectodomain shedding of EGFR ligands and the subsequent transactivation of the EGFR and its downstream signalling was investigated by performing shedding assays and ERK1/2 phosphorylation analyses. In COS7 cells, the N-terminally truncated but not the full-length or glycosylation-deficient ET_B receptor localised to caveolae. In contrast, in MDCK cells, only the full-length ET_B receptor was enriched in caveolae. In HEK293 cells, which do not form caveolae, only ET_B receptor constructs that were fused to caveolin-2, localised to low-density plasma membrane microdomains. When accumulated in caveolae, activation of the ET_B receptor disfavoured the shedding of EGF receptor ligands in COS7 cells. Nonetheless, the activation of ERK1/2 was efficient and long lasting. In HEK293 cells, the shedding activity was impaired by N-terminal truncation but not by simple removal of glycosylation of the ET_B receptor. The subsequent ERK1/2 phosphorylation was long lasting only for the full-length ET_B receptor. In MDCK cells, activation of ERK1/2 was

monophasic irrespective of a caveolar accumulation of the ET_B receptor. It can be concluded that the receptor localisation within plasma membrane microdomains is cell type-specific. In addition, a caveolar enrichment of ET_B receptors does not facilitate the release of EGF receptor ligands. Taken together these results suggest that cell type-specific mechanisms beyond receptor structure and localisation determine the kinetic properties of ERK1/2 phosphorylation.

Since the cellular background is based on protein composition and transcriptional responses, a genome-wide microarray approach was used to analyse the molecular basis of a long-lasting ERK1/2 phosphorylation in VSM cells. The protease-activated receptors (Par)-1 and -4 of neonatal rat aortic VSM cells were stimulated with thrombin, with a Par-1-selective thrombin receptor-activating peptide (TRAP), and with TRAP upon treatment with G_i-uncoupling pertussis toxin for 2 h to focus on mechanisms that may contribute to the induction of a long-lasting activity of ERK1/2. Gene expression was compared to unstimulated VSM cells and analysed using confidence analysis. Of the 31099 genes screened, 141 differentially regulated genes could be mapped to known signalling pathways of the KEGG pathway database. Special focus was laid on prothrombotic and MAPK signalling pathways of which 32 genes were regulated (22 upregulated genes) upon stimulation of Par-1 or Par-4. Among them were the EGFR ligands amphiregulin and HB-EGF (heparin-binding EGF-like growth factor), extracellular matrix components, MAPKs and their inhibitors, transcription factors, and plasminogen activator inhibitors. Five genes, namely amphiregulin, MAP3K8, ADAMTS (a disintegrin and metalloproteinase with thrombospondin motif)-1, TIMP (tissue inhibitor of metalloproteinases)-1 and COX (cyclooxygenase)-2 were investigated in more detail and their expression was reassessed by RT-PCR and immunoblot analyses. The data obtained from the microarray studies suggest novel important roles for amphiregulin, ADAMTS-1, MAP3K8, TIMP-1 and COX-2 in the phenotypic modulation of VSM cells. They might function as intermediates in the expression of contractile proteins. For future experiments, the role of the differentially regulated genes in the long-lasting activation of ERK1/2 and subsequent phenotypic modulation of VSM cells needs to be addressed by performing siRNA experiments or by applying small molecules that selectively inhibit the addressed protein. These approaches may help to better understand and also to prevent the progression of arteriosclerosis.

Zusammenfassung

Obwohl bekannt ist, dass eine phänotypische Veränderung glatter Gefäßmuskelzellen zur Entstehung und Entwicklung von Arteriosklerose beiträgt, so sind die molekularen Grundlagen dieser Veränderung noch immer nicht vollständig aufgeklärt. Eine Hypothese besagt, dass die Dauer einer EGF (epidermal growth factor)-Rezeptor-vermittelten Phosphorylierung der MAP (mitogen-activated protein)-Kinasen ERK1/2 (extracellular signal-regulated kinases 1/2) diesen Prozess kontrolliert. In diesem Zusammenhang wurde für verschiedene Zelltypen gezeigt, dass eine lang anhaltende Aktivierung von ERK1/2 zu einer Differenzierung von Zellen führt, während eine nur kurzlebige Aktivierung die Proliferation einer Zelle begünstigt, jedoch ist der genaue Mechanismus weiterhin nicht vollständig aufgeklärt. Diese Arbeit zielte darauf ab die verschiedenen Kinetiken der ERK1/2 Phosphorylierung aus zwei verschiedenen Gesichtspunkten zu analysieren.

Der Endothelin B (ET_B) Rezeptor gehört zur Familie der G-Protein-gekoppelten Rezeptoren (GPCR) und wird hauptsächlich in Endothelzellen exprimiert. Einzig für Krankheitszustände wie Arteriosklerose wurde gezeigt, dass der Rezeptor auch in glatten Gefäßmuskelzellen sehr stark exprimiert wird und somit eine wichtige Rolle in der Entwicklung dieser Krankheit spielen könnte. Nachdem der Rezeptor seinen Liganden gebunden hat, erfährt er eine N-terminale Proteolyse, wodurch ein verkürzter und unglycosylierter Rezeptor entsteht. In COS7-, HEK293- und MDCK-Zellen wurde untersucht, ob diese Rezeptorprozessierung einen Einfluss auf die Lokalisation des Rezeptors in Plasmamembran-Mikrodomänen hat und ob dies seine Signaltransduktion beeinflusst. Mittels detergensfreier Präparation von Caveolae sowie TIRF (total internal reflection fluorescence)-Mikroskopie wurde die subzelluläre Lokalisation verschiedener ET_B-Rezeptorkonstrukte sowie des EGF-Rezeptors und dessen Liganden untersucht. Weiterhin, wurde das ET_B-Rezeptor-induzierte Spalten (Shedding) von EGF-Rezeptorliganden und die anschließende Transaktivierung des EGF-Rezeptors sowie die Aktivierung von ERK1/2 analysiert. Während in COS7-Zellen der gespaltene, jedoch nicht der ungespaltene ET_B-Rezeptor in Caveolae angereichert war, zeigte der ungespaltene ET_B-Rezeptor eine caveoläre Anreicherung in MDCK-Zellen. In HEK293-Zellen, welche keine Caveolae bilden, war der ET_B-Rezeptor nur dann in Plasmamembran-Mikrodomänen angereichert, wenn er mit Caveolin-2 fusioniert war. Stimulation eines caveolär akkumulierten ET_B-Rezeptors resultierte in COS7-Zellen in einem weniger effizienten Shedding von EGF-Rezeptorliganden. Die Aktivierung von ERK1/2 war jedoch unabhängig von der Lokalisation effizient und lang

anhaltend. In HEK293-Zellen war die Shedding-Aktivität zusätzlich von der N-terminalen Proteolyse des ET_B-Rezeptors, jedoch nicht vom Glykosylierungsstatus des Rezeptors beeinflusst. Die anschließende Phosphorylierung von ERK1/2 war aber nur lang anhaltend, wenn der Rezeptor nicht prozessiert wurde. In MDCK-Zellen hatte die Prozessierung des ET_B-Rezeptors keinerlei Einfluss auf die Aktivierung von ERK1/2. Diese war stets kurzlebig. Zusammenfassend kann gesagt werden, dass eine zelltyp-spezifische Lokalisation des ET_B-Rezeptors vorliegt. Zusätzlich scheint eine caveoläre Anreicherung des ET_B-Rezeptors das Shedding von EGF-Rezeptorliganden nicht zu begünstigen. Schlussfolgernd kann gesagt werden, dass neben den zelltyp-spezifischen Rezeptorformen und -lokalisationen auch andere Faktoren die Kinetiken der ERK1/2-Phosphorylierung beeinflussen. Da auch das zelluläre Proteom sowie transkriptionelle Mechanismen die Signaltransduktion beeinflussen, wurde genomweit untersucht, inwiefern eine Par-1 und -4-induzierte lang anhaltende ERK1/2-Aktivierung transkriptionell reguliert wird.

Die Proteinase-aktivierten Rezeptoren (Par)-1 und -4 neonataler Gefäßmuskelzellen der Ratte wurden mit Thrombin, einem Par-1-selektiven Thrombin-Rezeptor-aktivierendem Peptid (TRAP) sowie mit TRAP nach Vorbehandlung mit Pertussistoxin, einem G_i-Inhibitor, für 2 h stimuliert. Die Genexpression dieser Proben wurde mit der in unbehandelten Gefäßmuskelzellen verglichen und mittels Konfidenzanalyse analysiert. 31099 Gene wurden untersucht, wovon 141 differentiell regulierte Gene verschiedenen Signaltransduktionswegen aus der KEGG-Datenbank zugeordnet werden konnten. Besonderer Fokus galt den prothrombotischen und den MAP-Kinase-Signalwegen, denen 32 differentiell regulierte (22 hochregulierte) Gene zugeordnet werden konnten. Zu ihnen gehörten die EGF-Rezeptorliganden Amphiregulin und HB-EGF (heparin-binding EGF-like growth factor), extrazelluläre Matrixkomponenten, MAP-Kinasen und deren Inhibitoren sowie Plasminogenaktivator-Inhibitoren. Die fünf Gene Amphiregulin, MAP3K8, ADAMTS (a disintegrin and metalloproteinase with thrombospondin motif)-1, TIMP (tissue inhibitor of metalloproteinases)-1 und COX (Cyclooxygenase)-2 wurden genauer analysiert und ihre Expression wurde mittels RT-PCR und Immunoblot bestimmt. Die durch die Genchip-Analysen erhaltenen Daten deuten darauf hin, dass Amphiregulin, ADAMTS-1, MAP3K8, TIMP-1 und COX-2 eine wichtige Rolle in der phänotypischen Modulation von glatten Gefäßmuskelzellen spielen. Sie könnten wichtige Intermediate bei der Expression kontraktiler Proteine darstellen. In weitergehenden Experimenten sollte die Rolle dieser Proteine in der lang anhaltenden Aktivierung von ERK1/2 durch siRNA oder kleine inhibitorische Moleküle weiter untersucht werden. Diese Ansätze könnten zu einem besseren Verständnis der Entstehung von Arteriosklerose führen und neue Möglichkeiten liefern, eine Progression zu verhindern.

Erklärung

„Ich, Solveig Großmann, erkläre, dass ich die vorgelegte Dissertationsschrift mit dem Thema: ‚Long-lasting activation of extracellular signal-regulated kinases 1/2: importance of G protein-coupled receptor localisation and transcriptional responses‘ selbst verfasst und keine anderen als die angegebenen Quellen und Hilfsmittel benutzt, ohne die (unzulässige) Hilfe Dritter verfasst und auch in Teilen keine Kopien anderer Arbeiten dargestellt habe.“

Ort, Datum

Unterschrift

Literature

Akiyama N, Hiraoka O, Fujii Y, et al. Biotin derivatives of endothelin: utilization for affinity purification of endothelin receptor. *Protein Expr Purif* 1992;3:427-33.

Anderson RGW. The caveolae membrane system. *Annu Rev Biochem* 1998;67:199-225.

Anderson RGW and Jacobson K. A role for lipid shells in targeting proteins to caveolae, rafts, and other lipid domains. *Science* 2002;296:1821-5.

Asakura M, Kitakaze M, Takashima S, et al. Cardiac hypertrophy is inhibited by antagonism of ADAM12 processing of HB-EGF: metalloproteinase inhibitors as a new therapy. *Nat Med* 2002;8:35-40.

Axelrod D. Total internal reflection fluorescence microscopy in cell biology. *Methods Enzymol* 2003;361:1-33.

Badimon JJ, Weng D, Chesebro JH, Fuster V, Badimon L. Platelet deposition induced by severely damaged vessel wall is inhibited by a boroarginine synthetic peptide with antithrombin activity. *Thromb Haemost* 1994a;71:511-6.

Badimon L, Badimon JJ, Lassila R, et al. Thrombin regulation of platelet interaction with damaged vessel wall and isolated collagen type I at arterial flow conditions in a porcine model: effects of hirudins, heparin, and calcium chelation. *Blood* 1991;78:423-34.

Badimon L, Meyer BJ, Badimon JJ. Thrombin in arterial thrombosis. *Haemostasis* 1994b;24:69-80.

Bagi Z, Erdei N, Toth A, et al. Type 2 diabetic mice have increased arteriolar tone and blood pressure: enhanced release of COX-2-derived constrictor prostaglandins. *Arterioscler Thromb Vasc Biol* 2005;25:1610-6.

Bar-Shavit R, Benezra M, Eldor A, et al. Thrombin immobilized to extracellular matrix is a potent mitogen for vascular smooth muscle cells: nonenzymatic mode of action. *Cell Regul* 1990;1:453-63.

Basile DP, Fredrich K, Chelladurai B, Leonard EC, Parrish AR. Renal ischemia reperfusion inhibits VEGF expression and induces ADAMTS-1, a novel VEGF inhibitor. *Am J Physiol Renal Physiol* 2008;294:F928-36.

- Beauchamp N, van Achterberg T, Engelse MA, Pannekoek H, de Vries C. Gene expression profiling of resting and activated vascular smooth muscle cells by serial analysis of gene expression and clustering analysis. *Genomics* 2003;82:288-99.
- Bokemeyer D, Lindemann M, Kramer HJ. Regulation of mitogen-activated protein kinase phosphatase-1 in vascular smooth muscle cells. *Hypertension* 1998;32:661-7.
- Bremnes T, Paasche JD, Mehлум A, et al. Regulation and intracellular trafficking pathways of the endothelin receptors. *J Biol Chem* 2000;275:17596-604.
- Brown DA and London E. Functions of lipid rafts in biological membranes. *Annu Rev Cell Dev Biol* 1998;14:111-36.
- Camacho M, Gerboles E, Escudero J, et al. Microsomal prostaglandin E synthase-1, which is not coupled to a particular cyclooxygenase isoenzyme, is essential for prostaglandin E2 biosynthesis in vascular smooth muscle cells. *J Thromb Haemost* 2007;5:1411-9.
- Carmeliet P, Moons L, Herbert JM, et al. Urokinase but not tissue plasminogen activator mediates arterial neointima formation in mice. *Circ Res* 1997;81:829-39.
- Carmeliet P. Proteinases in cardiovascular aneurysms and rupture: targets for therapy? *J Clin Invest* 2000;105:1519-20.
- Cheng CM, Hong HJ, Liu JC, et al. Crucial role of extracellular signal-regulated kinase pathway in reactive oxygen species-mediated endothelin-1 gene expression induced by endothelin-1 in rat cardiac fibroblasts. *Mol Pharmacol* 2003;63:1002-11.
- Chini B and Parenti M. G-protein coupled receptors in lipid rafts and caveolae: how, when and why do they go there? *J Mol Endocrinol* 2004;32:325-38.
- Chun M, Liyanage UK, Lisanti MP, Lodish HF. Signal transduction of a G protein-coupled receptor in caveolae: colocalization of endothelin and its receptor with caveolin. *PNAS* 1994;91:11728-32.
- Chun M, Lin HY, Henis YI, Lodish HF. Endothelin-induced endocytosis of cell surface ETA receptors. *J Biol Chem* 1995;270:10855-60.
- Colles SM, Irwin KC, Chisolm GM. Roles of multiple oxidized LDL lipids in cellular injury: dominance of 7 beta-hydroperoxycholesterol. *J Lipid Res.* 1996;37:2018-28.
- Coughlin SR. Thrombin signalling and protease-activated receptors. *Nature* 2000;407:258-64.

- Coughlin SR. Protease-activated receptors in hemostasis, thrombosis and vascular biology. *J Thromb Haemost* 2005;3:1800-14.
- Crotty T, Cai J, Sakane F, et al. Diacylglycerol kinase δ regulates protein kinase C and epidermal growth factor receptor signaling. *PNAS* 2006;103:15485-90.
- Dagassan PH, Breu V, Clozel M, et al. Up-regulation of endothelin-B receptors in atherosclerotic human coronary arteries. *J Cardiovasc Pharmacol* 1996;27:147-53.
- Das S, Cho J, Lambertz I, et al. Tpl2/Cot signals activate ERK, JNK, and NF- κ B in a cell-type and stimulus-specific manner. *J Biol Chem* 2005;280:23748-57.
- Daub H, Weiss UF, Wallasch C, Ullrich A. Role of transactivation of the EGF receptor in signalling by G-protein-coupled receptors. *Nature* 1996;379:557-60.
- Davenport AP. International union of pharmacology. XXIX. Update on endothelin receptor nomenclature. *Pharmacol Rev* 2002;54:219-26.
- Davies MJ, Richardson PD, Woolf N, Katz DR, Mann J. Risk of thrombosis in human atherosclerotic plaques: role of extracellular lipid, macrophage, and smooth muscle cell content. *Br Heart J* 1993;69:377-81.
- Dennis G, Sherman B, Hosack D, et al. DAVID: database for annotation, visualization, and integrated discovery. *Genome Biol* 2003;4:3.
- DeWire SM, Ahn S, Lefkowitz RJ, Shenoy SK. β -arrestins and cell signaling. *Annu Rev Physiol* 2007;69:483-510.
- Dschietzig T, Bartsch C, Richter C, et al. Relaxin, a pregnancy hormone, is a functional endothelin-1 antagonist: attenuation of endothelin-1-mediated vasoconstriction by stimulation of endothelin type-B receptor expression via ERK-1/2 and nuclear factor- κ B. *Circ Res* 2003;92:32-40.
- Dumitru CD, Ceci JD, Tsatsanis C, et al. TNF- α induction by LPS is regulated posttranscriptionally via a Tpl2/ERK-dependent pathway. *Cell* 2000;103:1071-83.
- Dupree P, Parton RG, Raposo G, Kurzchalia TV, Simons K. Caveolae and sorting in the trans-Golgi network of epithelial cells. *EMBO J* 1993;12:1597-605.
- Feldman LJ, Mazighi M, Scheuble A, et al. Differential expression of matrix metalloproteinases after stent implantation and balloon angioplasty in the hypercholesterolemic rabbit. *Circulation* 2001;102:3117-22.

Foster N, Loi TH, Owe-Young R, Stanley KK. Lysosomal traffic of liganded endothelin B receptor. *Biochim Biophys Acta* 2003;1642:45-52.

Fukuroda T, Fujikawa T, Ozaki S, et al. Clearance of circulating endothelin-1 by ETB receptors in rats. *Biochem Biophys Res Commun* 1994;199:1461-65.

Galbiati F, Rafani B, Lisanti MP. Emerging themes in lipid rafts and caveolae. *Cell* 2001;106:403-11.

Galis ZS, Sukhova GK, Lark MW, Libby P. Increased expression of matrix metalloproteinases and matrix degrading activity in vulnerable regions of human atherosclerotic plaques. *J Clin Invest* 1994;94:2493-503.

Gerits N, Kostenko S, Moens U. In vivo functions of mitogen-activated protein kinases: conclusions from knock-in and knock-out mice. *Transgenic Res* 2007;16:281-314.

Gerritsen ME, Tomlinson JE, Zlot C, Ziman M, Hwang S Using gene expression profiling to identify the molecular basis of the synergistic actions of hepatocyte growth factor and vascular endothelial growth factor in human endothelial cells. *Br J Pharmacol* 2003;140:595-610.

Gimpl G and Gehrig-Burger K. Cholesterol reporter molecules. *Biosci Rep* 2007;27:335-58.

Glass CK and Witztum JL. Atherosclerosis: the road ahead. *Cell* 2001;104:503-16.

Grantcharova E, Furkert J, Reusch HP, et al. The extracellular N terminus of the endothelin B (ETB) receptor is cleaved by a metalloprotease in an agonist-dependent process. *J Biol Chem* 2002;277:43933-41.

Grantcharova E, Reusch HP, Beyermann M, Rosenthal W, Oksche A. Endothelin A and endothelin B receptors differ in their ability to stimulate ERK1/2 activation. *Exp Biol Med (Maywood)* 2006a;231:757-60.

Grantcharova E, Reusch HP, Grossmann S, et al. N-terminal proteolysis of the endothelin B receptor abolishes its ability to induce EGF receptor transactivation and contractile protein expression in vascular smooth muscle cells. *Arterioscler Thromb Vasc Biol* 2006b;26:1288-96.

Gschwind A, Zwick E, Prenzel N, Leserer M, Ullrich A. Cell communication networks: epidermal growth factor receptor transactivation as the paradigm for interreceptor signal transmission. *Oncogene* 2001;20:1594-600.

Gschwind A, Hart S, Fischer OM, Ullrich A. TACE cleavage of proamphiregulin regulates GPCR-induced proliferation and motility of cancer cells. *EMBO J* 2003;22:2411-21.

Guzzi F, Zanchetta D, Cassoni P, et al. Localization of the human oxytocin receptor in caveolin-1 enriched domains turns the receptor-mediated inhibition of cell growth into a proliferative response. *Oncogene* 2002;21:1658-67.

Hagiwara H, Kozuka M, Sakaguchi H, et al. Separation and purification of 34- and 52-kDa species of bovine lung endothelin receptors and identification of the 34-kDa species as a degradation product. *J Cardiovasc Pharmacol* 1991;17 Suppl 7:S117-8.

Hall JP, Kurdi Y, Hsu S, et al. Pharmacologic inhibition of Tpl2 blocks inflammatory responses in primary human monocytes, synoviocytes, and blood. *J Biol Chem* 2007;282:33295-304.

Hansson GK. Cell-mediated immunity in atherosclerosis. *Curr Opin Lipidol* 1997;8:301-11.

Harder T, Scheiffele P, Verkade P, Simons K. Lipid domain structure of the plasma membrane revealed by patching of membrane components. *J Cell Biol* 1998;141:929-42.

Haynes WG and Webb DJ. Contribution of endogenous generation of endothelin-1 to basal vascular tone. *Lancet* 1994;344:852-4.

Henley JR, Krueger EWA, Oswald BJ, McNiven MA. Dynamin-mediated internalization of caveolae. *J Cell Biol* 1998;141:85-99.

Higashiyama S, Ibrahim J, Miller J, Fiddes J, Klagsbrun M. A heparin-binding growth factor secreted by macrophage-like cells that is related to EGF. *Science* 1991;251:936-9.

Higashiyama S and Nanba D. ADAM-mediated ectodomain shedding of HB-EGF in receptor cross-talk. *Biochim Biophys Acta* 2005;1751:110-7.

Hirano K. The roles of proteinase-activated receptors in the vascular physiology and pathophysiology. *Arterioscler Thromb Vasc Biol* 2007;27:27-36.

Hollenberg MD and Compton SJ. International union of pharmacology. XXVIII. proteinase-activated receptors. *Pharmacol Rev* 2002;54:203-17.

Hsieh H, Wu C, Sun C, et al. Sphingosine-1-phosphate induces COX-2 expression via PI3K/Akt and p42/p44 MAPK pathways in rat vascular smooth muscle cells. *J Cell Physiol* 2006;207:757-66.

Hsieh H, Sun C, Wang T, Yang C. PKC- δ /c-Src-mediated EGF receptor transactivation regulates thrombin-induced COX-2 expression and PGE₂ production in rat vascular smooth muscle cells. *Biochim Biophys Acta* 2008;1783:1563-75.

Hunley TE and Kon V. Update on endothelins - biology and clinical implications. *Pediatr Nephrol* 2001;16:752-62.

Inoue A, Yanagisawa M, Kimura S, et al. The human endothelin family: three structurally and pharmacologically distinct isopeptides predicted by three separate genes. *PNAS* 1989;86:2863-7.

Ishihara H, Connolly AJ, Zeng D, et al. Protease-activated receptor 3 is a second thrombin receptor in humans. *Nature* 1997;386:502-6.

Iwasaki S, Homma T, Matsuda Y, Kon V. Endothelin receptor subtype B mediates autoinduction of endothelin-1 in rat mesangial cells. *J Biol Chem* 1995;270:6998-7003.

Johannes L and Lamaze C. Clathrin-dependent or not: is it still the question? *Traffic* 2002;3:443-51.

Jönsson-Rylander AC, Nilsson T, Fritsche-Danielson R, et al. Role of ADAMTS-1 in atherosclerosis: remodeling of carotid artery, immunohistochemistry, and proteolysis of versican. *Arterioscler Thromb Vasc Biol* 2005;25:180-5.

Kaplan-Albuquerque N, Bogaert YE, Van Putten V, Weiser-Evans MC, Nemenoff RA. Patterns of gene expression differentially regulated by platelet-derived growth factor and hypertrophic stimuli in vascular smooth muscle cells: markers for phenotypic modulation and response to injury. *J Biol Chem* 2005;280:19966-76.

Kedzierski M and Yanagisawa M. Endothelin system: the double-edged sword in health and disease. *Annu Rev Pharmacol Toxicol* 2001;41:851-76.

Keren O and Sarne Y. Multiple mechanisms of CB1 cannabinoid receptors regulation. *Brain Res* 2003;980:197-205.

Kimura H and Schubert D. Schwannoma-derived growth factor promotes the neuronal differentiation and survival of PC12 cells. *J Cell Biol* 1992;116:777-83.

Kinney CM, Chandrasekharan UM, Mavrakis L, DiCorleto PE. VEGF and thrombin induce MKP-1 through distinct signaling pathways: role for MKP-1 in endothelial cell migration. *Am J Physiol Cell Physiol* 2008;294:C241-50.

Kochl R, Alken M, Rutz C, et al. The signal peptide of the G protein-coupled human endothelin B receptor is necessary for translocation of the N-terminal tail across the endoplasmic reticulum membrane. *J Biol Chem* 2002;277:16131-8.

Kunigal S, Kusch A, Tkachuk N, et al. Monocyte-expressed urokinase inhibits vascular smooth muscle cell growth by activating Stat1. *Blood* 2003;102:4377-83.

Kurzchalia TV, Dupree P, Monier S. VIP21-caveolin, a protein of the trans-Golgi network and caveolae. *FEBS Letters* 1994;346:88-91.

Kurzchalia TV and Parton RG. Membrane microdomains and caveolae. *Curr Opin Cell Biol* 1999;11:424-31.

Kusserow H and Unger T. Vasoactive peptides, their receptors and drug development. *Basic Clin Pharmacol Toxicol* 2004;94:5-12.

Lai K, Wang H, Lee W, et al. Mitogen-activated protein kinase phosphatase-1 in rat arterial smooth muscle cell proliferation. *J Clin Invest* 1996;98:1560-7.

Le PU, Guay G, Altschuler Y, Nabi IR. Caveolin-1 is a negative regulator of caveolae-mediated endocytosis to the endoplasmic reticulum. *J Biol Chem* 2002;277:3371-9.

Lee RT and Libby P. The unstable atheroma. *Arterioscler Thromb Vasc Biol* 1997;17:1859-67.

Leger AJ, Covic L, Kuliopulos A. Protease-activated receptors in cardiovascular diseases. *Circulation* 2006;114:1070-7.

Lenz JC, Reusch HP, Albrecht N, Schultz G, Schaefer M. Ca²⁺-controlled competitive diacylglycerol binding of protein kinase C isoenzymes in living cells. *J Cell Biol* 2002;159:291-302.

Liebmann C. Regulation of MAP kinase activity by peptide receptor signalling pathway: paradigms of multiplicity. *Cell Signal* 2001;13:777-85.

Lisanti MP, Tang ZL, Sargiacomo M. Caveolin forms a hetero-oligomeric protein complex that interacts with an apical GPI-linked protein: implications for the biogenesis of caveolae. *J Cell Biol* 1993;123:595-604.

Lisanti MP, Tang Z, Scherer PE, et al. Caveolae, transmembrane signalling and cellular transformation. *Mol Membr Biol* 1995;12:124.

Liu Y, Xu Y, Yu Q. Full-length ADAMTS-1 and the ADAMTS-1 fragments display pro- and antimetastatic activity, respectively. *Oncogene* 2005;25:2452-67.

Liu Y-T, Song L, Templeton DM. Heparin suppresses lipid raft-mediated signaling and ligand-independent EGF receptor activation. *J Cell Physiol* 2007;211:205-12.

London E and Brown DA. Insolubility of lipids in Triton X-100: physical origin and relationship to sphingolipid/cholesterol membrane domains (rafts). *Biochim Biophys Acta* 2000;1508:182-95.

Lusis AJ. Atherosclerosis. *Nature* 2000;407:233-41.

Macfarlane SR, Seatter MJ, Kanke T, Hunter GD, Plevin R. Proteinase-activated receptors. *Pharmacol Rev* 2001;53:245-82.

Maguire JJ and Davenport AP. ETA receptor-mediated constrictor responses to endothelin peptides in human blood vessels in vitro. *Br J Pharmacol* 1995;115:191-7.

Mahtouk K, Hose D, Reme T, et al. Expression of EGF-family receptors and amphiregulin in multiple myeloma. Amphiregulin is a growth factor for myeloma cells. *Oncogene* 2005;24:3512-24.

Mandl M, Slack DN, Keyse SM. Specific inactivation and nuclear anchoring of extracellular signal-regulated kinase 2 by the inducible dual-specificity protein phosphatase DUSP5. *Mol Cell Biol* 2005;25:1830-45.

Marais R, Light Y, Mason C, et al. Requirement of Ras-GTP-Raf complexes for activation of Raf-1 by protein kinase C. *Science* 1998;280:109-12.

Marshall CJ. Specificity of receptor tyrosine kinase signaling: transient versus sustained extracellular signal-regulated kinase activation. *Cell* 1995;80:179-85.

Martorell L, Martínez-González J, Rodríguez C, et al. Thrombin and protease-activated receptors (PARs) in atherothrombosis. *Thromb Haemost* 2008;99:305-15.

Masaki T. Historical review: endothelin. *Trends Pharmacol Sci* 2004;25:219-24.

Mayor S and Maxfield FR. Insolubility and redistribution of GPI-anchored proteins at the cell surface after detergent treatment. *Mol Biol Cell* 1995;6:929-44.

Medcalf RL and Stasinopoulos SJ. The undecided serpin. The ins and outs of plasminogen activator inhibitor type 2. *FEBS J* 2005;272:4858-67.

Mifune M, Ohtsu H, Suzuki H, et al. G protein coupling and second messenger generation are indispensable for metalloprotease-dependent, heparin-binding epidermal growth factor shedding through angiotensin II type-1 receptor. *J Biol Chem* 2005;280:26592-9.

Miwa S, Iwamuro Y, Zhang X-F, et al. Ca²⁺ entry channels in rat thoracic aortic smooth muscle cells activated by endothelin-1. *Jpn J Pharmacol* 1999;80:281-8.

Muda M, Theodosiou A, Rodrigues N, et al. The dual specificity phosphatases M3/6 and MKP-3 are highly selective for inactivation of distinct mitogen-activated protein kinases. *J Biol Chem* 1996;271:27205-8.

Nakanishi-Matsui M, Zheng YW, Sulciner DJ, et al. PAR3 is a cofactor for PAR4 activation by thrombin. *Nature* 2000;404:609-13.

Napoli C, D'Armiento FP, Mancini FP, et al. Fatty streak formation occurs in human fetal aortas and is greatly enhanced by maternal hypercholesterolemia. *J Clin Invest* 1997;100:2680-90.

Nelken NA, Soifer SJ, O'Keefe J, et al. Thrombin receptor expression in normal and atherosclerotic human arteries. *J Clin Invest* 1992;90:1614-21.

Nilsson A, Moller K, Dahlin L, Lundborg GR, Kanje M. Early changes in gene expression in the dorsal root ganglia after transection of the sciatic nerve; effects of amphiregulin and PAI-1 on regeneration. *Brain Res Mol Brain Res* 2005;136:65-74.

Noorbakhsh F, Vergnolle N, Hollenberg MD, Power C. Proteinase-activated receptors in the nervous system. *Nat Rev Neurosci* 2003;4:981-90.

O'Brien PJ, Prevost N, Molino M, et al. Thrombin responses in human endothelial cells. Contributions from receptors other than PAR1 include the transactivation of PAR2 by thrombin-cleaved PAR1. *J Biol Chem* 2000;275:13502-9.

Oh P, McIntosh DP, Schnitzer JE. Dynamin at the neck of caveolae mediates their budding to form transport vesicles by GTP-driven fission from the plasma membrane of endothelium. *J Cell Biol* 1998;141:101-14.

Ohtsu H, Dempsey PJ, Eguchi S. ADAMs as mediators of EGF receptor transactivation by G protein-coupled receptors. *Am J Physiol Cell Physiol* 2006;291:C1-10.

Oksche A, Boese G, Horstmeyer A, et al. Late endosomal/lysosomal targeting and lack of recycling of the ligand-occupied endothelin B receptor. *Mol Pharmacol* 2000;57:1104-13.

Oster H and Leitges M. Protein kinase C α but not PKC ζ suppresses intestinal tumor formation in *Apc*^{Min/+} mice. *Cancer Res* 2006;66:6955-63.

Ostrom RS, Gregorian C, Drenan RM, et al. Receptor number and caveolar co-localization determine receptor coupling efficiency to adenylyl cyclase. *J Biol Chem* 2001;276:42063-9.

Ostrom RS, Liu X, Head BP, et al. Localization of adenylyl cyclase isoforms and G protein-coupled receptors in vascular smooth muscle cells: expression in caveolin-rich and noncaveolin domains. *Mol Pharmacol* 2002;62:983-92.

Owens DM and Keyse SM. Differential regulation of MAP kinase signalling by dual-specificity protein phosphatases. *Oncogene* 2007;26:3203-13.

Owens GK, Kumar MS, Wamhoff BR. Molecular regulation of vascular smooth muscle cell differentiation in development and disease. *Physiol Rev* 2004;84:767-801.

Palade GE. Fine structure of blood capillaries. *J Appl Phys* 1953;24:1424-36.

Paulsson G, Zhou X, Tornquist E, Hansson GK. Oligoclonal T cell expansions in atherosclerotic lesions of apolipoprotein E-deficient mice. *Arterioscler Thromb Vasc Biol* 2000;20:10-7.

Peavy RD, Hubbard KB, Lau A, et al. Differential effects of $G_q\alpha$, $G_{14\alpha}$, and $G_{15\alpha}$ on vascular smooth muscle cell survival and gene expression profiles. *Mol. Pharmacol.* 2005;67:2102-14.

Pelkmans L and Helenius A. Endocytosis via caveolae. *Traffic* 2002;3:311-20.

Pérez Sastre A, Grossmann S, Reusch HP, Schaefer M. Requirement of an intermediate gene expression for biphasic ERK1/2 activation in thrombin-stimulated vascular smooth muscle cells. *J Biol Chem* 2008; 283:25871-8.

Pike LJ. Growth factor receptors, lipid rafts and caveolae: an evolving story. *Biochim Biophys Acta* 2005;1746:260-73.

Prenzel N, Zwick E, Daub H, et al. EGF receptor transactivation by G-protein-coupled receptors requires metalloproteinase cleavage of proHB-EGF. *Nature* 1999;402:884-8.

Prenzel N, Zwick E, Leserer M, Ullrich A. Tyrosine kinase signalling in breast cancer: epidermal growth factor receptor - convergence point for signal integration and diversification. *Breast Cancer Res* 2000;2:184-90.

Pritchard KA Jr, O'Banion MK, Miano JM, et al. Induction of cyclooxygenase-2 in rat vascular smooth muscle cells in vitro and in vivo. *J Biol Chem* 1994;269:8504-9.

Ramachandran R and Hollenberg MD. Proteinases and signalling: pathophysiological and therapeutic implications via PARs and more. *Br J Pharmacol* 2007;153:S263-82.

Reusch HP, Schaefer M, Plum C, Schultz G, Paul M. $G\beta\gamma$ mediate differentiation of vascular smooth muscle cells. *J Biol Chem* 2001a;276:19540-7.

Reusch HP, Zimmermann S, Schaefer M, Paul M, Moelling K. Regulation of Raf by Akt controls growth and differentiation in vascular smooth muscle cells. *J Biol Chem* 2001b;276:33630-7.

Rimoldi V, Riversi A, Taverna E, et al. Oxytocin receptor elicits different EGFR/MAPK activation patterns depending on its localization in caveolin-1 enriched domains. *Oncogene* 2003;22:6054-60.

Ross R. Cell biology of atherosclerosis. *Annu Rev Physiol* 1995;57:791-804.

Ross R. Atherosclerosis - an inflammatory disease. *N Engl J Med* 1999;340:115-26.

Roubert P, Gillard-Roubert V, Pourmarin L, et al. Endothelin receptor subtypes A and B are up-regulated in an experimental model of acute renal failure. *Mol Pharmacol* 1994;45:182-8.

Rozengurt E. Mitogenic signaling pathways induced by G protein-coupled receptors. *J Cell Physiol* 2007;213:589-602.

Russell FD, Skepper JN, Davenport AP. Human endothelial cell storage granules: a novel intracellular site for isoforms of the endothelin-converting enzyme. *Circ Res* 1998;83:314-21.

Rybin VO, Xu X, Lisanti MP, Steinberg SF. Differential targeting of β -adrenergic receptor subtypes and adenylyl cyclase to cardiomyocyte caveolae. A mechanism to functionally regulate the cAMP signaling pathway. *J Biol Chem* 2000;275:41447-57.

Sahin U, Weskamp G, Kelly K, et al. Distinct roles for ADAM10 and ADAM17 in ectodomain shedding of six EGFR ligands. *J Cell Biol* 2004;164:769-79.

Sahin U, Weskamp G, Zheng Y, et al. A sensitive method to monitor ectodomain shedding of ligands of the epidermal growth factor receptor. *Methods Mol Biol* 2006;327:99-113.

Saito Y, Mizuno T, Itakura M, et al. Primary structure of bovine endothelin ET_B receptor and identification of signal peptidase and metal proteinase cleavage sites. *J Biol Chem* 1991;266:23433-7.

Sanderson MP, Abbott CA, Tada H, et al. Hydrogen peroxide and endothelin-1 are novel activators of betacellulin ectodomain shedding. *J Cell Biochem* 2006;99:609-23.

Sargiacomo M, Sudol M, Tang Z, Lisanti MP. Signal transducing molecules and glycosyl-phosphatidylinositol-linked proteins form a caveolin-rich insoluble complex in MDCK cells. *J Cell Biol* 1993;122:789-807.

Sarközi R, Miller B, Pollack V, et al. ERK1/2-driven and MKP-mediated inhibition of EGF-induced ERK5 signaling in human proximal tubular cells. *J Cell Physiol* 2007;211:88-100.

Schafer B, Gschwind A, Ullrich A. Multiple G-protein-coupled receptor signals converge on the epidermal growth factor receptor to promote migration and invasion. *Oncogene* 2004a;23:991-9.

Schafer B, Marg B, Gschwind A, Ullrich A. Distinct ADAM metalloproteinases regulate G protein-coupled receptor-induced cell proliferation and survival. *J Biol Chem* 2004b;279:47929-38.

Schinelli S, Zanassi P, Paolillo M, et al. Stimulation of endothelin B receptors in astrocytes induces cAMP response element-binding protein phosphorylation and c-fos expression via multiple mitogen-activated protein kinase signaling pathways. *J Neurosci* 2001;21:8842-53.

Shah BH. Epidermal growth factor receptor transactivation in angiotensin II-induced signaling: role of cholesterol-rich microdomains. *Trends Endocrinol Metab* 2002;13:1-2.

Shah BH and Catt KJ. Matrix metalloproteinase-dependent EGF receptor activation in hypertension and left ventricular hypertrophy. *Trends Endocrinol. Metab.* 2004;15:241-3.

Shah BH, Baukal AJ, Chen H-D, Shah AB, Catt KJ. Mechanisms of endothelin-1-induced MAP kinase activation in adrenal glomerulosa cells. *J Steroid Biochem Mol Biol* 2006;102:79-88.

Shin HS, Lee HJ, Nishida M, et al. Betacellulin and amphiregulin induce upregulation of cyclin D1 and DNA synthesis activity through differential signaling pathways in vascular smooth muscle cells. *Circ Res* 2003;93:302-10.

Smart EJ, Ying Y, Mineo C, Anderson RGW. A detergent-free method for purifying caveolae membrane from tissue culture cells. *PNAS* 1995;92:10104-8.

Steinberg SF. The cardiovascular actions of protease-activated receptors. *Mol Pharmacol* 2005;67:2-11.

Steinhoff M, Buddenkotte J, Shpacovitch V, et al. Proteinase-activated receptors: transducers of proteinase-mediated signaling in inflammation and immune response. *Endocr Rev* 2005;26:1-43.

Tagawa A, Mezzacasa A, Hayer A, et al. Assembly and trafficking of caveolar domains in the cell: caveolae as stable, cargo-triggered, vesicular transporters. *J Cell Biol* 2005;170:769-79.

Takasuka T, Satoh N, Horii I, Furuichi Y, Watanabe T. Heterogeneity of endothelin receptor. *J Cardiovasc Pharmacol* 1991;17 Suppl 7:S109-12.

Takayanagi R, Ohnaka K, Takasaki C, Ohashi M, Nawata H. Multiple subtypes of endothelin receptors in porcine tissues: characterization by ligand binding, affinity labeling and regional distribution. *Regul Pept* 1991;32:23-37.

Tall AR, Jiang XC, Luo Y, Silver D. 1999 George Lyman Duff memorial lecture: lipid transfer proteins, HDL metabolism, and atherogenesis. *Arterioscler Thromb Vasc Biol* 2000;20:1185-8.

Teixeira A, Chaverot N, Schroder C, et al. Requirement of caveolae microdomains in extracellular signal-regulated kinase and focal adhesion kinase activation induced by endothelin-1 in primary astrocytes. *J Neurochem* 1999;72:120-8.

Tokumaru S, Higashiyama S, Endo T, et al. Ectodomain shedding of epidermal growth factor receptor ligands is required for keratinocyte migration in cutaneous wound healing. *J Cell Biol* 2000;151:209-20.

Tonnessen T, Lunde PK, Giaid A, Sejersted OM, Christensen G. Pulmonary and cardiac expression of preproendothelin-1 mRNA are increased in heart failure after myocardial infarction in rats. Localization of preproendothelin-1 mRNA and endothelin peptide. *Cardiovasc Res* 1998;39:633-43.

Torii S, Nakayama K, Yamamoto T, Nishida E. Regulatory mechanisms and function of ERK MAP kinases. *J Biochem* 2004;136:557-61.

Traynelis SF and Trejo J. Protease-activated receptor signaling: new roles and regulatory mechanisms. *Curr Opin Hematol* 2007;14:230-5.

Trejo J, Altschuler Y, Fu HW, Mostov KE, Coughlin SR. Protease-activated receptor-1 down-regulation. A mutant HeLa cell line suggests novel requirements for PAR1 phosphorylation and recruitment to clathrin-coated pits. *J Biol Chem* 2000;275:31255-65.

Ushio-Fukai M, Hilenski L, Santanam N, et al. Cholesterol depletion inhibits epidermal growth factor receptor transactivation by angiotensin II in vascular smooth muscle cells. Role of cholesterol-rich microdomains and focal adhesion in angiotensin II signaling. *J Biol Chem* 2001;276:48269-75.

Vichi P, Whelchel A, Knot H, et al. Endothelin-stimulated ERK activation in airway smooth-muscle cells requires calcium influx and Raf activation. *Am J Respir Cell Mol Biol* 1999;20:99-105.

Wackenfors A, Emilson M, Ingemansson R, et al. Ischemic heart disease induce upregulation of endothelin receptor mRNA in human coronary arteries. *Eur J Pharmacol* 2004;484:103-9.

Wang M, Zukas AM, Hui Y, et al. Deletion of microsomal prostaglandin E synthase-1 augments prostacyclin and retards atherogenesis. *PNAS* 2006;103:14507-12.

Waugh MG, Lawson D, Hsuan JJ. Epidermal growth factor receptor activation is localized within low-buoyant density, non-caveolar membrane domains. *Biochem J* 1999;337:591-7.

Waugh MG, Minogue S, Anderson JS, dos Santos M, Hsuan JJ. Signalling and non-caveolar rafts. *Biochem Soc Trans* 2001;29:509-11.

Yamada Y, Doi T, Hamakubo T, Kodama T. Scavenger receptor family proteins: roles for atherosclerosis, host defence and disorders of the central nervous system. *Cell Mol Life Sci* 1998;54:628-40.

Yamaguchi T, Murata Y, Fujiyoshi Y, Doi T. Regulated interaction of endothelin B receptor with caveolin-1. *Eur J Biochem* 2003;270:1816-27.

Yan Y, Shirakabe K, Werb Z. The metalloprotease Kuzbanian (ADAM10) mediates the transactivation of EGF receptor by G protein-coupled receptors. *J Cell Biol* 2002;158:221-6.

Zhao Y, Xiao W, Templeton DM. Suppression of mitogen-activated protein kinase phosphatase-1 (MKP-1) by heparin in vascular smooth muscle cells. *Biochem Pharmacol* 2003;66:769-76.

Publications list

Publications

Grantcharova E, Reusch HP, Grossmann S, Eichhorst J, Krell HW, Beyermann M, Rosenthal W, Oksche A. N-terminal proteolysis of the endothelin B receptor abolishes its ability to induce EGF receptor transactivation and contractile protein expression in vascular smooth muscle cells. *Arteriosclerosis, Thrombosis, and Vascular Biology* (2006). 26:1288-1296.

Pérez Sastre A, Grossmann S, Reusch HP, Schaefer M. Requirement of an intermediate gene expression for biphasic ERK1/2 activation in thrombin-stimulated vascular smooth muscle cells. *Journal of Biological Chemistry* (2008). 283:25871-25878.

Grossmann S, Tannert A, Higashiyama S, Oksche A, Schaefer M. Localisation of endothelin B receptor variants to plasma membrane microdomains and its effects on downstream signalling. *Molecular Membrane Biology* (2008) *submitted*

Grossmann S, Schaefer M. Genome-wide analysis of short-term transcriptional responses in thrombin-stimulated vascular smooth muscle cells. *Atherosclerosis* (2008) *submitted*

Oral Presentations

Importance of the glycosylated N terminus of the ET_B receptor for ERK1/2 activation. Seminar, Institut für molekulare Zellbiologie und Pharmakologie, Charité-Universitätsmedizin Berlin. 2005

Role of glycosylation and localisation for endothelin B receptor-mediated mitogenic signalling. Workshop of the GRK 865, Berlin. 2006

Endothelin B Receptor Isoforms: Localisation and Signalling. Evaluation of the GRK865, Berlin. 2007

Abstracts

Grossmann S, Grantcharova E, Reusch HP, Higashiyama S, Oksche A. Mechanisms leading to endothelin B receptor-mediated transactivation of the epidermal growth factor receptor. *Nauyn-Schmiedeberg's archives of pharmacology* (2006). 372: 36-36 96 Suppl. 1

Grantcharova E, Grossmann S, Reusch HP, Rosenthal W, Oksche A. Delayed transactivation of the epidermal growth factor receptor via the endothelin B receptor promotes differentiation of vascular smooth muscle cells. *Nauyn-Schmiedeberg's archives of pharmacology* (2006). 372:31-31 72 Suppl. 1

Poster

Grossmann S, Grantcharova E, Valet S, Rosenthal W, Oksche A. Endothelin B receptor-mediated signalling cascades: the role of lipid rafts. Workshop of the GRK 865, Berlin. 2005

Grossmann S, Grantcharova E, Reusch HP, Valet S, Rosenthal W, Oksche A. ERK1/2 activation via the endothelin B receptor: the role of lipid rafts and internalization. International Symposium of the SFB 593. Mechanisms of Cellular Compartmentalization. Marburg. 2005

Grossmann S, Grantcharova E, Reusch HP, Valet S, Rosenthal W, Oksche A. The role of lipid rafts in ET_B receptor mediated signalling. Molecular Interactions Workshop. Berlin. 2005

Grossmann S, Grantcharova E, Reusch HP, Higashiyama S, Rosenthal W, Oksche A. Importance of the glycosylated N terminus of the ET_B receptor for ERK1/2 activation. 1st international meeting on anchored cAMP signaling pathways. Berlin. 2005

Grossmann S, Grantcharova E, Reusch HP, Higashiyama S, Oksche A. Mechanisms leading to Endothelin B receptor-mediated transactivation of the epidermal growth factor receptor. 47. Frühjahrstagung der DGPT. Mainz. 2006

Grossmann S, Reusch HP, Schaefer M. Short-term modification of gene expression in thrombin-stimulated VSM cells. Evaluation of the GRK865. Berlin. 2007

Grossmann S, Reusch HP, Schaefer M. Thrombin-induced short-term modification of gene expression in vascular smooth muscle cells. Kinin 2007. 2nd international conference on "Exploring the future of vascular and inflammatory mediators". Berlin. 2007

Acknowledgements

I thank Dr. Alexander Oksche and Prof. Dr. Michael Schaefer for giving me the opportunity to work on this project. Their supervision, support and advice were of great help throughout the years.

I also thank all the people I have worked with. Nadine Albrecht, Berit Bohnekamp, Anke Klein, Chihab Klose, Katja Lautz, Alejandra Pérez Sastre, Isabel Schwieger, Isabelle Straub, Astrid Tannert and Philipp Voigt made the lab a wonderful place to work at. All of them contributed in some way to this thesis. Nadine endlessly seeded cells and helped with the calcium measurements. Astrid taught me how to use the TIRF microscope. Philipp was the one who always had an answer to every question. Isabel, Alejandra, Katja and Berit were and still are fantastic friends not only in the lab. I am very grateful for having met them. I will miss our coffee breaks in the afternoon that were always accompanied by a lot of laughter.

I want to thank Frank for our sometimes endless but always fruitful discussions. His continuous support made everything a lot easier.

Last but not least, I thank my family and friends for their encouragement and support throughout the years.